FLUXGATE MAGNETOMETER CALIBRATION FOR

BEPICOLOMBO

BC–MAG–TR–0085

Issue: 1 Revision: 3

May 06, 2013

Protocol and Analysis of the

BepiColombo MPO Calibration for

Sensor BS_10 & BS_11

connected to the FM_1 Electronics

Dr. Ingo Richter

Institut für Geophysik und extraterrestrische Physik
Technische Universität Braunschweig
Mendelssohnstraße 3, 38106 Braunschweig
Germany

Contents

1 Introduction

This document describes the ground calibration of the BepiColombo MPO-FM1 magnetometer using the Sensors BS_10 & BS_11. The calibration was conducted at the Magnetsrode Calibration facility operated by the Institute for Geophysics and extraterrestrial Physics, TU Braunschweig. The tests were executed from April 02 - April 11, 2013.

Part Identification:

Sensor:	BS_10 (connected to J02, IB)
	BS_11 (connected to J01, OB)
Electronics	MPO FM1

Key Personnel:

Karl-Heinz Fornaçon:	operating FGM
Ingo Richter:	operating MRode Facility

General Setup

- Sensor mounted in thermal box. CoC. Box vertical.
- Sensor is operated with thick MPO hat installed
- FM1 Electronics placed in House 2 / Mainroom.
- The EGSE Laptop placed in House 2 / Anteroom.
- The Spacewire Brick placed in House 2 / Anteroom.
- The FM1 Electronics was powered by the Thurlby Power Supply in House 1.
  Voltage: +28V / Current: +0.163A
- DUT parameters Sensor BS_10:
  Phase: 146
  K1X: 24927
  K1Y: 14331
  K1Z: 56105
  KF: 102
  Relais: on , Excitation: on

- DUT parameters Sensor BS_11:
  Phase: 146
  K1X: 40402
  K1Y: 22671
  K1Z: 55926
  KF: 102
  Relais: on , Excitation: on

- Position 1: Standard Alignment
  $X_m = X_c, Y_m = Y_c, Z_m = Z_c$
  Elevation= 0°. Azimuth= 180°.

- Position 2: Turned Position for XY Offset Measurements
  $X_m = -X_c, Y_m = -Y_c, Z_m = Z_c$
  Elevation= 0°. Azimuth= 0°.

- Position 3: Normal Position for Z Offset Measurements
  $X_m = -Z_c, Y_m = -Y_c, Z_m = -X_c$
  Elevation=90°. Azimuth= 0°.

- Position 4: Turned Position for Z Offset Measurements
  $X_m = -Z_c, Y_m = Y_c, Z_m = X_c$
  Elevation=90°. Azimuth= 180°.

- The sensor pictures were taken before rotating the box to the vertical orientation.

- TEMPCTRL-Parameters for Heating:
  Field-Active-Time: 25s
  SOL controlled, Delay after SOL: 8s
  Max. Heating Time: 20s
  Heating-Profile: *manual*
  Heater-Select: automatic
  Smart_heat: off

- TEMPCTRL-Parameters for Cooling:
  Field-Active-Time: 25s
  SOL controlled, Delay after SOL: 8s
  Max. Heating Time: 25s
  Max. Cooling Time: 7s
  Heating-Profile: *manual*
  Heater-Select: *automatic*
  Smart_heat: *on*

- IP-Adressses:
  FM1-EGSE: 192.168.124.37
  MRode-Terminal: 192.168.124.50

REMARKS:

- The Analysis has been performed using a nominal conversion factor of 1 nT/V (nT/ADCcounts).
- The magnetometer was operated always in 2048 nT range with a sampling rate of 128 vectors per second if not stated different.
- **All values (e.g Offsets) given in engineering nanotesla (enT) have to be multiplied with the calculated sensitivities to obtain real nanotesla values.**
- The X-sensor shows non-linearities at fields of ±2000 nT. Therefore, only values up to ±1900 nT were used for the analysis.
- In open loop mode the X-sensor shows non-linearities at fields of ±1300 nT. Therefore, only values up to ±1300 nT were used for the analysis.
- In open loop mode the Y-sensor shows non-linearities at fields of ±1100 nT. Therefore, only values up to ±1100 nT were used for the analysis.
- In open loop mode the Z-sensor shows non-linearities at fields of ±1700 nT. Therefore, only values up to ±1700 nT were used for the analysis.
- All TEMB frames contain the MPO temperatures in the first three channels:

TEMB-CH0: $T_{\text{ELEC-IB}}$
TEMB-CH1: $T_{\text{IB-1}}$ – Sensor Temperature
TEMB-CH2: $T_{\text{IB-2}}$ – Sensor Temperature
TEMB-CH3: $T_{\text{ELEC-OB}}$
TEMB-CH4: $T_{\text{OB-1}}$ – Sensor Temperature
TEMB-CH5: $T_{\text{OB-2}}$ – Sensor Temperature

- MRode-Terminal software:
  TERMINAL_16.vi using *MPO/EXTRACT_MPO_HK_PACKETS.vi*

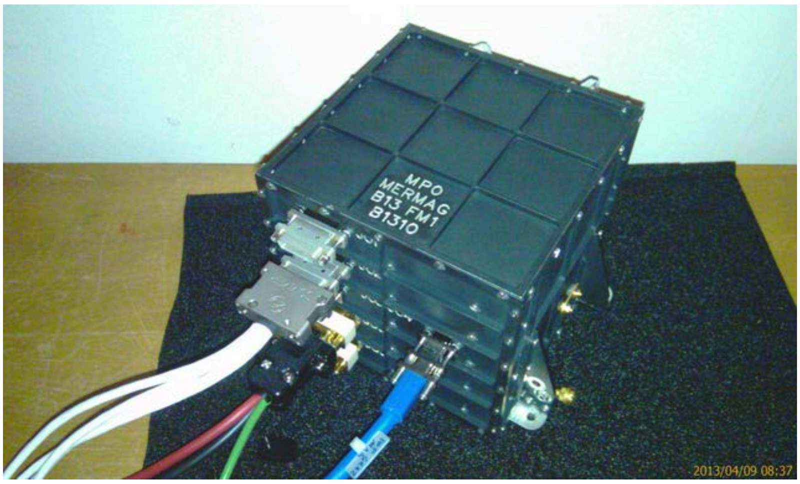

Figure 1: FM1 Electronics in H2, Mainroom

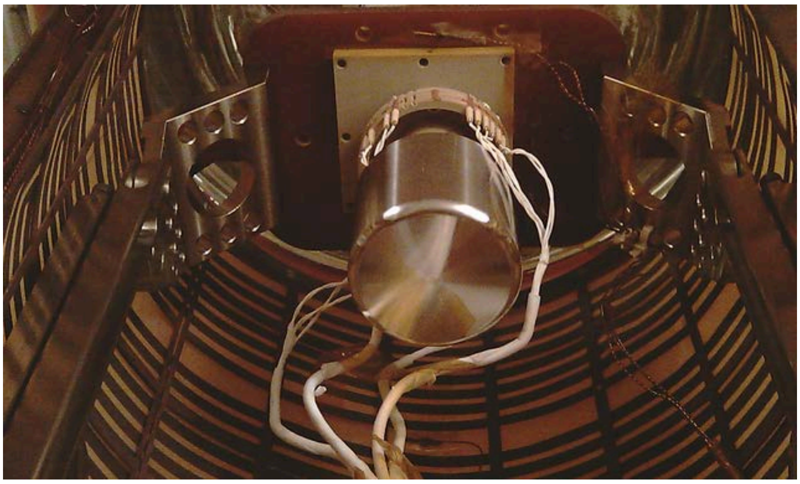

Figure 2: Sensor in Standard Position, POSITION 1, View from South

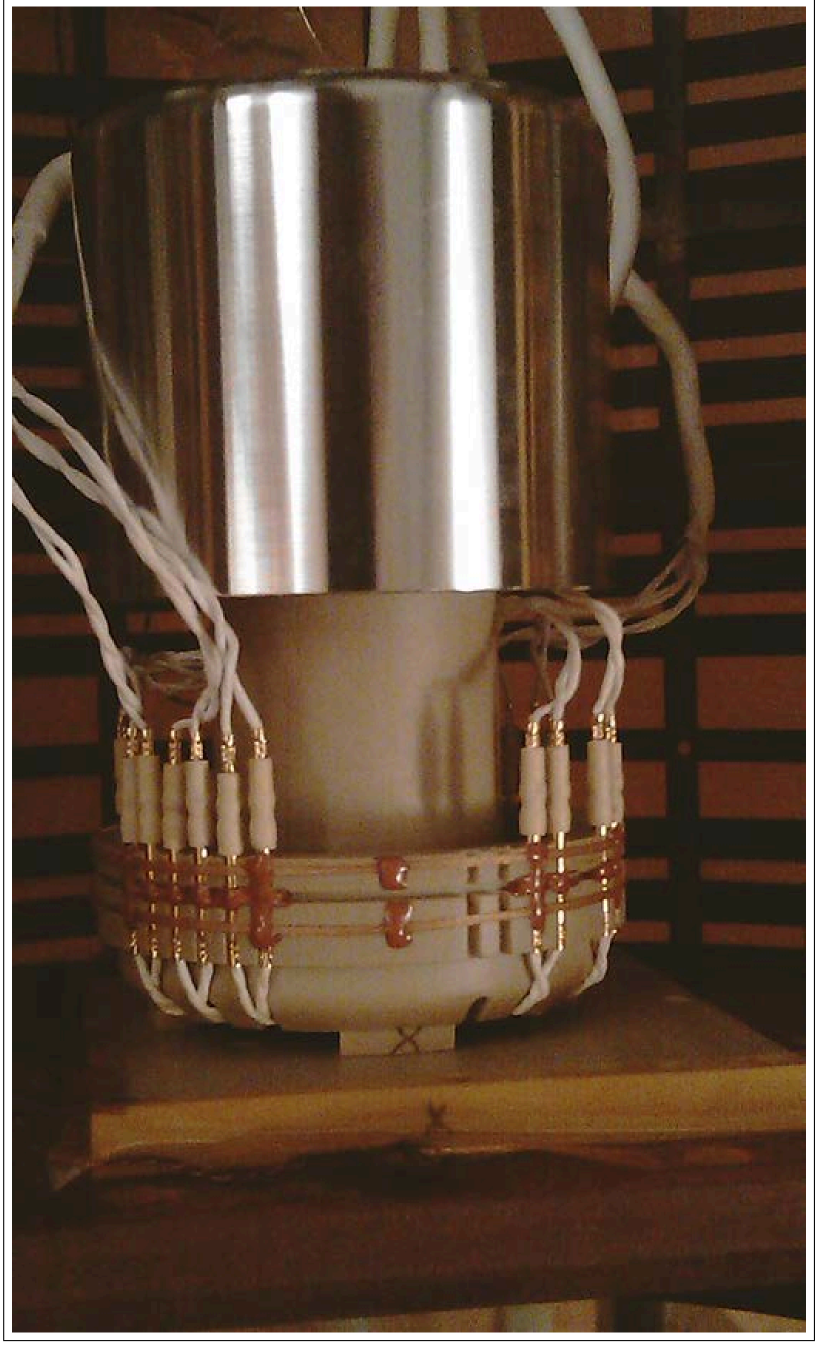

Figure 3: Sensor in Standard Position, POSITION 1, View from Top

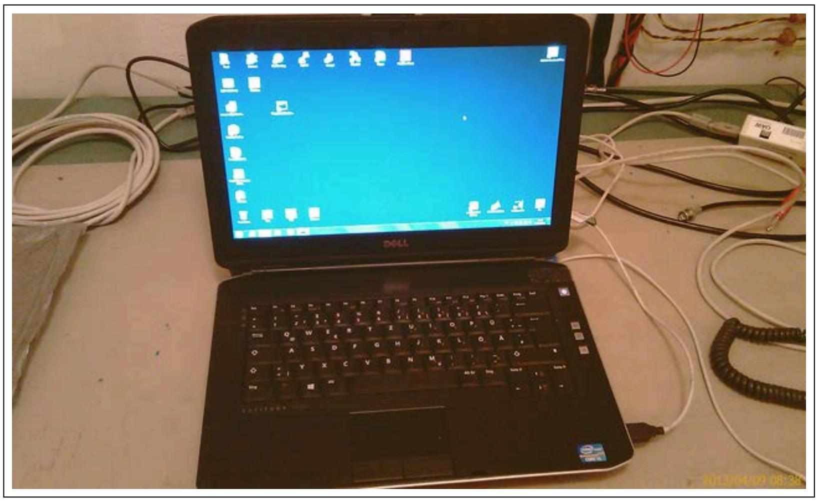

Figure 4: EGSE Laptop in H2, Anteroom

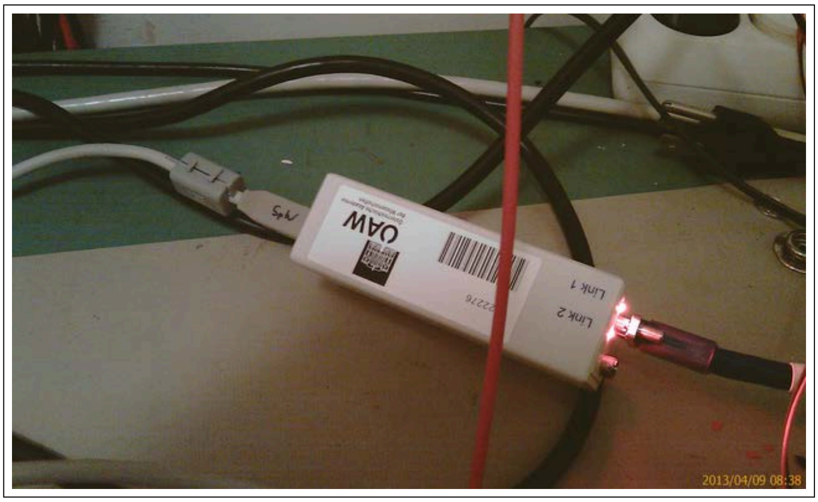

Figure 5: FM1 Brick in H2, Anteroom

2 Measurements on April 2, 2013

The FM1 Magnetometer was installed in House 2. Sensor BS_11 was placed at CoC in the thermal box. Sensor BS_10 was placed south of the coilsystem inside a small μ-Metal can.

Due to lack of time and a needed quick setup the sensor was operated by EGSE control only. No data were stored at the MRode CDRS. The magnetometer was operated in dynamical compensated zerofield conditions.

Over night the sensor measured in normal science mode, 4 Hz sampling rate, 2048 nT range, room temperature, measurements started at about 12:30.

3 Measurements on April 3, 2013

The measurement over night was performed without any problem.

3.1 Coilsystem Residual Field Check

Figure 6: Overhauser Magnetometer Sensor in Diagonal in Space Orientation, CoC, View from South-West

Prior to the real MPO calibration the residual field of the MCF has been checked using the Overhauser magnetometer. The OVH was placed diagonal in space at CoC. Fields of ±49000 nT were applied sequentially to each axis in order to determine the actual residual field:

Component	Applied Field	Measured Modulus	Calc. Residual
X_c	+49000 nT	49002 nT	
	-49000 nT	49007 nT	-2.5 nT
Y_c	+49000 nT	49002 nT	
	-49000 nT	49004 nT	-1 nT
Z_c	+49000 nT	48960 nT	
	-49000 nT	49040 nT	-40 nT

After these initial measurements the residual field was nulled with the offset potentiometers at the Power Amplifiers.

Component	Applied Field	Measured Modulus	Calc. Residual
X_c	+49000 nT	49005 nT	
	-49000 nT	49005 nT	0 nT
Y_c	+49000 nT	49003 nT	
	-49000 nT	49003 nT	0 nT
Z_c	+49000 nT	48993 nT	
	-49000 nT	49007 nT	-7 nT

The z-component could not be nulled exactly, as the offset controlling potentiometer of the Zc-PA reached the limit of its rotation range.

After the removal of the Overhauser magnetometer and shifting the thermal box, with sensor BS_11 installed, to the default CoC position, the setup was finished.

3.2 Calibration Initialisation

Initial reading of the thermistors:

T_{59}	=	17.3°C
$T_{\mathrm{ELEC-IB}}$	=	26.5°C
$T_{\mathrm{IB-1}}$	=	15.7°C
$T_{\mathrm{IB-2}}$	=	16.7°C
$T_{\mathrm{ELEC-OB}}$	=	27.35°C
$T_{\mathrm{OB-1}}$	=	19.9°C
$T_{\mathrm{OB-2}}$	=	20.1°C

A first test of the BS_11 Sensor revealed the correct soldering of the components.

Application of 1000 nT fields in all main axes in Standard orientation yielded (in the default position 1):

X_{m}	=	X_{c}
Y_{m}	=	Y_{c}
Z_{m}	=	Z_{c}

3.3 Data

CCD File	Configuration File	Remark
13-04-03\09-22-38.CCR	LIN2000XYZE.MAG	
13-04-03\09-53-35.CCR	OFFSET_200.MAG	
13-04-03\10-07-54.CCR	LIN2000XYZE.MAG	
13-04-03\10-15-00.CCR	LIN2000XYZE.MAG	
13-04-03\10-45-19.CCR	LIN2000XYZE.MAG	
13-04-03\11-15-38.CCR	LIN2000XYZE.MAG	
13-04-03\11-45-56.CCR	LIN2000XYZE.MAG	
13-04-03\12-16-15.CCR	LIN2000XYZE.MAG	
13-04-03\12-47-57.CCR	OFFSET_200.MAG	
13-04-03\12-59-48.CCR	FREQ2000.MAG	
13-04-03\13-45-53.CCR	FREQ2000.MAG	
13-04-03\14-41-31.CCR	FREQ2000.MAG	
13-04-03\15-24-42.CCR	LIN2000XYZE.MAG	
13-04-03\15-55-48.CCR	OFFSET_200.MAG	
13-04-03\16-08-54.CCR	NULL_LANG.MAG	

3.4 DC-Analysis at Room Temperature - OB Sensor, Science mode 0

A standard linearity and offset measurement was performed at 17.3°C.

3.4.1 Calibration on 3 Linear Axes

Used Files:

CCD File	Configuration File	Remark
`13-04-03\09-22-38.CCR`	`LIN2000XYZE.MAG`	

Parameter File: `PARAMETER_LIN__13-04-03_09-22-38.CPF`

Facility Parameter:

Nominal Sensor Setup $\underline{B}_{\mathrm{DUT}} = \underline{\underline{R}}_{\mathrm{nom}} \underline{B}_{\mathrm{C}}$

$$\underline{\underline{R}}_{\mathrm{nom}} = \begin{pmatrix} +1.000000 & +0.000000 & +0.000000 \\ +0.000000 & +1.000000 & +0.000000 \\ +0.000000 & +0.000000 & +1.000000 \end{pmatrix}$$

Calculated Sensor Rotation:

$$\underline{\underline{\rho}} = \begin{pmatrix} +0.999800 & +0.018895 & +0.006519 \\ -0.018810 & +0.999740 & -0.012858 \\ -0.006760 & +0.012733 & +0.999896 \end{pmatrix}$$

Rotation Angles:

$$\begin{aligned} \text{Angle } (X_c, X_m): \quad & \lambda_{\mathrm{x}} = +1^\circ\ 8'43'' \\ \text{Angle } (Y_c, Y_m): \quad & \mu_{\mathrm{y}} = +1^\circ\ 18'20'' \\ \text{Angle } (Z_c, Z_m): \quad & \nu_{\mathrm{z}} = +0^\circ\ 49'34'' \end{aligned}$$

Determinant of Rotation Matrix: 1.00000
Nominal Field Source: FLDS
Fields applied for 24.0 s
Mean Sensor Temperature: 17.2°C
Automatic Coil Correction: used

Earthfield Compensation: X = DYNAMIC
Y = DYNAMIC
Z = DYNAMIC

Offset Treatment:

A polynomial offset trend of order 2 has been fitted and subtracted from the raw data before creating the sensor model.

Mean Coil System Residual + Sensor Offset: $\underline{B}^{or}$ = (-0.208 , -0.272 , -10.561) nT

Raw Data Quality:

Standard Deviation of used Raw Data Blocks:

[Values in eng nT]	s_x	s_y	s_z
Minimum	0.000	0.342	0.316
Mean	2.383	0.407	0.676
Maximum	3.318	1.087	0.892

Calibration Parameter:

$$\text{Transfermatrix:}\quad \underline{\underline{\phi}} = \underline{\underline{R}}_{\text{nom}}\,\underline{\underline{\rho}}\,\underline{\underline{\omega}}\,\underline{\underline{\sigma}} = \begin{pmatrix} +0.972083 & +0.018824 & +0.006445 \\ -0.021899 & +0.995935 & -0.012713 \\ -0.005695 & +0.012883 & +0.988644 \end{pmatrix}$$

$$\text{Reduced Transfermatrix:}\quad \tilde{\underline{\underline{\phi}}} = \underline{\underline{\omega}}\,\underline{\underline{\sigma}} = \begin{pmatrix} +0.972339 & +0.000000 & +0.000000 \\ -0.003598 & +0.996196 & +0.000000 \\ +0.000923 & +0.000198 & +0.988747 \end{pmatrix}$$

$$\text{Sensitivity:}\quad \underline{\underline{\sigma}} = \begin{pmatrix} +0.972339 & +0.000000 & +0.000000 \\ +0.000000 & +0.996189 & +0.000000 \\ +0.000000 & +0.000000 & +0.988747 \end{pmatrix}$$

$$\text{Misalignment:}\quad \underline{\underline{\omega}} = \begin{pmatrix} +1.000000 & +0.000000 & +0.000000 \\ -0.003701 & +1.000007 & +0.000000 \\ +0.000950 & +0.000199 & +1.000000 \end{pmatrix}$$

Sensor Misalignment Angles:

$$\xi_{\text{x,y}} = +89^\circ\ 47'17''$$
$$\xi_{\text{x,z}} = +90^\circ\ 3'16''$$
$$\xi_{\text{y,z}} = +90^\circ\ 0'42''$$

Model Quality:

Standard Deviation, Maximum and Minimum Error of Calculated Model:

[Values in nT]	X	Y	Z
Standard Deviation	0.051	0.068	0.067
Maximum Error	0.121	0.120	0.176
Minimum Error	-0.124	-0.183	-0.147

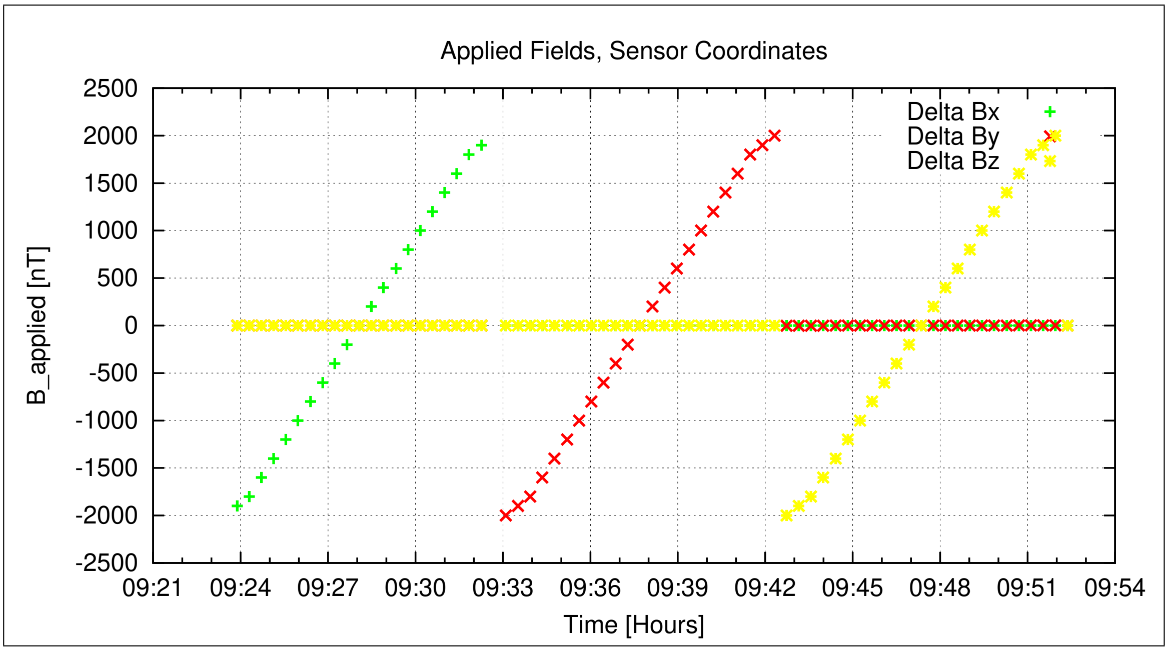

Figure 7: Applied Fields

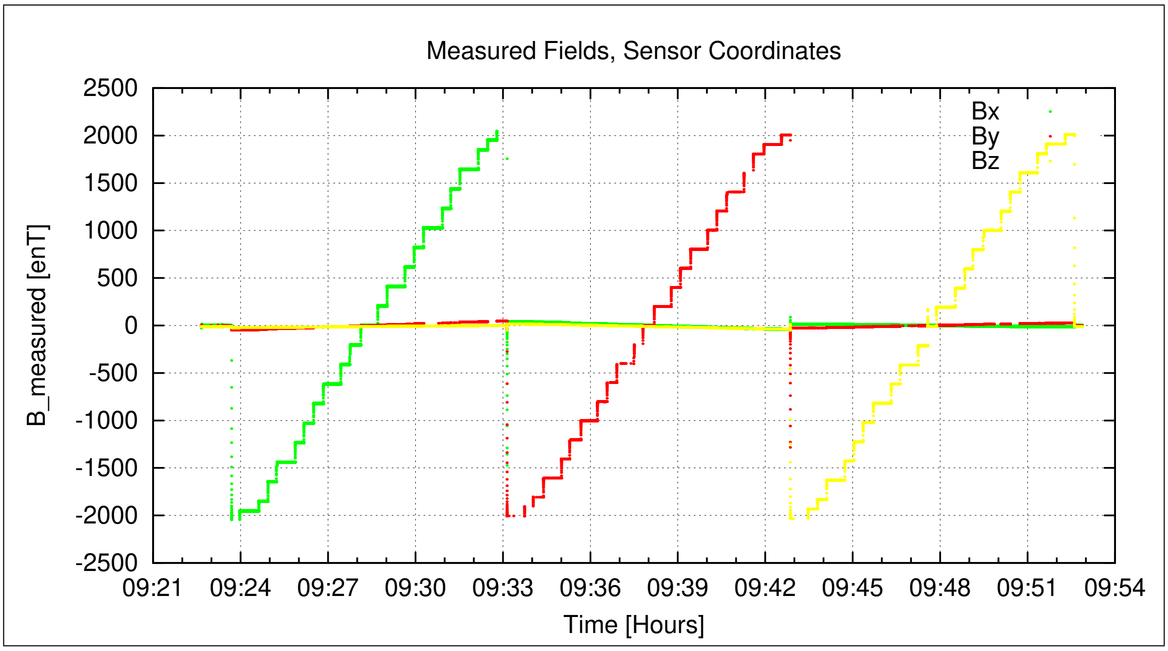

Figure 8: Measured Data

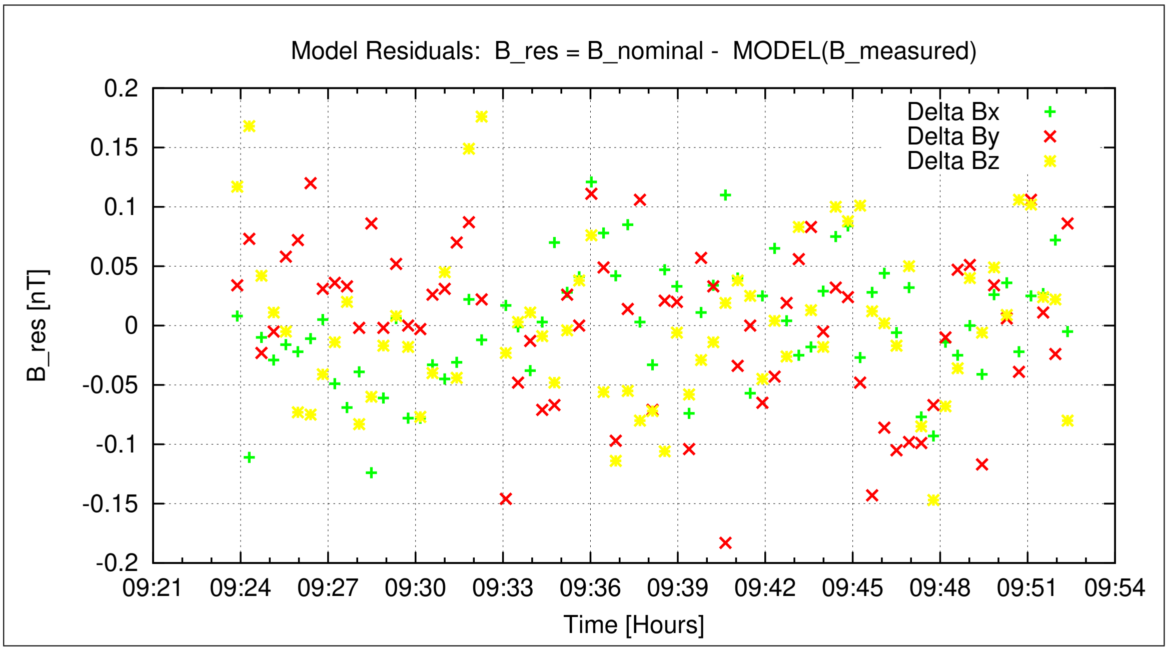

Figure 9: Model Quality - Differences of applied field and modelled measurement data

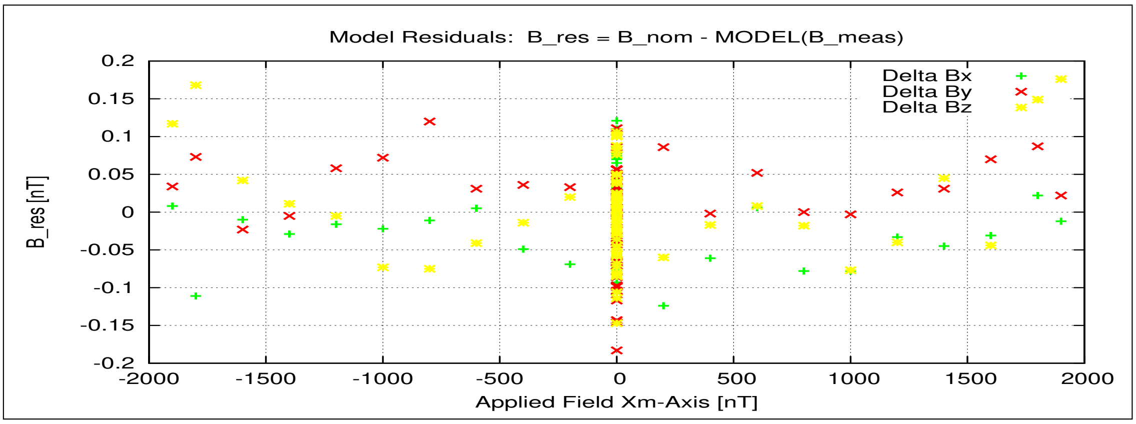

Figure 10: RESIDUALS vs FLD X

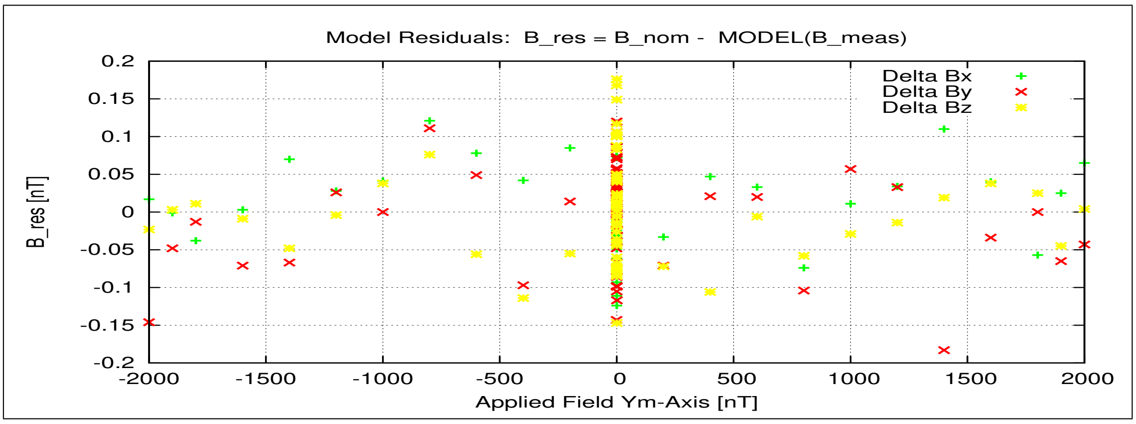

Figure 11: RESIDUALS vs FLD Y

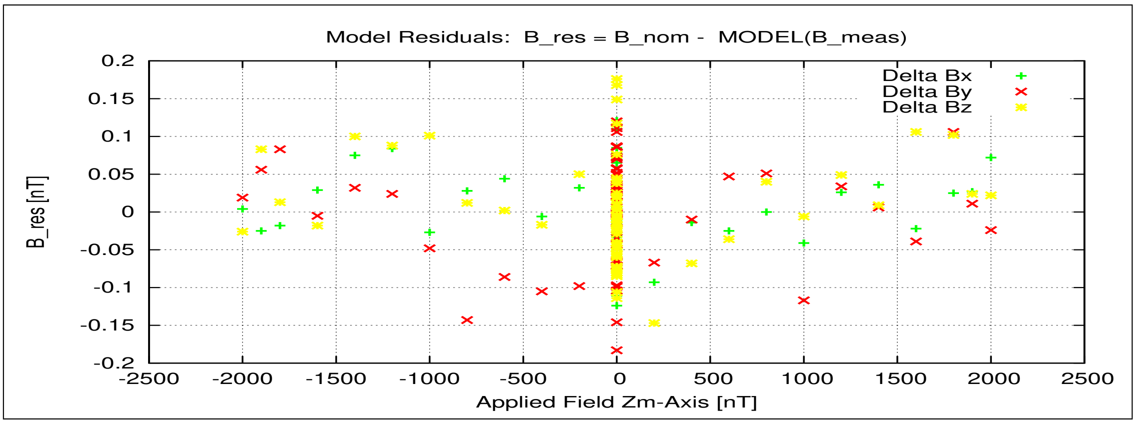

Figure 12: RESIDUALS vs FLD Z

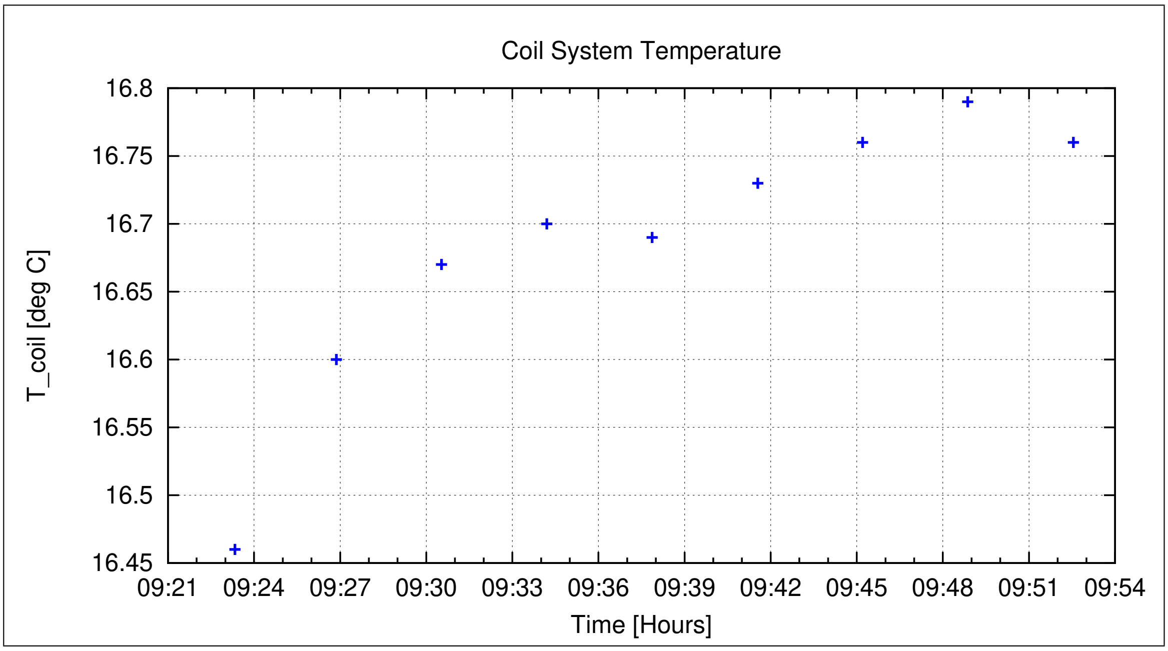

Figure 13: Coil System Temperature

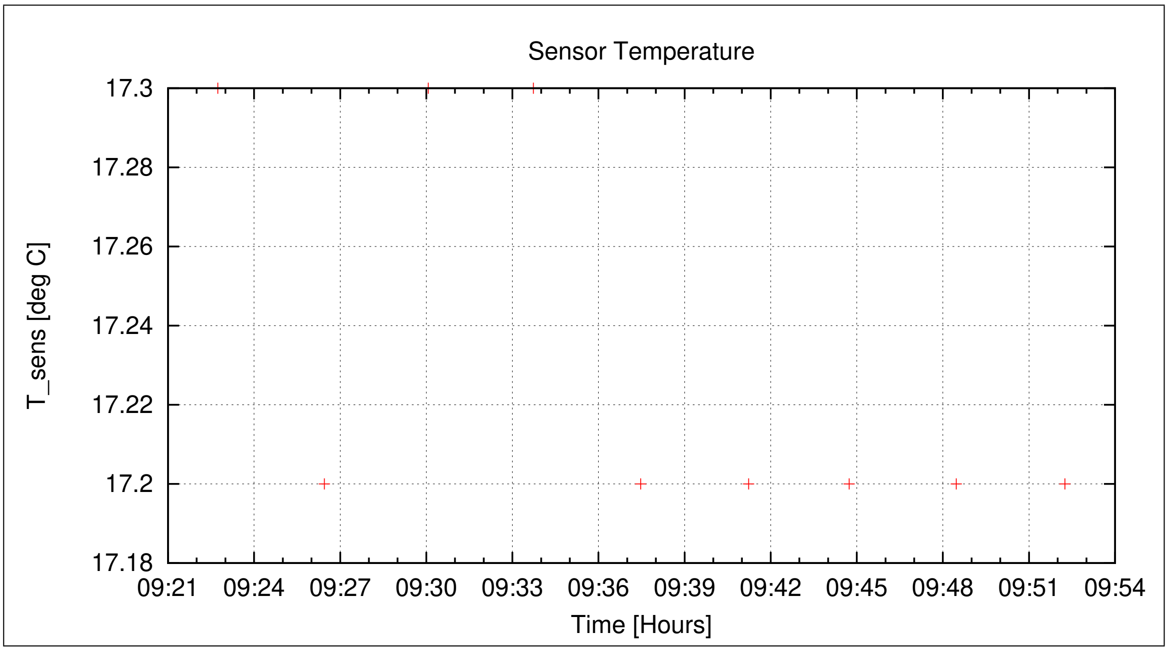

Figure 14: Sensor Temperature

3.4.2 OFFSET Calculation

In this section the instrument offsets and the residual field of the Coil System will be evaluated. Measurements at two orientations for each component act as input for the offset calculation. From the "normal" (0-degrees) and "turned" (180-degrees) orientations the offsets and residual fields can be derived:

$$B_{\text{off}} = \frac{B_{\text{normal}} + B_{\text{turned}}}{2}$$
$$B_{\text{res}} = \frac{B_{\text{normal}} - B_{\text{turned}}}{2}$$

Used Offset Measurements:

CCD File	Configuration File	Remark
13-04-03\09-53-35.CCR	OFFSET_200.MAG	

Parameter File: OFF_PARAMETER__13-04-03-09-53-35.OPF

Calibration Parameter:

Sensor Offsets:

Component	Offset [enT]	Standard deviation [enT]
X	0.10	0.097
Y	-0.14	0.091
Z	0.65	0.081

Residual Field of the Coil System:

Component	B_{res} [enT]
X	-0.44
Y	0.17
Z	0.66

Remark: Residual field is given in actual DUT coordinates, not in coil-coordinates!

Afterwards the thermal system was started and the box was cooled down to -70°C starting at 10:15. The initial pressure of the N_2-bottle was 85 bar, 35 kg of LN_2 were available.

3.5 DC-Analysis at very low Temperature - OB Sensor

Linearity and offset measurements were performed at $T_{59} = -71$°C in cal mode 4 and cal mode 0.

Thermal Analysis: refer to section 12.

3.6 AC-Analysis at very low Temperature - OB Sensor, Science mode 0

A frequency measurement was performed at -70°C.

Setup:

- Sensor mounted in thermal box. CoC. Box vertical.
- Sensor rotated to:
  Elevation= 45°
  Azimuth= 126°
- Field applied on Y_c.
- No attenuator

3.6.1 Frequency Measurements

This section is dedicated to the frequency behavior of the instrument. The analysis of the performed AC measurements allows to calculate the actual sampling frequency f_s of the instrument and the frequency response (amplitude vs. frequency). The measurements have been performed with the sensor placed at CoC in a diagonal in space orientation. The AC-fields have been applied on the Y_c axis only. Using this setup it can be guaranteed that only one frequency is applied at a time and no beat effects occur.

Used Frequency Measurements:

CCD File	Configuration File	Remark
13-04-03\12-59-48.CCR	FREQ2000.MAG	

Parameter File: `FREQ_PARAMETER__13-04-03-12-59-48.FPF`

Calibration Parameter:

Sampling Frequency:

Component	f_s [Hz]	Standard deviation [Hz]
X	127.9989	0.000066
Y	127.9988	0.000058
Z	127.9990	0.000056
Mean Sampling Frequency	127.9989	0.000138

3 dB Corner Frequency:

Component	$f_{3\mathrm{dB}}$ [Hz]
X	64.59
Y	64.02
Z	55.45

Applied Frequencies and Measured Amplitudes

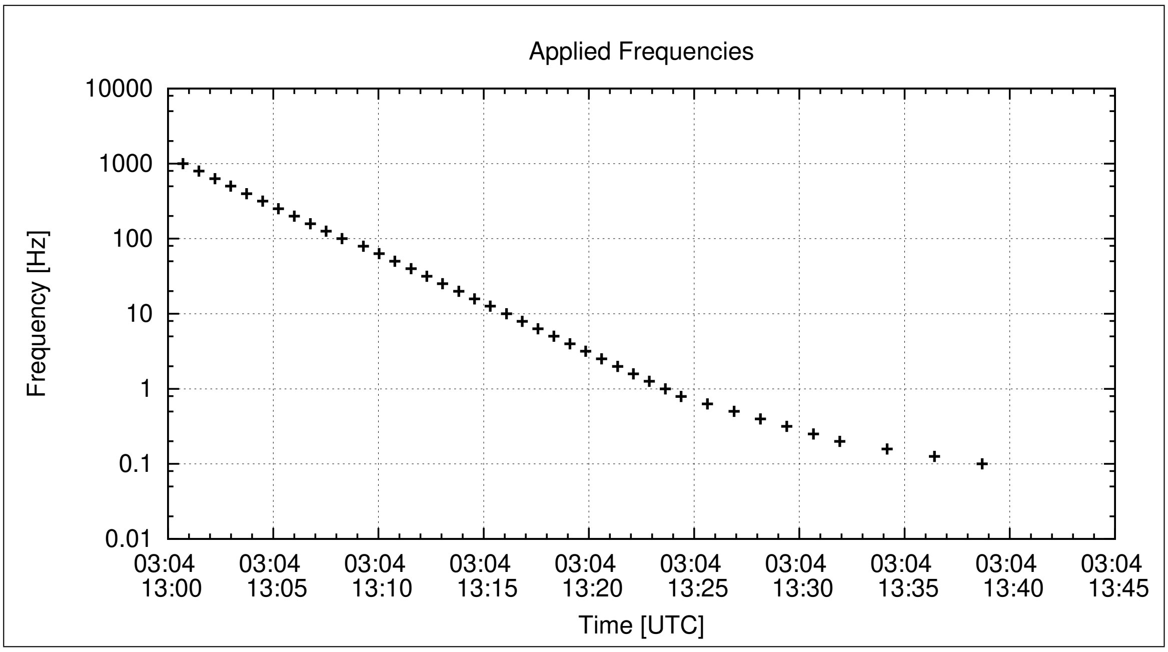

Figure 15: Applied Frequencies for AC Analysis

Applied Frequency [Hz]	Bx [enT]	By [enT]	Bz [enT]
1000.000	1.93	1.77	0.69
794.000	10.30	9.61	4.11
631.000	15.74	14.81	6.97
501.000	23.35	22.14	11.64
398.000	18.89	18.03	10.37
316.000	37.04	35.01	21.00
251.000	46.26	44.23	29.94
199.000	105.65	100.40	71.59
158.000	54.24	52.31	43.02
126.000	61.87	59.36	49.76
100.000	148.72	144.04	133.77
79.400	340.65	326.34	298.36
63.100	442.44	422.76	387.03
50.100	514.93	494.05	471.04
39.800	561.95	541.63	541.95
31.600	589.20	569.67	588.78
25.100	603.14	583.57	610.07
19.900	609.00	588.76	613.88
15.800	609.33	588.29	608.45
12.600	610.46	588.61	603.77
10.000	608.93	586.51	597.48
7.900	607.11	584.29	592.19
6.310	608.06	584.89	590.83
5.010	606.56	583.25	587.84
3.980	606.81	583.34	587.07
3.160	607.81	584.21	587.37
2.510	606.75	583.14	585.94
1.990	606.46	582.83	585.40
1.580	608.15	584.44	586.87
1.260	607.69	583.97	586.31
1.000	608.11	584.37	586.64
0.790	607.53	583.80	586.04
0.631	608.56	584.78	587.01
0.501	608.41	584.63	586.85
0.398	608.01	584.25	586.42
0.316	608.20	584.43	586.58
0.251	608.72	584.93	587.11
0.199	608.78	584.98	587.16
0.158	609.30	585.49	587.62
0.126	608.88	585.04	587.21
0.100	609.90	586.07	588.19

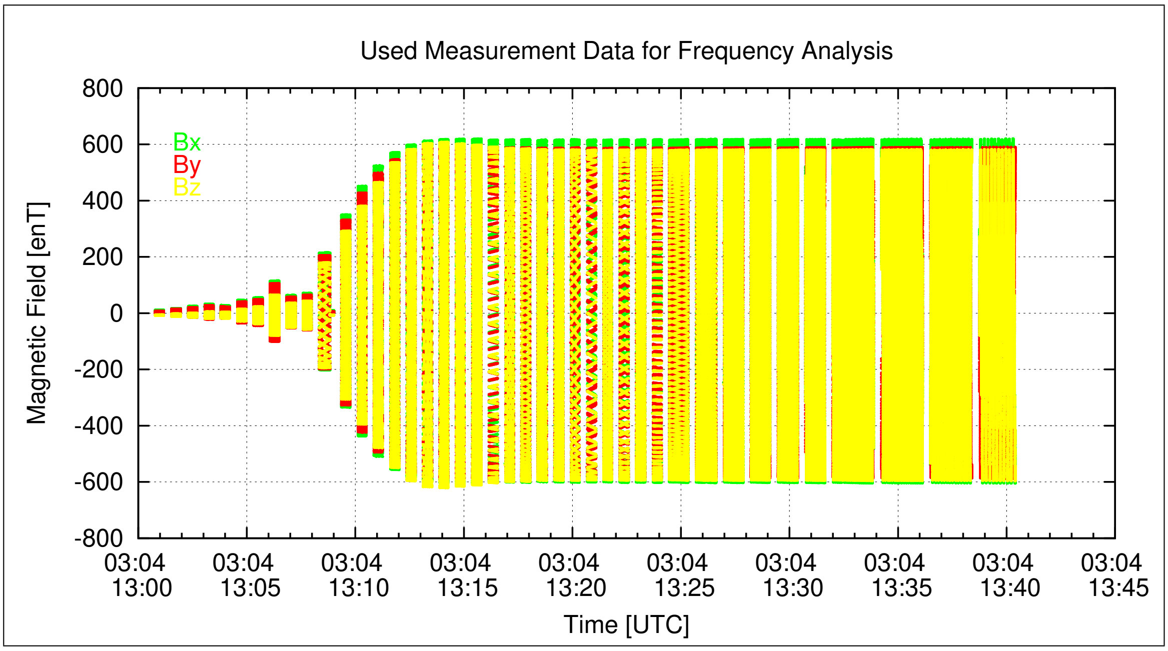

Figure 16: Used packets of Measured data for the Frequency analysis

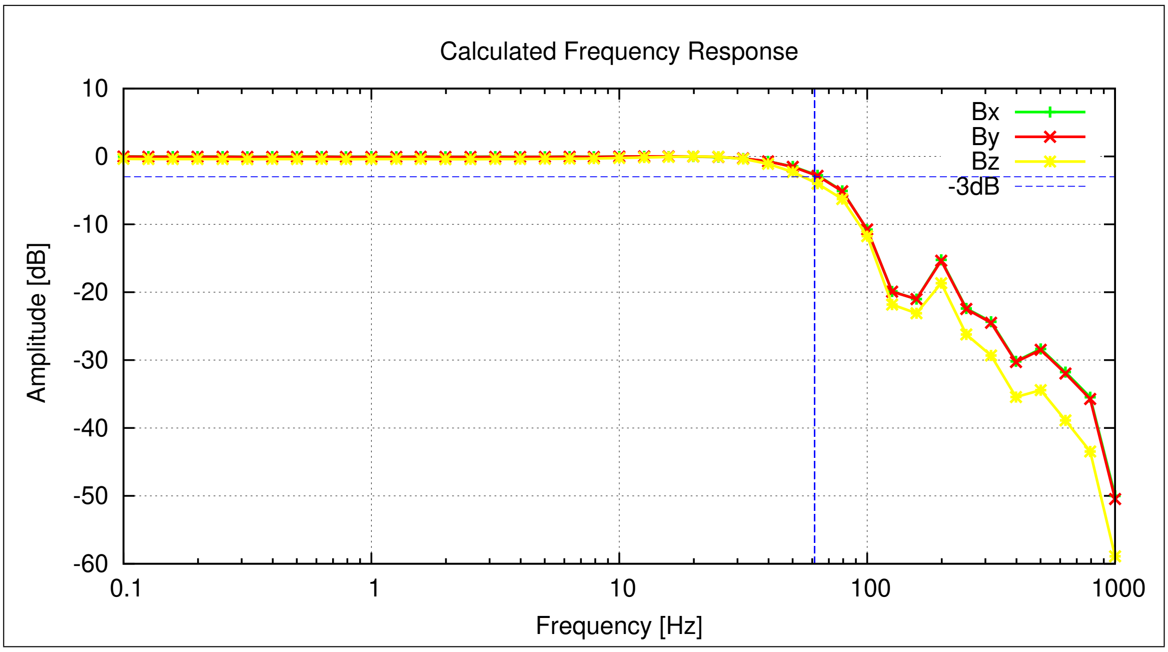

Figure 17: Calculated Frequency Response

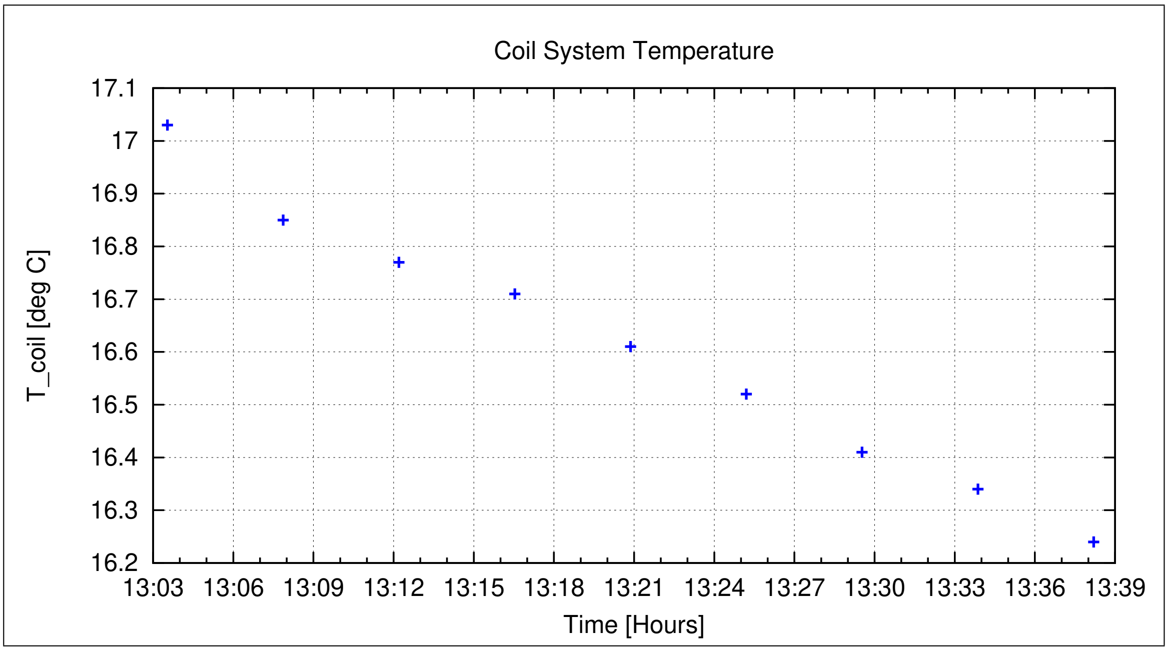

Figure 18: Coil System Temperature

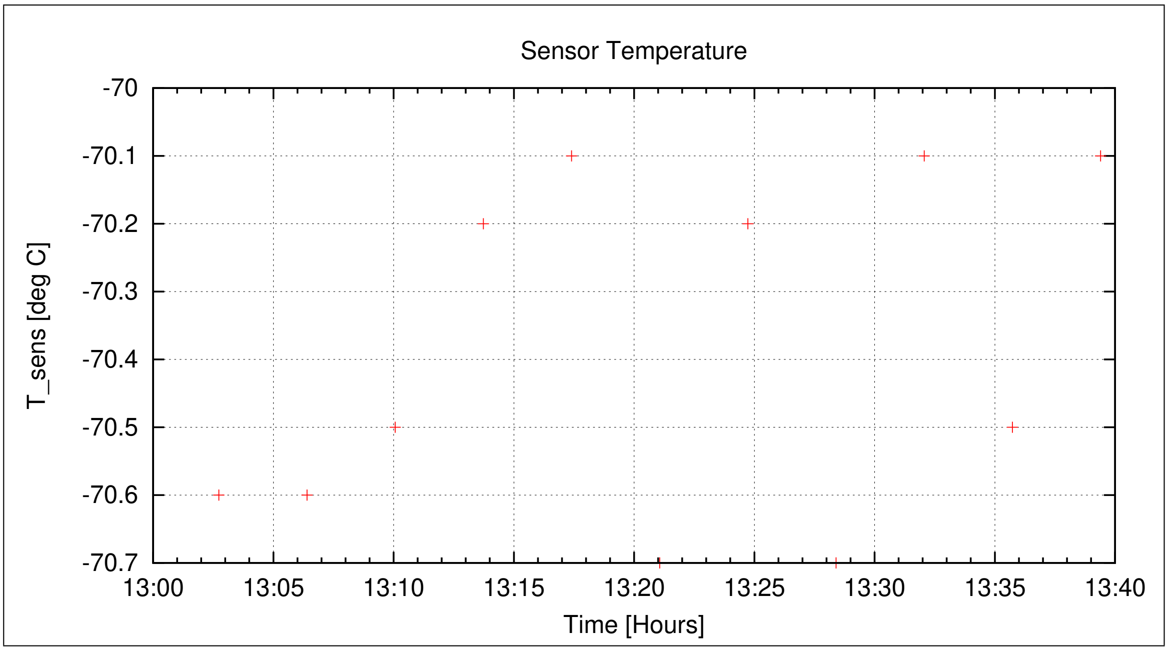

Figure 19: Sensor Temperature

3.7 AC-Analysis at very low Temperature - OB Sensor, Cal mode 4, open loop

A frequency measurement was performed at -70°C.

Setup:

- Sensor mounted in thermal box. CoC. Box vertical.
- Sensor rotated to:
  Elevation= 45°
  Azimuth= 126°
- Field applied on Y_c.
- No attenuator

3.7.1 Frequency Measurements

This section is dedicated to the frequency behavior of the instrument. The analysis of the performed AC measurements allows to calculate the actual sampling frequency f_s of the instrument and the frequency response (amplitude vs. frequency). The measurements have been performed with the sensor placed at CoC in a diagonal in space orientation. The AC-fields have been applied on the Y_c axis only. Using this setup it can be guaranteed that only one frequency is applied at a time and no beat effects occur.

Used Frequency Measurements:

CCD File	Configuration File	Remark
13-04-03\14-41-31.CCR	FREQ2000.MAG	

Parameter File: FREQ_PARAMETER__13-04-03-14-41-31.FPF

Calibration Parameter:

Sampling Frequency:

Component	f_s [Hz]	Standard deviation [Hz]
X	127.9989	0.000019
Y	127.9990	0.001444
Z	127.9988	0.000024
Mean Sampling Frequency	127.9989	0.000103

3 dB Corner Frequency:

Component	f_{3dB} [Hz]
X	58.34
Y	58.29
Z	54.47

Applied Frequencies and Measured Amplitudes

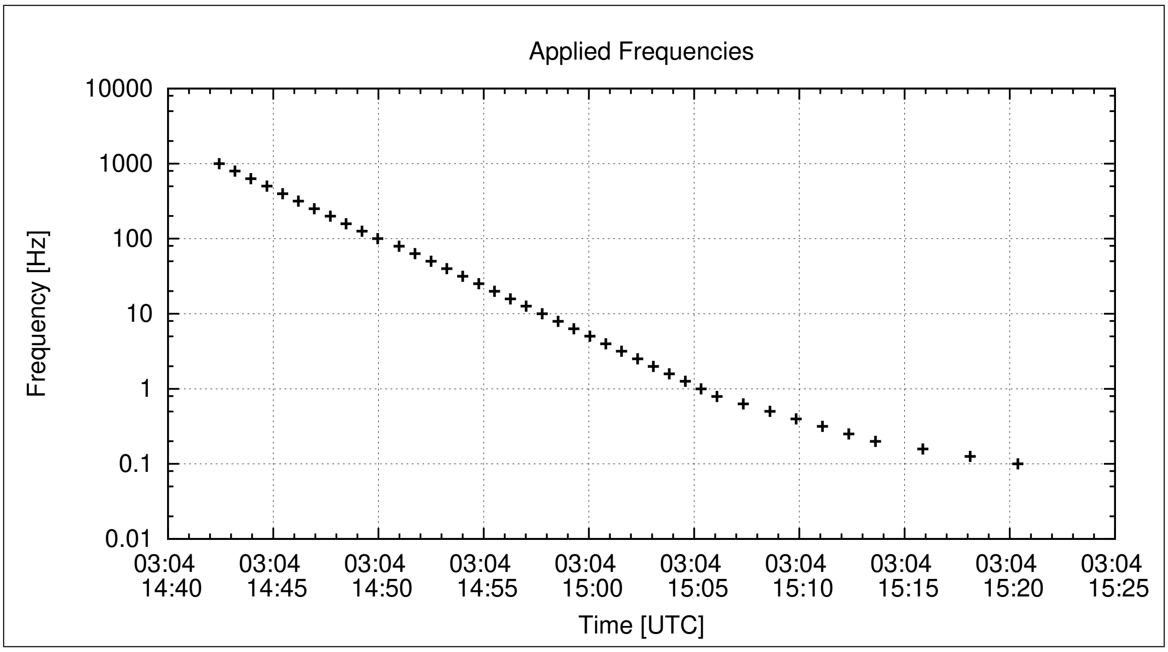

Figure 20: Applied Frequencies for AC Analysis

Applied Frequency [Hz]	Bx [enT]	By [enT]	Bz [enT]
1000.000	1.94	1.77	0.66
794.000	10.33	9.59	4.04
631.000	16.53	15.50	7.29
501.000	24.24	22.84	11.94
398.000	19.51	18.53	10.63
316.000	36.05	34.35	21.58
251.000	46.83	44.84	30.68
199.000	102.85	98.44	73.06
158.000	50.73	48.85	39.72
126.000	65.18	62.56	53.23
100.000	152.32	146.33	131.15
79.400	110.79	106.08	99.16
63.100	430.62	414.14	397.73
50.100	501.72	482.62	472.95
39.800	478.17	461.86	481.30
31.600	363.37	349.57	350.24
25.100	604.13	581.36	585.98
19.900	563.38	542.37	548.66
15.800	624.38	600.89	609.36
12.600	632.59	608.80	618.30
10.000	634.45	610.58	620.71
7.900	636.31	612.41	622.95
6.310	549.54	528.85	538.13
5.010	640.68	616.61	627.58
3.980	640.26	616.19	627.24
3.160	641.32	617.21	628.33
2.510	640.31	616.25	627.39
1.990	616.40	593.22	603.95
1.580	640.80	616.73	627.90
1.260	641.36	617.26	628.44
1.000	613.35	590.29	601.07
0.790	642.64	618.49	629.71
0.631	641.81	617.70	628.91
0.501	641.86	617.75	628.94
0.398	467.42	449.82	457.86
0.316	642.21	618.07	629.29
0.251	489.19	470.72	479.17
0.199	344.90	332.03	338.07
0.158	567.47	545.98	555.76
0.126	549.68	528.87	538.26
0.100	643.28	619.12	630.30

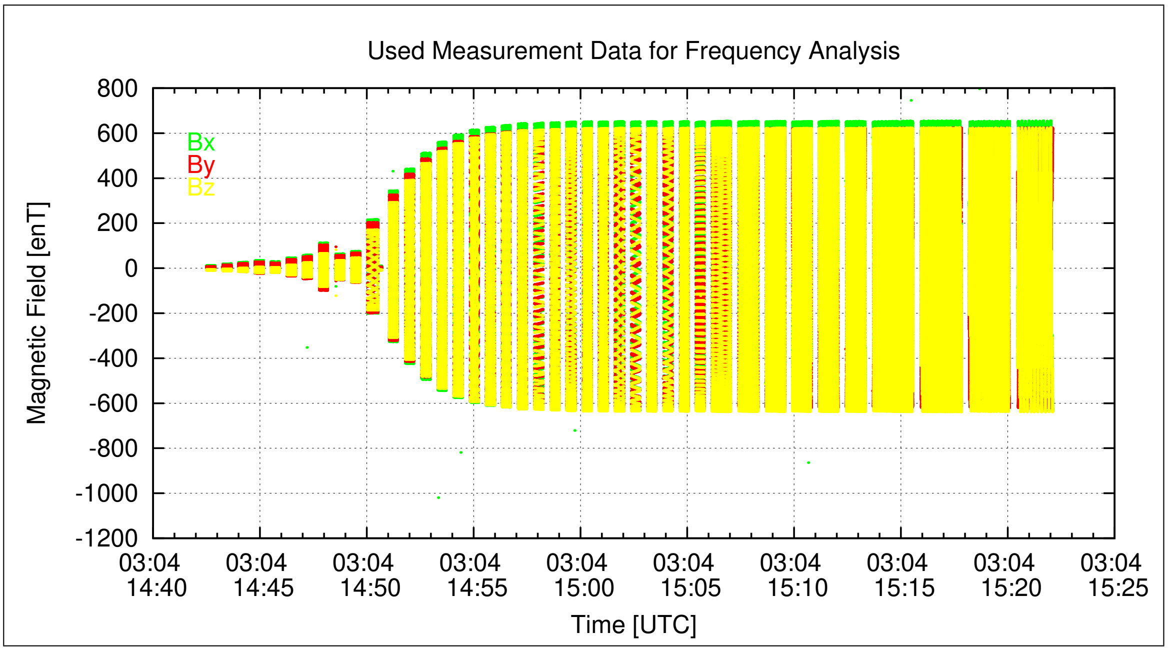

Figure 21: Used packets of Measured data for the Frequency analysis

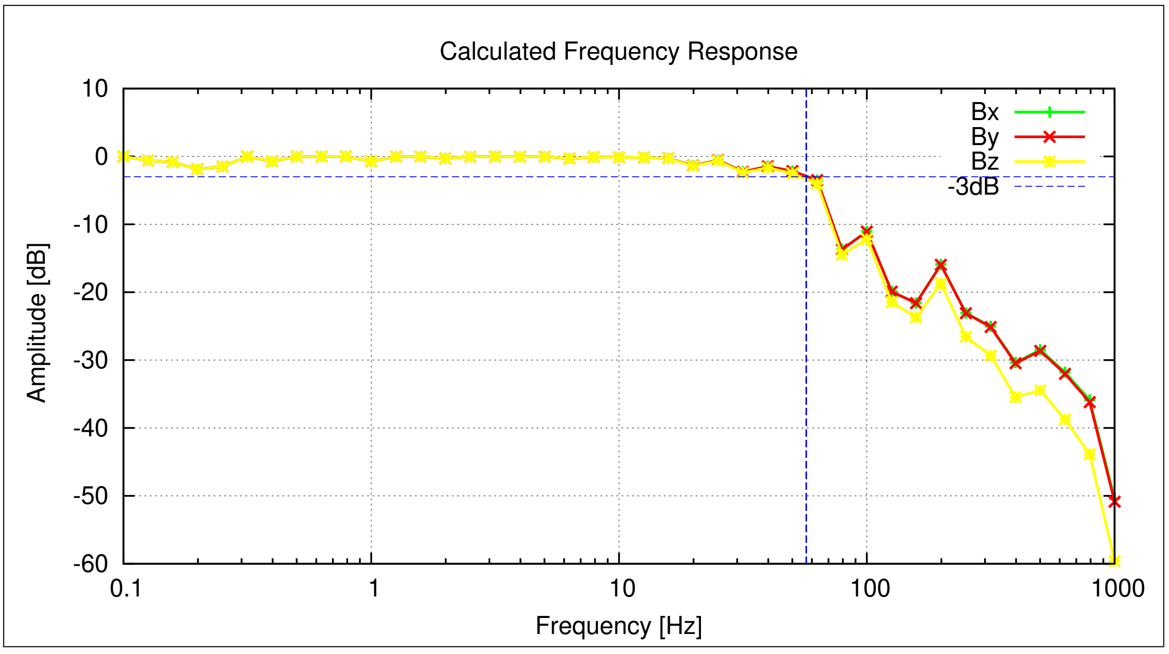

Figure 22: Calculated Frequency Response

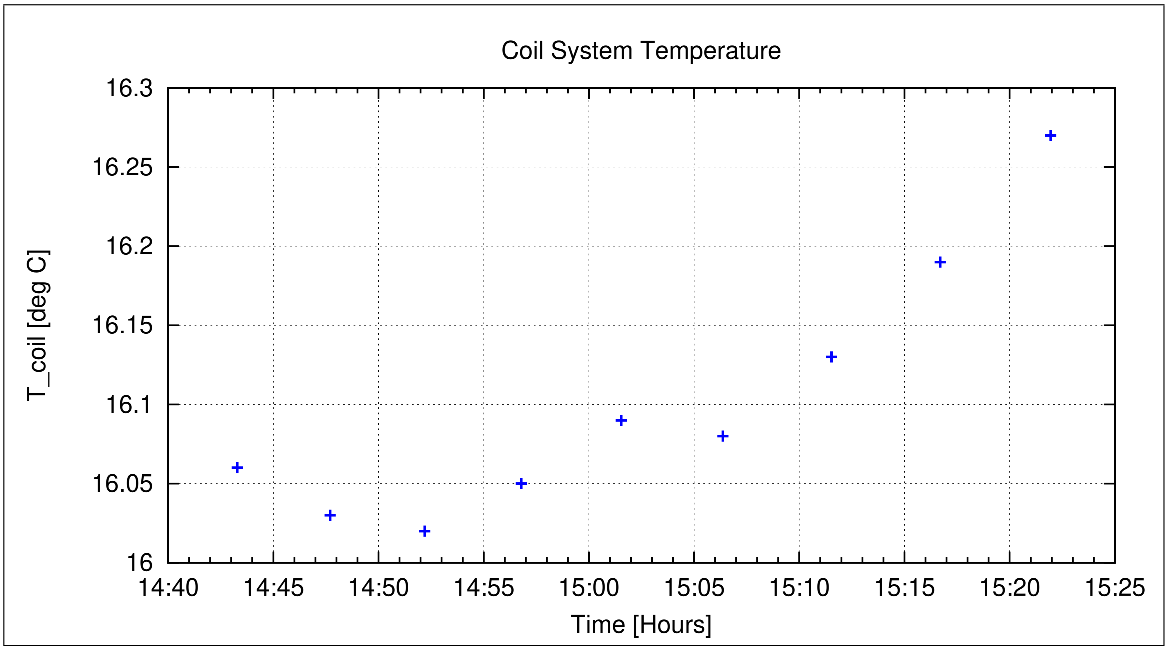

Figure 23: Coil System Temperature

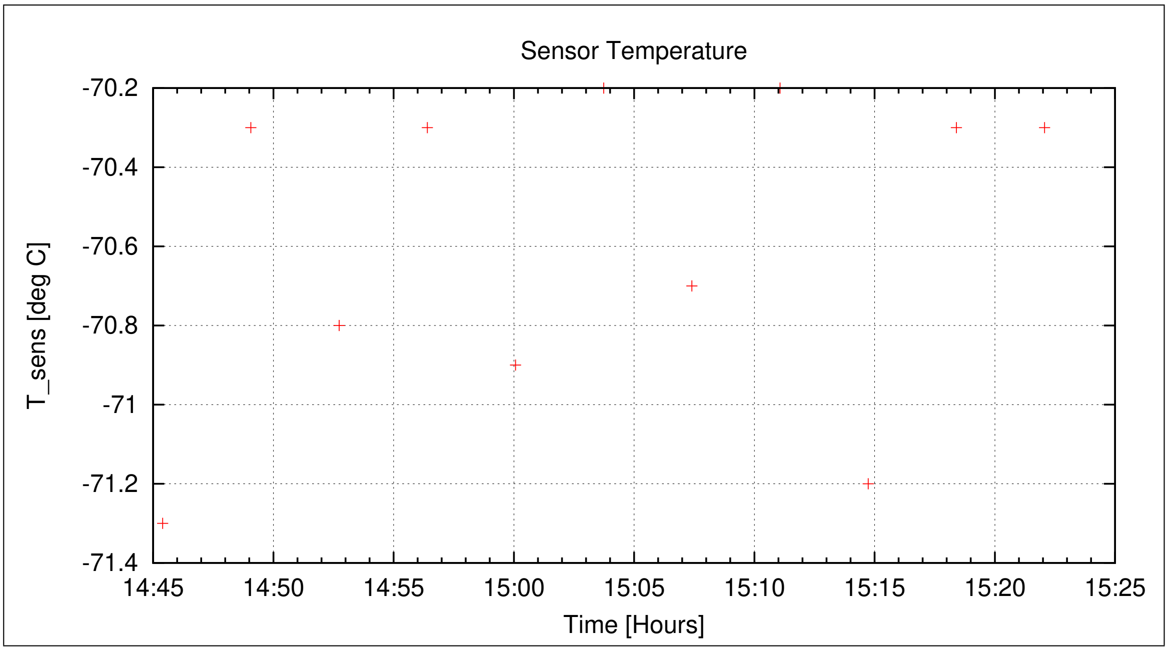

Figure 24: Sensor Temperature

Afterwards the thermal system was switched off for smooth heating up to -20°C.

Zerofield measurements (open loop, cal mode 4) in dynamically compensated earthfield conditions were conducted during the night. Measurements started at 16:08.

4 Measurements on April 4, 2013

The measurements over night were conducted without any problem. At 06:37 the temperature indicated by T_{59} was $-21°$. The MPO-sensor temperatures sensors showed the same temperature.

4.1 Data

CCD File	Configuration File	Remark
13-04-04\06-41-24.CCR	LIN2000XYZE.MAG	
13-04-04\07-18-40.CCR	LIN2000XYZE.MAG	
13-04-04\07-54-10.CCR	OFFSET_200.MAG	
13-04-04\08-08-11.CCR	LIN2000XYZE.MAG	
13-04-04\08-39-48.CCR	OFFSET_200.MAG	
13-04-04\08-50-42.CCR	LIN2000XYZE.MAG	
13-04-04\09-21-00.CCR	LIN2000XYZE.MAG	
13-04-04\09-51-19.CCR	LIN2000XYZE.MAG	
13-04-04\10-21-37.CCR	LIN2000XYZE.MAG	
13-04-04\10-26-52.CCR	OFFSET_200.MAG	
13-04-04\10-51-43.CCR	LIN2000XYZE.MAG	
13-04-04\11-22-26.CCR	OFFSET_200.MAG	
13-04-04\11-33-17.CCR	LIN2000XYZE.MAG	
13-04-04\12-03-52.CCR	LIN2000XYZE.MAG	
13-04-04\12-34-10.CCR	LIN2000XYZE.MAG	
13-04-04\13-05-27.CCR	OFFSET_200.MAG	
13-04-04\13-14-59.CCR	FREQ2000.MAG	
13-04-04\14-11-50.CCR	FREQ2000.MAG	
13-04-04\14-55-20.CCR	LIN2000XYZE.MAG	
13-04-04\15-26-56.CCR	OFFSET_200.MAG	
13-04-04\15-40-25.CCR	NULL_LANG.MAG	

4.2 DC-Analysis at Low Temperature - OB Sensor

Linearity and offset measurements were performed at $T_{59} = -21°C$ in cal mode 4 and cal mode 0.

Thermal Analysis: refer to section 12.

Afterwards the system was heated up to $T_{59} = +30°$.

4.3 DC-Analysis at moderate Temperature - OB Sensor

Linearity and offset measurements were performed at $T_{59} = +30°C$ in cal mode 4 and cal mode 0.

Thermal Analysis: refer to section 12.

Afterwards the system was heated up to $T_{59} = +80°$.

4.4 DC-Analysis at high Temperature - OB Sensor

Linearity and offset measurements were performed at $T_{59} = +80°C$ in cal mode 4 and cal mode 0.
Thermal Analysis: refer to section 12.

4.5 AC-Analysis at high Temperature - OB Sensor

The sensor was rotated to the diagonal in space orientation and the usual AC measurements were conducted at at $T_{59} = +80°C$ in cal mode 4 and cal mode 0.
Thermal Analysis: refer to section 12.

Afterward the sensor was rotated back to the standard orientation (POS1). The thermal system was switched off for smooth cooling during the night. Measurements in dynamically compensated zerofield conditions , starting at 15:40, were conducted during the night and the weekend in cal mode 0.

5 Measurements on April 5, 2013

No personnel around today. Zerofield measurements continued.

5.1 Data

CCD File	Configuration File	Remark
13-04-05\15-40-58.CCR	NULL_LANG.MAG	

6 Measurements on April 6, 2013

No personnel around today. Zerofield measurements continued.

6.1 Data

CCD File	Configuration File	Remark
13-04-06\15-41-30.CCR	NULL_LANG.MAG	

7 Measurements on April 7, 2013

No personnel around today. Zerofield measurements continued.

7.1 Data

CCD File	Configuration File	Remark
13-04-07\15-42-17.CCR	NULL_LANG.MAG	

8 Measurements on April 8, 2013

The zerofield measurements were stopped at 06:20. T_{59} showed 18.1°C. It showed up that MPO stopped sending data on April 7. Reason unknown. After reboot, the instrument worked properly again.

Additionally the Opto-Isolator of the MRode GPIB bus did not work anymore. Therefore, it was decided to couple all GPIB devices directly to the MRode-Controller, although a higher noise level was a expected this way. But there was no change to do it in a different way, as the GPIB Bus is essential for controlling the field generation devices.

During the GPIB analysis the thermal system was already activated. The goal temperature was set to $T_{59} = +130°$.

8.1 Data

CCD File	Configuration File	Remark
13-04-08\06-43-09.CCR	NULL_LANG.MAG	
13-04-08\08-29-20.CCR	LIN2000XYZE.MAG	
13-04-08\08-59-25.CCR	LIN2000XYZE.MAG	
13-04-08\09-30-44.CCR	OFFSET_200.MAG	
13-04-08\09-40-37.CCR	FREQ2000.MAG	
13-04-08\10-31-48.CCR	FREQ2000.MAG	
13-04-08\11-15-40.CCR	LIN2000XYZE.MAG	
13-04-08\11-46-06.CCR	OFFSET_200.MAG	
13-04-08\11-55-12.CCR	LIN2000XYZE.MAG	
13-04-08\12-25-15.CCR	LIN2000XYZE.MAG	
13-04-08\12-55-19.CCR	LIN2000XYZE.MAG	
13-04-08\13-25-22.CCR	LIN2000XYZE.MAG	
13-04-08\13-56-15.CCR	OFFSET_200.MAG	
13-04-08\14-06-16.CCR	FREQ2000.MAG	
13-04-08\15-02-45.CCR	LIN2000XYZE.MAG	
13-04-08\15-06-16.CCR	LIN2000XYZE.MAG	
13-04-08\15-36-36.CCR	OFFSET_200.MAG	
13-04-08\15-46-19.CCR	FREQ2000.MAG	
13-04-08\16-34-53.CCR	NULL.MAG	
13-04-08\22-35-12.CCR	NULL.MAG	

8.2 DC-Analysis at very high Temperature - OB Sensor

Linearity and offset measurements were performed at T_{59} = +130°C in cal mode 4 and cal mode 0 starting at 08:30.

Thermal Analysis: refer to section 12.

8.3 AC-Analysis at very high Temperature - OB Sensor

The sensor was rotated to the diagonal in space orientation and the usual AC measurements were conducted at T_{59} = +130°C in cal mode 4 and cal mode 0.

Thermal Analysis: refer to section 12.

Afterwards the thermal box was heated up to the final temperature of +180°C.

8.4 DC-Analysis at highest Temperature - OB Sensor

Linearity and offset measurements were performed at T_{59} = +180°C in cal mode 4 and cal mode 0 starting at 08:30.

Thermal Analysis: refer to section 12.

8.5 AC-Analysis at highest Temperature - OB Sensor

The sensor was rotated to the diagonal in space orientation and the usual AC measurements were conducted at at T_{59} = +180°C in cal mode 4 and cal mode 0.

Thermal Analysis: refer to section 12.

Afterwards the thermal system was switched off to let the temperature fall smoothly. Over night zerofield measurements in dynamically compensated earthfield conditions were conducted in cal mode 0. The measurements started at 16:34. Sensor alignment: Standard, Azimuth =180°, Elevation=0°.

9 Measurements on April 9, 2013

The measurements overnight were conducted smoothly. At 06:32 the box temperature was about $T_{59} = +71°C$.

The box was opened and the OB sensor was removed.

The BS_11 = OB calibration finished at 06:45.

9.1 Data

CCD File	Configuration File	Remark
13-04-09\04-35-30.CCR	NULL.MAG	
13-04-09\06-32-42.CCR	NULL.MAG	
		Change to IB Sensor
13-04-09\07-22-11.CCR	LIN2000XYZE.MAG	
13-04-09\07-52-14.CCR	LIN2000XYZE.MAG	
13-04-09\08-22-17.CCR	LIN2000XYZE.MAG	
13-04-09\08-52-20.CCR	LIN2000XYZE.MAG	
13-04-09\09-22-23.CCR	LIN2000XYZE.MAG	
13-04-09\09-52-27.CCR	LIN2000XYZE.MAG	
13-04-09\10-23-29.CCR	OFFSET_200.MAG	
13-04-09\10-34-40.CCR	LIN2000XYZE.MAG	
13-04-09\11-05-13.CCR	OFFSET_200.MAG	
13-04-09\11-14-46.CCR	OFFSET_200.MAG	
13-04-09\11-24-12.CCR	LIN2000XYZE.MAG	
13-04-09\11-54-15.CCR	LIN2000XYZE.MAG	
13-04-09\12-26-36.CCR	FREQ2000.MAG	
13-04-09\13-08-27.CCR	OFFSET_200.MAG	
13-04-09\13-18-15.CCR	OFFSET_200.MAG	
13-04-09\13-27-51.CCR	FREQ2000.MAG	
13-04-09\14-12-36.CCR	LIN2000XYZE.MAG	
13-04-09\14-53-47.CCR	NULL.MAG	
13-04-09\20-54-03.CCR	NULL.MAG	

The IB sensor BS_10 was installed in the thermal box. The box was erected to the vertical orientation and shifted to CoC.

Cooling of the system down to −20°C started at 07:22.

9.2 DC-Analysis at Low Temperature - IB Sensor, cal mode 0

Linearity and offset measurements were performed at $T_{59} = -20°C$ in cal mode 0.

9.2.1 Calibration on 3 Linear Axes

Used Files:

CCD File	Configuration File	Remark
13-04-09\09-52-27.CCR	LIN2000XYZE.MAG	

Parameter File: `PARAMETER_LIN__13-04-09_09-52-27.CPF`

Facility Parameter:

Nominal Sensor Setup $\underline{B}_{\mathrm{DUT}} = \underline{\underline{R}}_{\mathrm{nom}} \underline{B}_{\mathrm{C}}$

$$\underline{\underline{R}}_{\mathrm{nom}} = \begin{pmatrix} +1.000000 & +0.000000 & +0.000000 \\ +0.000000 & +1.000000 & +0.000000 \\ +0.000000 & +0.000000 & +1.000000 \end{pmatrix}$$

Calculated Sensor Rotation:

$$\underline{\underline{\rho}} = \begin{pmatrix} +0.999974 & +0.003127 & +0.006434 \\ -0.003132 & +0.999995 & +0.000706 \\ -0.006432 & -0.000726 & +0.999979 \end{pmatrix}$$

Rotation Angles:

$$\begin{aligned} \text{Angle } (X_c, X_m): &\quad \lambda_{\mathrm{x}} = && +0^\circ\ 24'36'' \\ \text{Angle } (Y_c, Y_m): &\quad \mu_{\mathrm{y}} = && +0^\circ\ 11'2'' \\ \text{Angle } (Z_c, Z_m): &\quad \nu_{\mathrm{z}} = && +0^\circ\ 22'15'' \end{aligned}$$

Determinant of Rotation Matrix: 1.00000
Nominal Field Source: SOLARTRON
Fields applied for 24.0 s
Mean Sensor Temperature: -30.6°C
Automatic Coil Correction: used

Earthfield Compensation:	X	=	DYNAMIC
	Y	=	DYNAMIC
	Z	=	DYNAMIC

Offset Treatment:

A polynomial offset trend of order 2 has been fitted and subtracted from the raw data before creating the sensor model.

Mean Coil System Residual + Sensor Offset: $\underline{B}^{or}$ = (-3.954 , -0.950 , -11.069) nT

Raw Data Quality:

Standard Deviation of used Raw Data Blocks:

[Values in eng nT]	s_x	s_y	s_z
Minimum	0.000	0.376	0.242
Mean	2.315	0.449	0.452
Maximum	2.860	1.274	1.210

Calibration Parameter:

$$\text{Transfermatrix:}\quad \underline{\underline{\phi}} = \underline{\underline{R}}_{\text{nom}}\,\underline{\underline{\rho}}\,\underline{\underline{\omega}}\,\underline{\underline{\sigma}} = \begin{pmatrix} +0.976259 & +0.003130 & +0.006347 \\ -0.010380 & +0.988528 & +0.000696 \\ -0.007349 & +0.005271 & +0.986472 \end{pmatrix}$$

$$\text{Reduced Transfermatrix:}\quad \underline{\underline{\tilde{\phi}}} = \underline{\underline{\omega}}\,\underline{\underline{\sigma}} = \begin{pmatrix} +0.976314 & +0.000000 & +0.000000 \\ -0.007321 & +0.988529 & +0.000000 \\ -0.001075 & +0.005989 & +0.986493 \end{pmatrix}$$

$$\text{Sensitivity:}\quad \underline{\underline{\sigma}} = \begin{pmatrix} +0.976314 & +0.000000 & +0.000000 \\ +0.000000 & +0.988501 & +0.000000 \\ +0.000000 & +0.000000 & +0.986474 \end{pmatrix}$$

$$\text{Misalignment:}\quad \underline{\underline{\omega}} = \begin{pmatrix} +1.000000 & +0.000000 & +0.000000 \\ -0.007499 & +1.000028 & +0.000000 \\ -0.001101 & +0.006058 & +1.000019 \end{pmatrix}$$

Sensor Misalignment Angles:

$$\xi_{\text{x,y}} = +89^\circ\ 34'13''$$
$$\xi_{\text{x,z}} = +89^\circ\ 56'22''$$
$$\xi_{\text{y,z}} = +90^\circ\ 20'48''$$

Model Quality:

Standard Deviation, Maximum and Minimum Error of Calculated Model:

[Values in nT]	X	Y	Z
Standard Deviation	0.130	0.170	0.163
Maximum Error	0.280	0.460	0.445
Minimum Error	-0.225	-0.244	-0.287

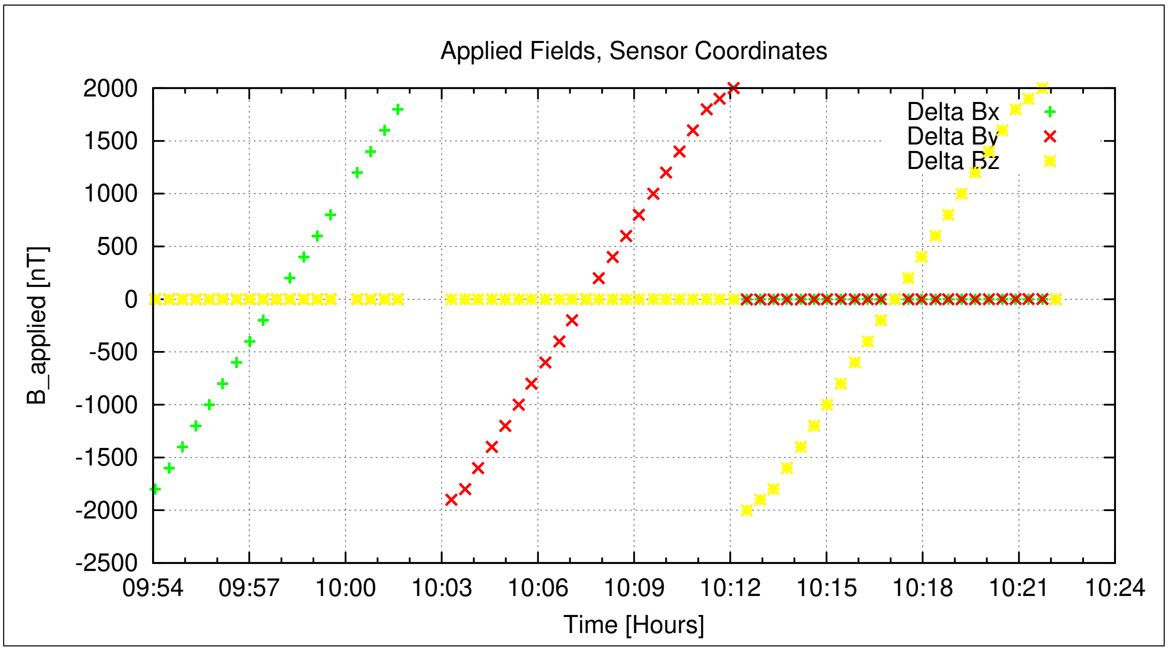

Figure 25: Applied Fields

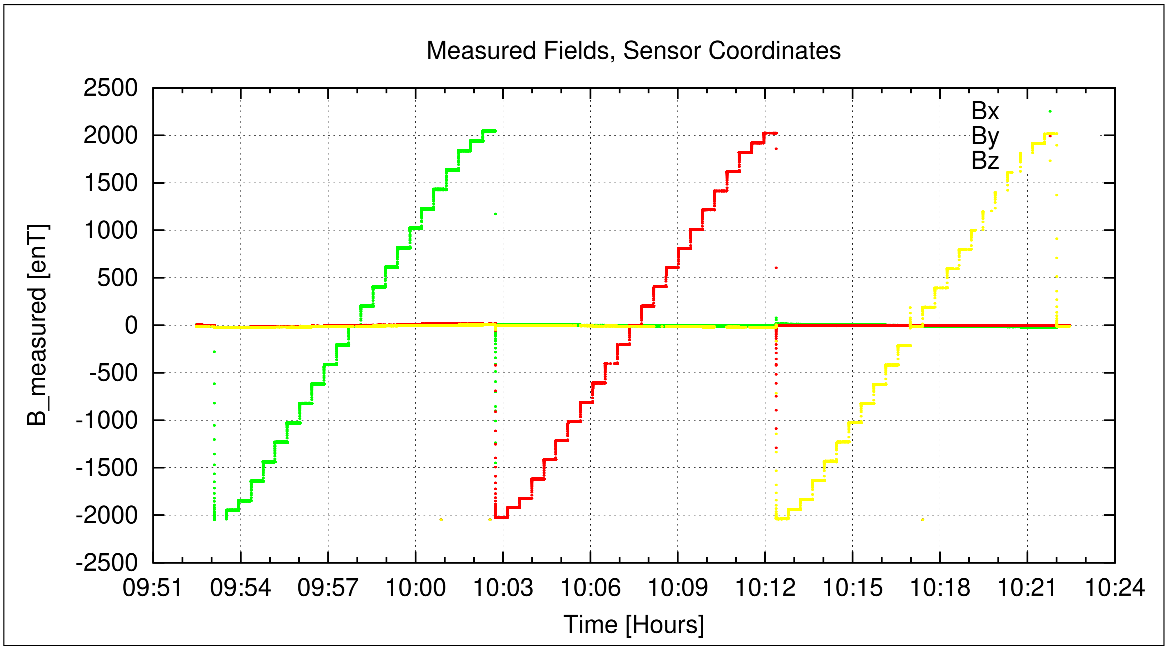

Figure 26: Measured Data

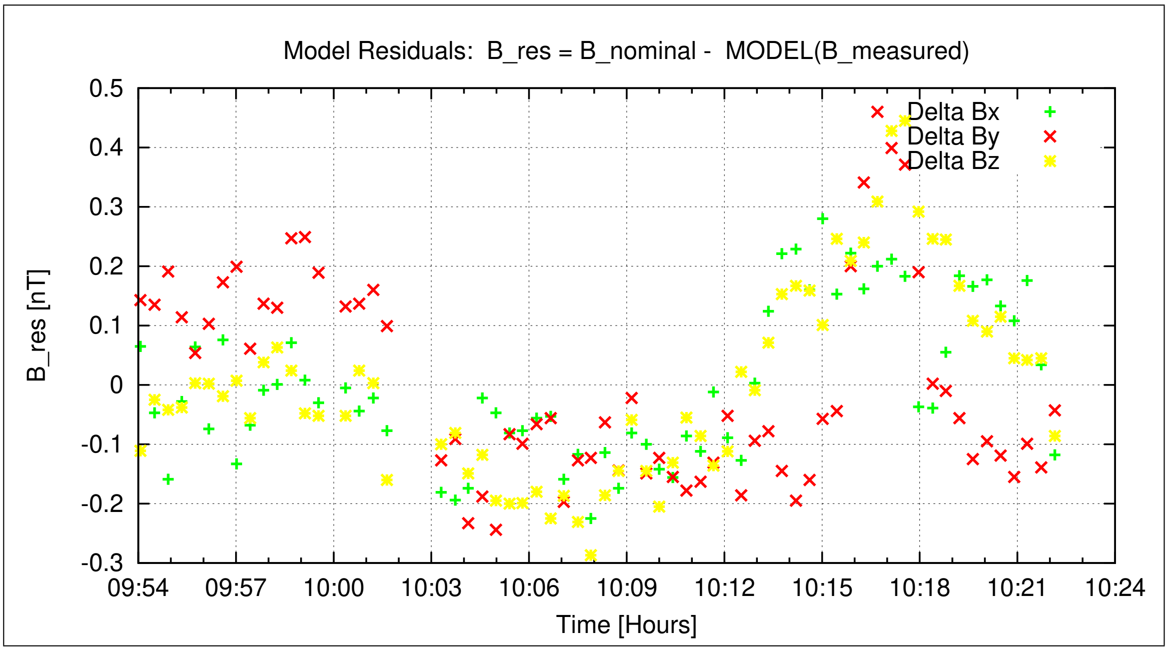

Figure 27: Model Quality - Differences of applied field and modelled measurement data

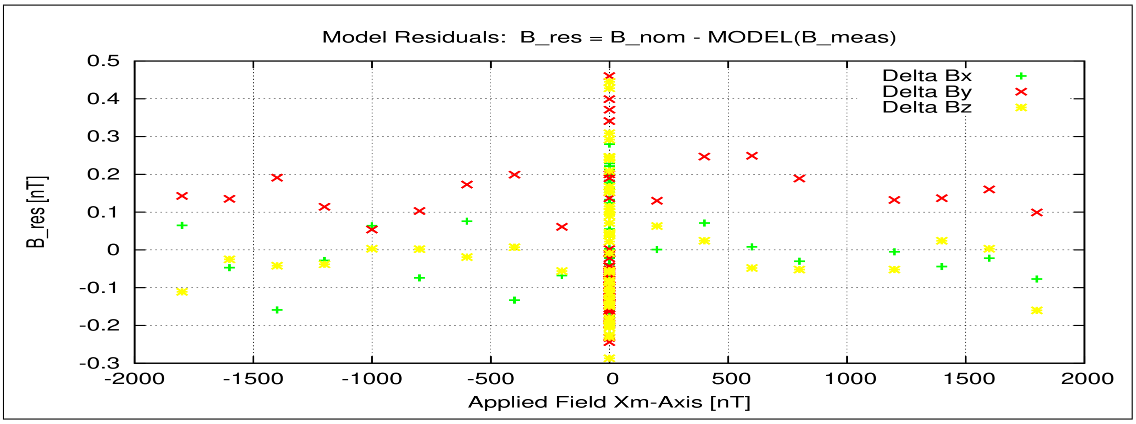

Figure 28: RESIDUALS vs FLD X

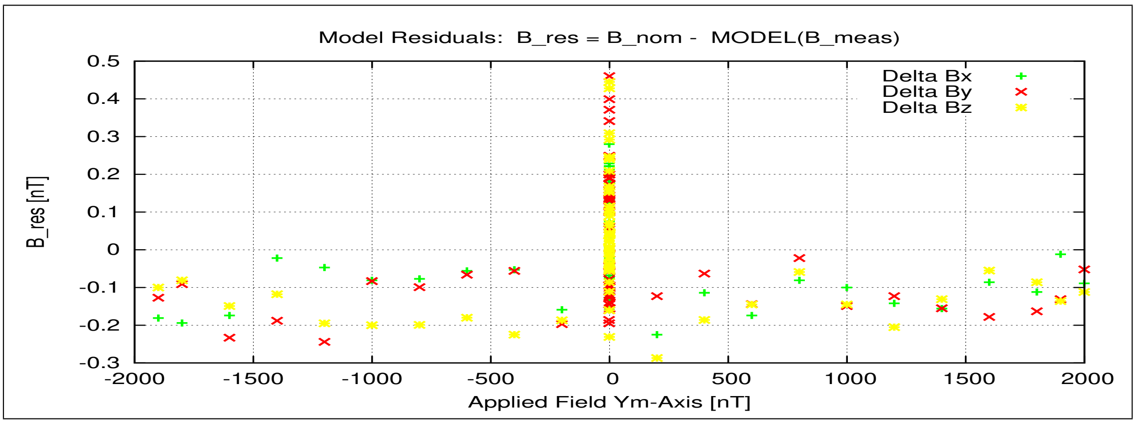

Figure 29: RESIDUALS vs FLD Y

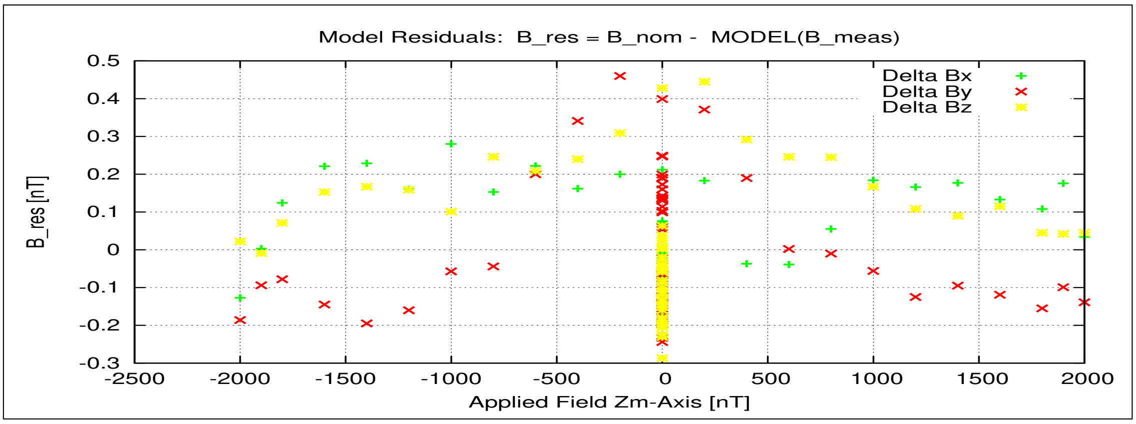

Figure 30: RESIDUALS vs FLD Z

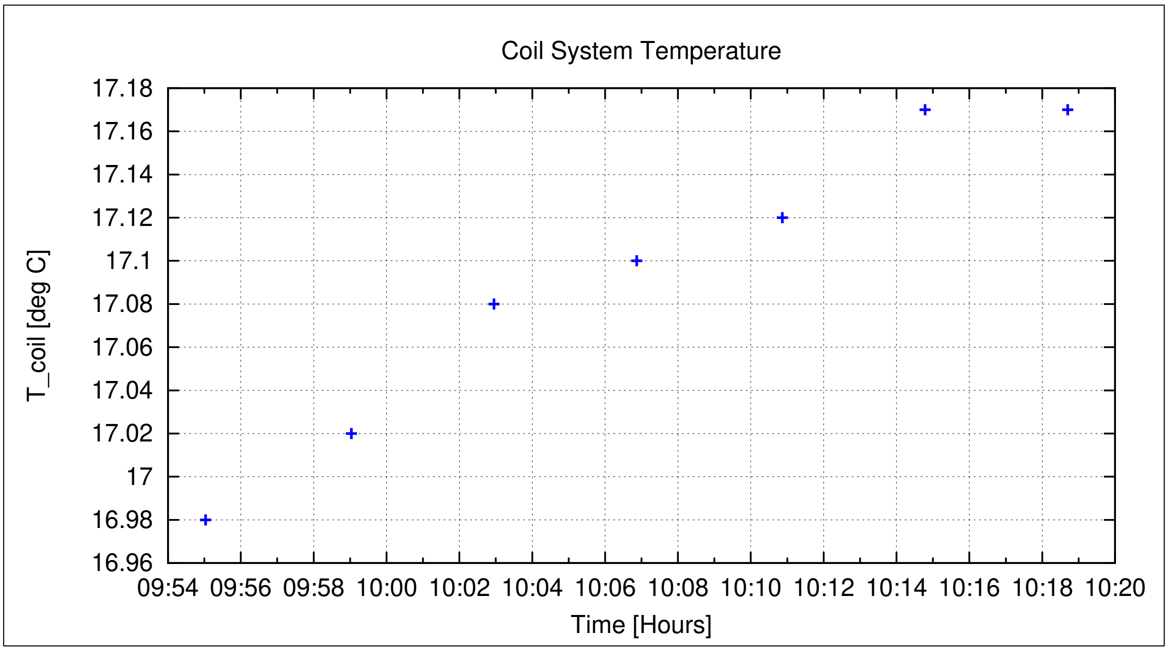

Figure 31: Coil System Temperature

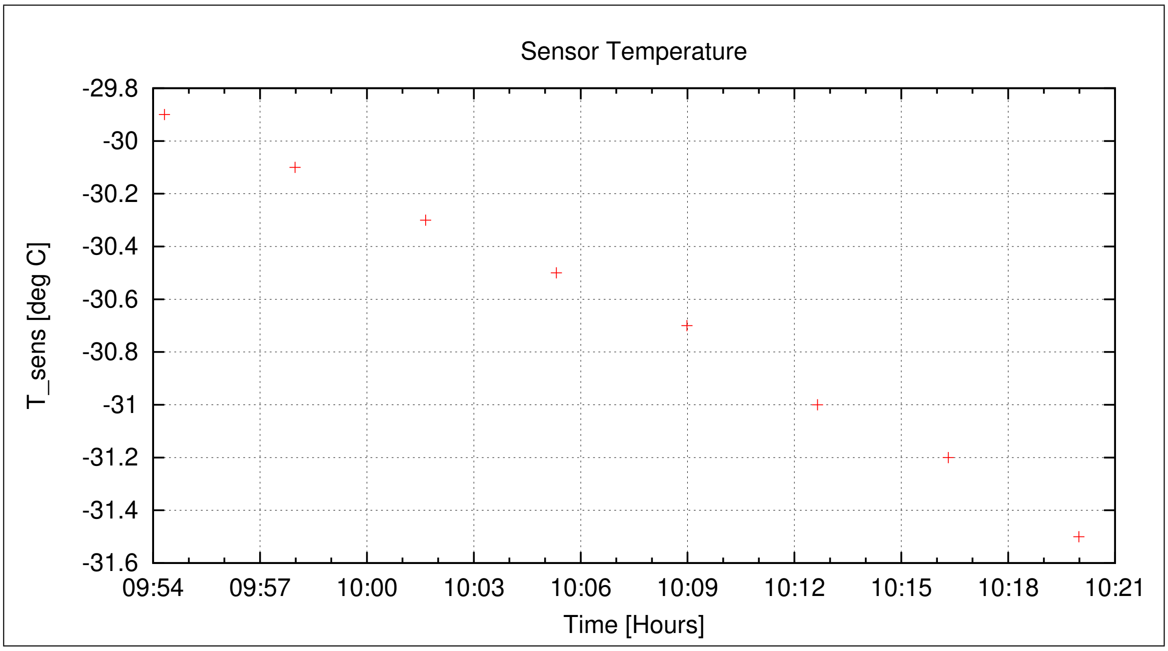

Figure 32: Sensor Temperature

9.2.2 OFFSET Calculation

In this section the instrument offsets and the residual field of the Coil System will be evaluated. Measurements at two orientations for each component act as input for the offset calculation. From the "normal" (0-degrees) and "turned" (180-degrees) orientations the offsets and residual fields can be derived:

$$B_{\mathrm{off}} = \frac{B_{\mathrm{normal}} + B_{\mathrm{turned}}}{2}$$
$$B_{\mathrm{res}} = \frac{B_{\mathrm{normal}} - B_{\mathrm{turned}}}{2}$$

Used Offset Measurements:

CCD File	Configuration File	Remark
13-04-09\11-14-46.CCR	OFFSET_200.MAG	

Parameter File: OFF_PARAMETER__13-04-09-11-14-46.OPF

Calibration Parameter:

Sensor Offsets:

Component	Offset [enT]	Standard deviation [enT]
X	-0.64	0.111
Y	-0.78	0.104
Z	-0.38	0.100

Residual Field of the Coil System:

Component	B_{res} [enT]
X	-2.07
Y	-0.46
Z	2.01

Remark: Residual field is given in actual DUT coordinates, not in coil-coordinates!

Thermal Analysis: refer to section 13.

9.3 DC-Analysis at Low Temperature - IB Sensor, cal mode 4

Linearity and offset measurements were performed at $T_{59} = -20°C$ in cal mode 4.

9.3.1 Calibration on 3 Linear Axes

Used Files:

CCD File	Configuration File	Remark
13-04-09\10-34-40.CCR	LIN2000XYZE.MAG	

Parameter File: PARAMETER_LIN__13-04-09_10-34-40.CPF

Facility Parameter:

Nominal Sensor Setup $\underline{B}_{\mathrm{DUT}} = \underline{\underline{R}}_{\mathrm{nom}} \underline{B}_{\mathrm{C}}$

$$\underline{\underline{R}}_{\mathrm{nom}} = \begin{pmatrix} +1.000000 & +0.000000 & +0.000000 \\ +0.000000 & +1.000000 & +0.000000 \\ +0.000000 & +0.000000 & +1.000000 \end{pmatrix}$$

Calculated Sensor Rotation:

$$\underline{\underline{\rho}} = \begin{pmatrix} +0.999707 & +0.023539 & +0.005617 \\ -0.023561 & +0.999715 & +0.003876 \\ -0.005524 & -0.004007 & +0.999977 \end{pmatrix}$$

Rotation Angles:

$$\begin{aligned} \text{Angle } (X_c, X_m): \quad & \lambda_{\mathrm{x}} = +1^\circ\ 23'12'' \\ \text{Angle } (Y_c, Y_m): \quad & \mu_{\mathrm{y}} = +1^\circ\ 22'6'' \\ \text{Angle } (Z_c, Z_m): \quad & \nu_{\mathrm{z}} = +0^\circ\ 23'28'' \end{aligned}$$

Determinant of Rotation Matrix: 1.00000
Nominal Field Source: FLDS
Fields applied for 25.0 s
Mean Sensor Temperature: -32.9°C
Automatic Coil Correction: used

Earthfield Compensation: X = DYNAMIC
Y = DYNAMIC
Z = DYNAMIC

Offset Treatment:

A polynomial offset trend of order 2 has been fitted and subtracted from the raw data before creating the sensor model.

Mean Coil System Residual + Sensor Offset: $\underline{B}^{or}$ = (-2.786 , -1.095 , -10.723) nT

Raw Data Quality:

Standard Deviation of used Raw Data Blocks:

[Values in eng nT]	s_x	s_y	s_z
Minimum	1.638	0.191	0.000
Mean	2.299	0.391	0.478
Maximum	2.952	2.520	1.822

Calibration Parameter:

$$\text{Transfermatrix:} \quad \underline{\underline{\phi}} = \underline{\underline{R}}_{\text{nom}}\, \underline{\underline{\rho}}\, \underline{\underline{\omega}}\, \underline{\underline{\sigma}} \quad = \begin{pmatrix} +0.976121 & +0.023140 & +0.005394 \\ -0.020240 & +0.980345 & +0.003723 \\ -0.013290 & +0.006444 & +0.960428 \end{pmatrix}$$

$$\text{Reduced Transfermatrix:} \quad \underline{\underline{\tilde{\phi}}} = \underline{\underline{\omega}}\, \underline{\underline{\sigma}} \quad = \begin{pmatrix} +0.976385 & +0.000000 & +0.000000 \\ +0.002795 & +0.980584 & +0.000000 \\ -0.007885 & +0.010374 & +0.960450 \end{pmatrix}$$

$$\text{Sensitivity:} \quad \underline{\underline{\sigma}} \quad = \begin{pmatrix} +0.976385 & +0.000000 & +0.000000 \\ +0.000000 & +0.980580 & +0.000000 \\ +0.000000 & +0.000000 & +0.960365 \end{pmatrix}$$

$$\text{Misalignment:} \quad \underline{\underline{\omega}} \quad = \begin{pmatrix} +1.000000 & +0.000000 & +0.000000 \\ +0.002863 & +1.000004 & +0.000000 \\ -0.008076 & +0.010579 & +1.000089 \end{pmatrix}$$

Sensor Misalignment Angles:

$$\begin{aligned} \xi_{\text{x,y}} &= +90^\circ\ 9'51'' \\ \xi_{\text{x,z}} &= +89^\circ\ 32'8'' \\ \xi_{\text{y,z}} &= +90^\circ\ 36'27'' \end{aligned}$$

Model Quality:

Standard Deviation, Maximum and Minimum Error of Calculated Model:

[Values in nT]	X	Y	Z
Standard Deviation	0.124	0.222	0.129
Maximum Error	0.325	0.249	0.309
Minimum Error	-0.320	-0.800	-0.357

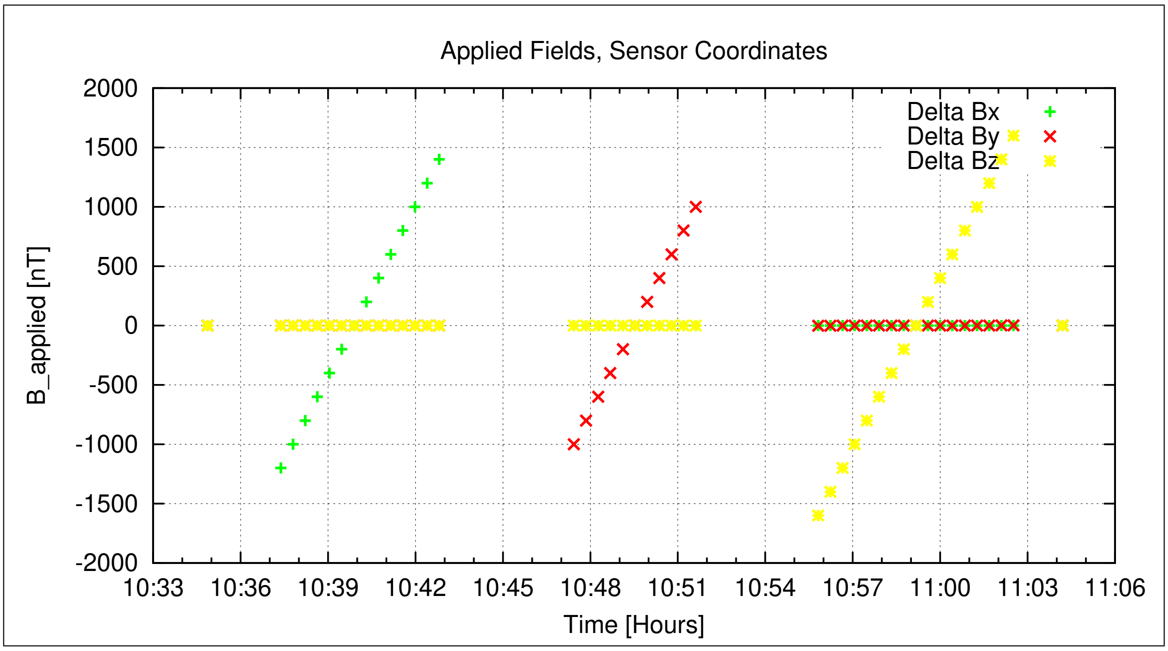

Figure 33: Applied Fields

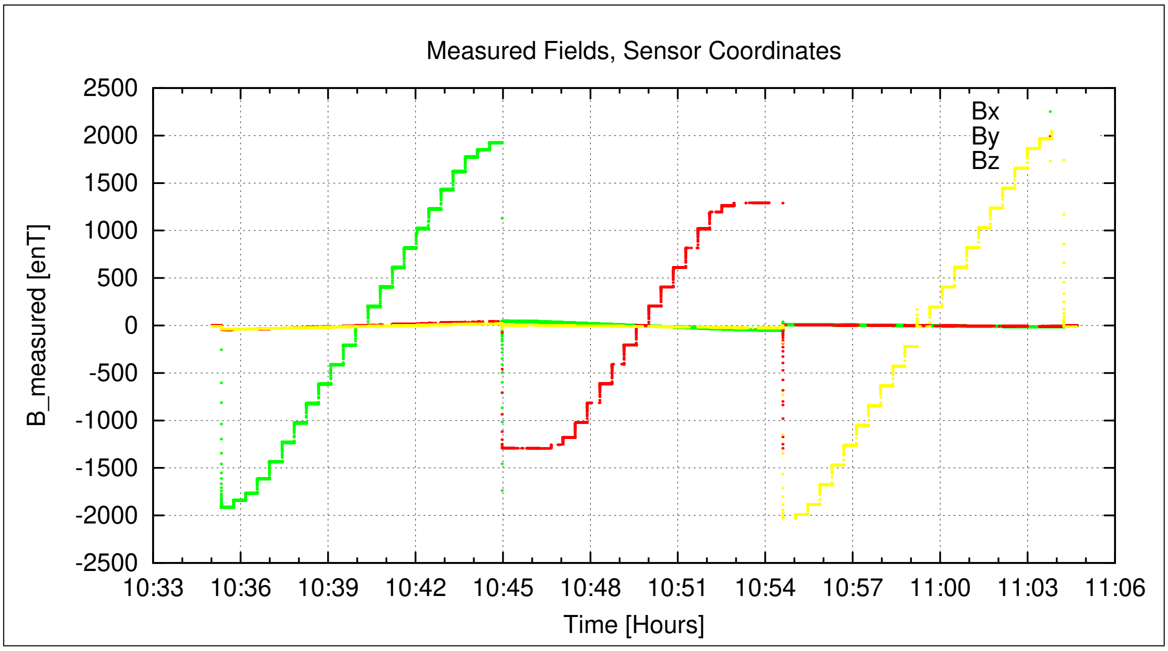

Figure 34: Measured Data

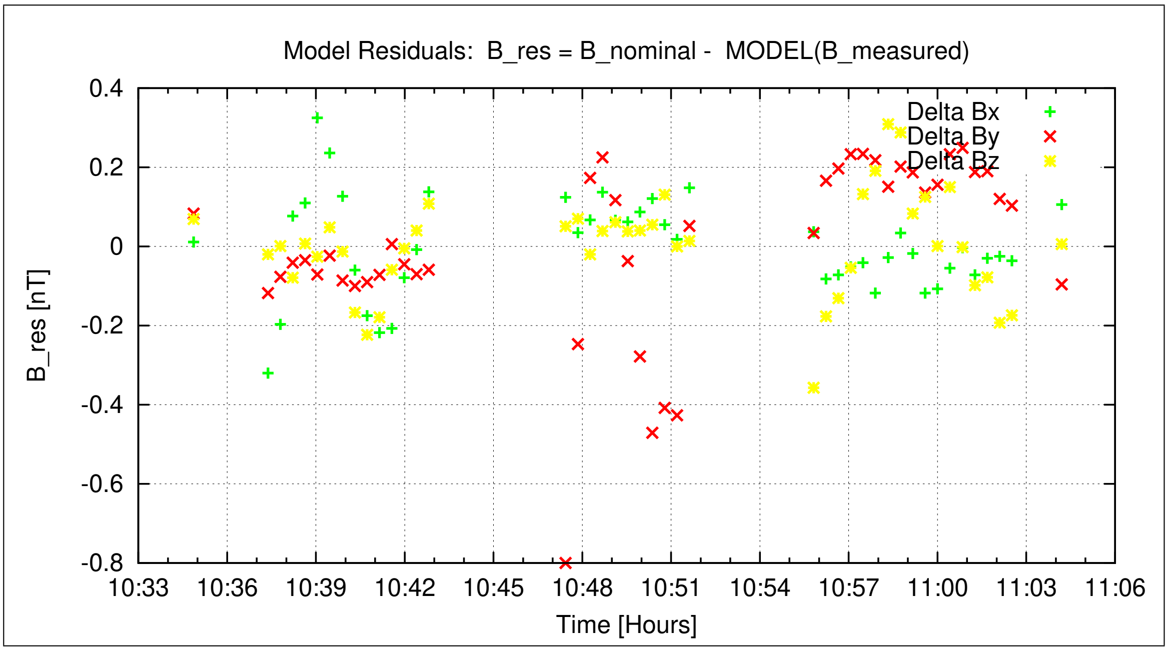

Figure 35: Model Quality - Differences of applied field and modelled measurement data

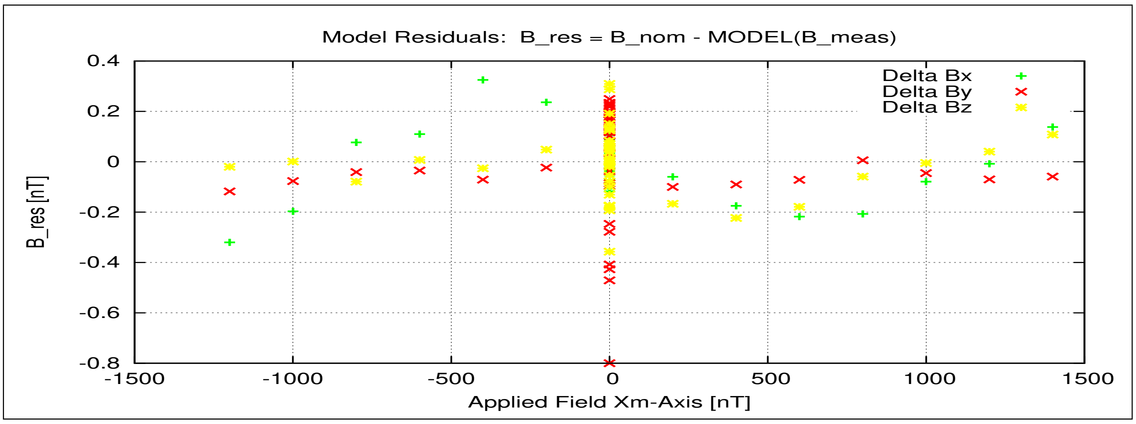

Figure 36: RESIDUALS vs FLD X

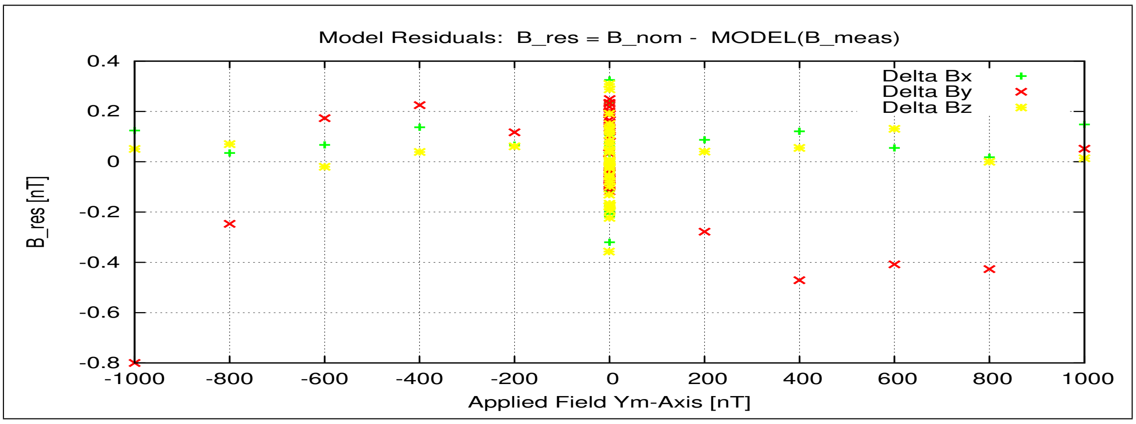

Figure 37: RESIDUALS vs FLD Y

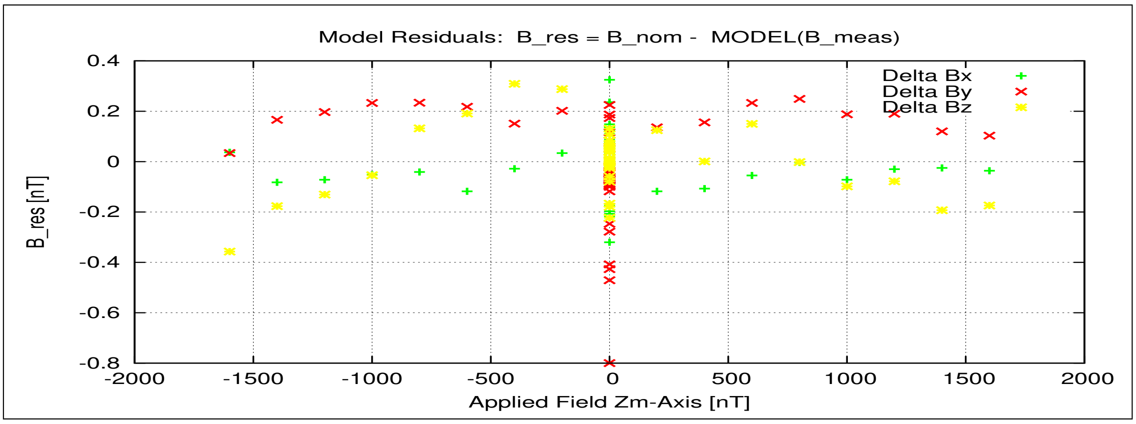

Figure 38: RESIDUALS vs FLD Z

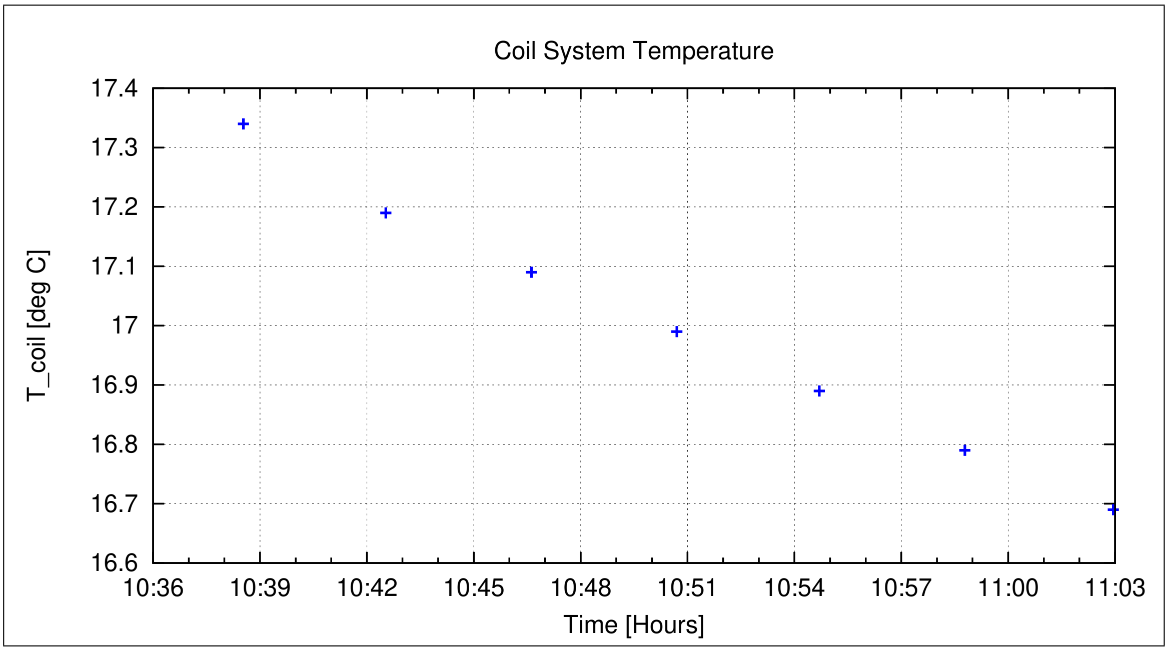

Figure 39: Coil System Temperature

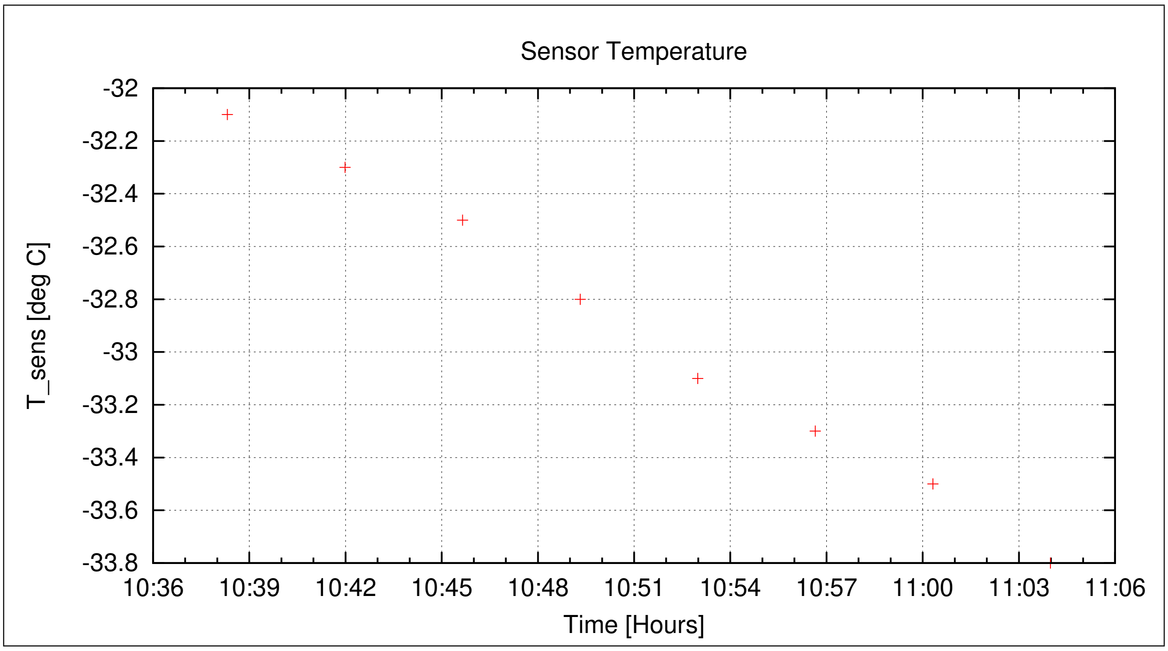

Figure 40: Sensor Temperature

9.3.2 OFFSET Calculation

In this section the instrument offsets and the residual field of the Coil System will be evaluated. Measurements at two orientations for each component act as input for the offset calculation. From the "normal" (0-degrees) and "turned" (180-degrees) orientations the offsets and residual fields can be derived:

$$B_{\mathrm{off}} = \frac{B_{\mathrm{normal}} + B_{\mathrm{turned}}}{2}$$

$$B_{\mathrm{res}} = \frac{B_{\mathrm{normal}} - B_{\mathrm{turned}}}{2}$$

Used Offset Measurements:

CCD File	Configuration File	Remark
13-04-09\11-05-13.CCR	OFFSET_200.MAG	

Parameter File: OFF_PARAMETER__13-04-09-11-05-13.OPF

Calibration Parameter:

Sensor Offsets:

Component	Offset [enT]	Standard deviation [enT]
X	-0.70	0.088
Y	-0.79	0.101
Z	-0.29	0.097

Residual Field of the Coil System:

Component	B_{res} [enT]
X	-2.06
Y	-0.60
Z	2.09

Remark: Residual field is given in actual DUT coordinates, not in coil-coordinates!

Thermal Analysis: refer to section 13.

Afterwards the system was cooled down up to $T_{59} = -70°$.

9.4 DC-Analysis at very low Temperature - IB Sensor

Linearity and offset measurements were performed at $T_{59} = -70°C$ in cal mode 4 and cal mode 0.

Thermal Analysis: refer to section 13.

9.5 AC-Analysis at very low Temperature - IB Sensor, cal mode 0

A frequency measurement was performed at -70°C.

Setup:

- Sensor mounted in thermal box. CoC. Box vertical.
- Sensor rotated to:
  Elevation= 45°
  Azimuth= 126°
- Field applied on Y_c.
- No attenuator

9.5.1 Frequency Measurements

This section is dedicated to the frequency behavior of the instrument. The analysis of the performed AC measurements allows to calculate the actual sampling frequency f_s of the instrument and the frequency response (amplitude vs. frequency). The measurements have been performed with the sensor placed at CoC in a diagonal in space orientation. The AC-fields have been applied on the Y_c axis only. Using this setup it can be guaranteed that only one frequency is applied at a time and no beat effects occur.

Used Frequency Measurements:

CCD File	Configuration File	Remark
`13-04-09\12-26-36.CCR`	`FREQ2000.MAG`	

Parameter File: `FREQ_PARAMETER__13-04-09-12-26-36.FPF`

Calibration Parameter:

Sampling Frequency:

Component	f_s [Hz]	Standard deviation [Hz]
X	127.9995	0.000100
Y	127.9979	0.000104
Z	127.9998	0.000768
Mean Sampling Frequency	127.9991	0.001029

3 dB Corner Frequency:

Component	f_{3dB} [Hz]
X	66.93
Y	65.62
Z	55.63

Applied Frequencies and Measured Amplitudes

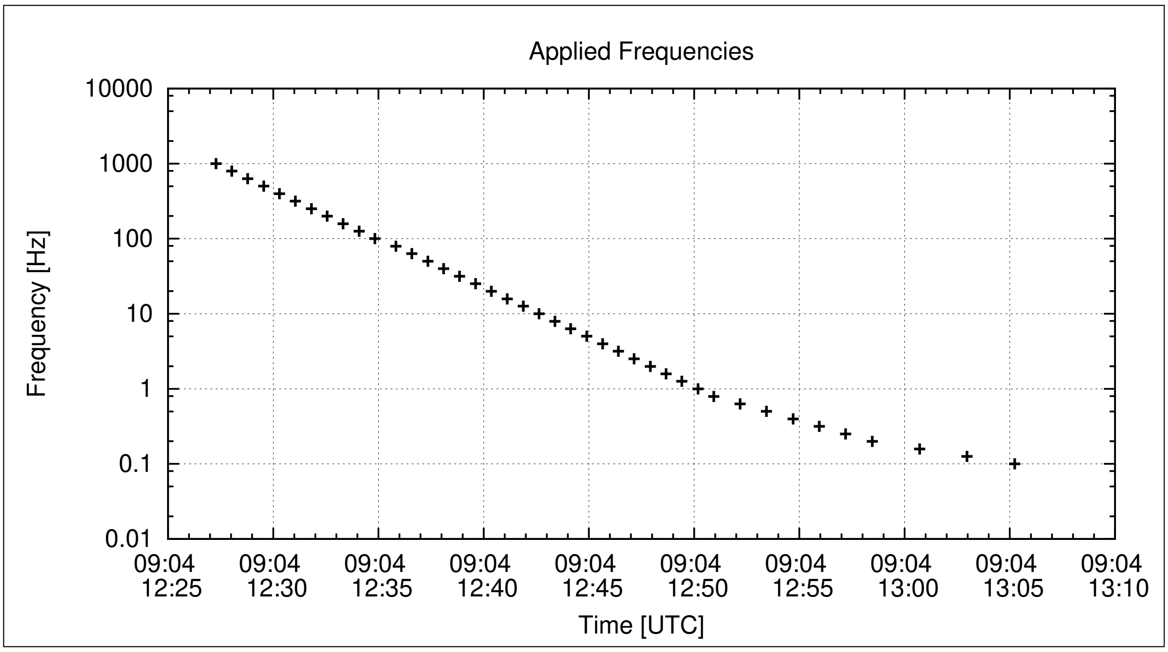

Figure 41: Applied Frequencies for AC Analysis

Applied Frequency [Hz]	Bx [enT]	By [enT]	Bz [enT]
1000.000	1.75	1.73	0.65
794.000	9.77	9.75	3.94
631.000	14.97	15.01	6.11
501.000	22.69	22.82	11.39
398.000	18.64	18.76	10.21
316.000	38.87	37.93	20.91
251.000	45.98	46.00	29.75
199.000	111.79	108.81	71.31
158.000	56.12	55.59	42.55
126.000	61.36	61.02	48.96
100.000	160.41	158.02	137.96
79.400	359.88	349.71	294.00
63.100	469.32	453.74	380.80
50.100	546.55	529.59	464.21
39.800	592.13	578.12	533.62
31.600	613.77	603.51	578.31
25.100	623.00	615.22	600.10
19.900	622.22	615.62	602.77
15.800	619.18	613.02	598.53
12.600	612.13	604.57	589.20
10.000	611.92	605.81	586.46
7.900	606.86	600.69	579.65
6.310	607.76	601.50	579.19
5.010	603.74	597.45	574.43
3.980	606.09	599.75	576.08
3.160	601.83	595.50	571.64
2.510	606.75	600.34	576.06
1.990	605.51	599.12	574.73
1.580	605.52	599.09	574.61
1.260	605.68	599.24	574.69
1.000	607.14	600.70	576.05
0.790	605.42	598.98	574.38
0.631	605.63	599.21	574.58
0.501	604.94	598.52	573.91
0.398	606.96	600.54	575.84
0.316	602.16	595.79	571.27
0.251	608.72	602.26	577.45
0.199	608.18	601.74	576.95
0.158	609.52	603.10	578.20
0.126	606.59	600.19	575.44
0.100	606.65	600.26	575.47

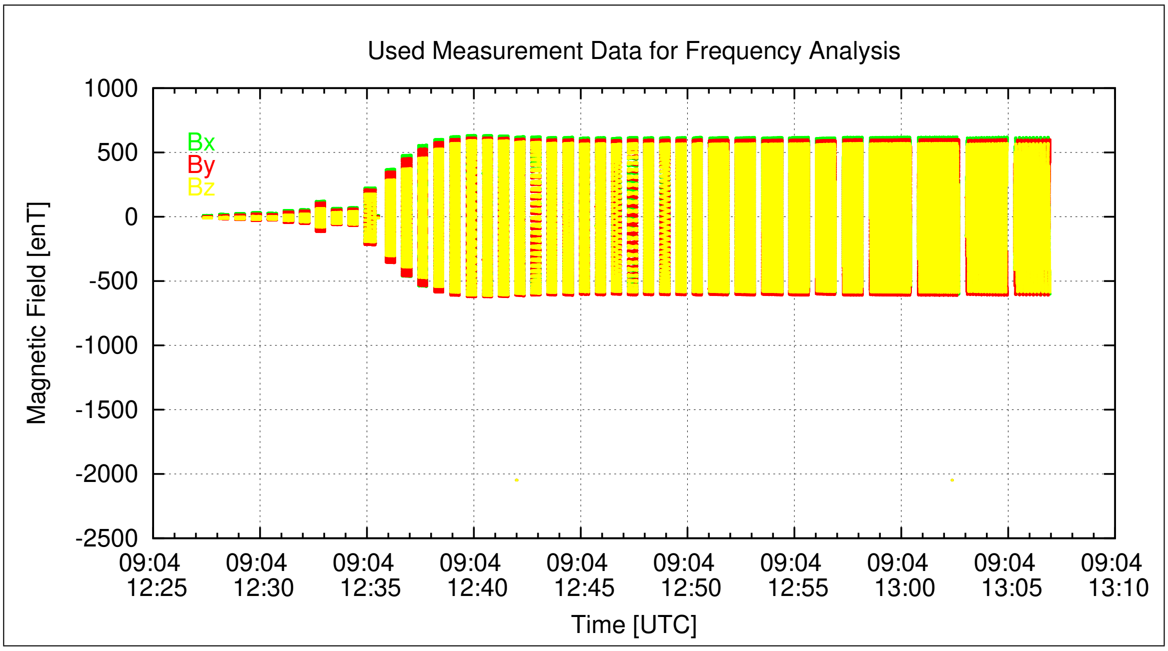

Figure 42: Used packets of Measured data for the Frequency analysis

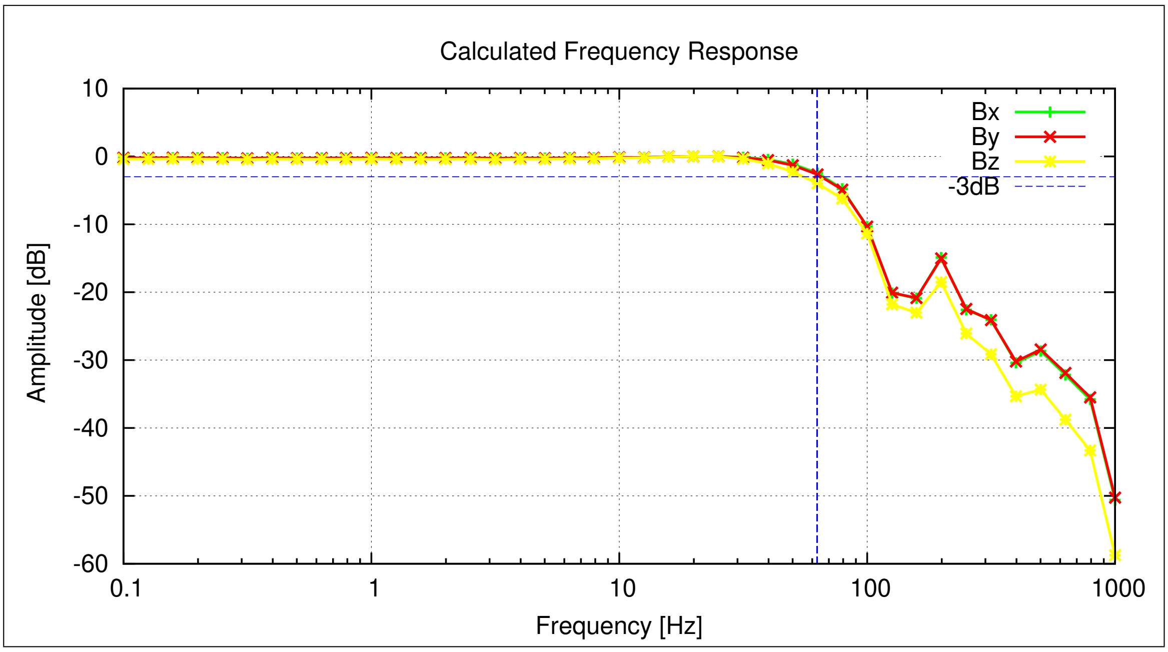

Figure 43: Calculated Frequency Response

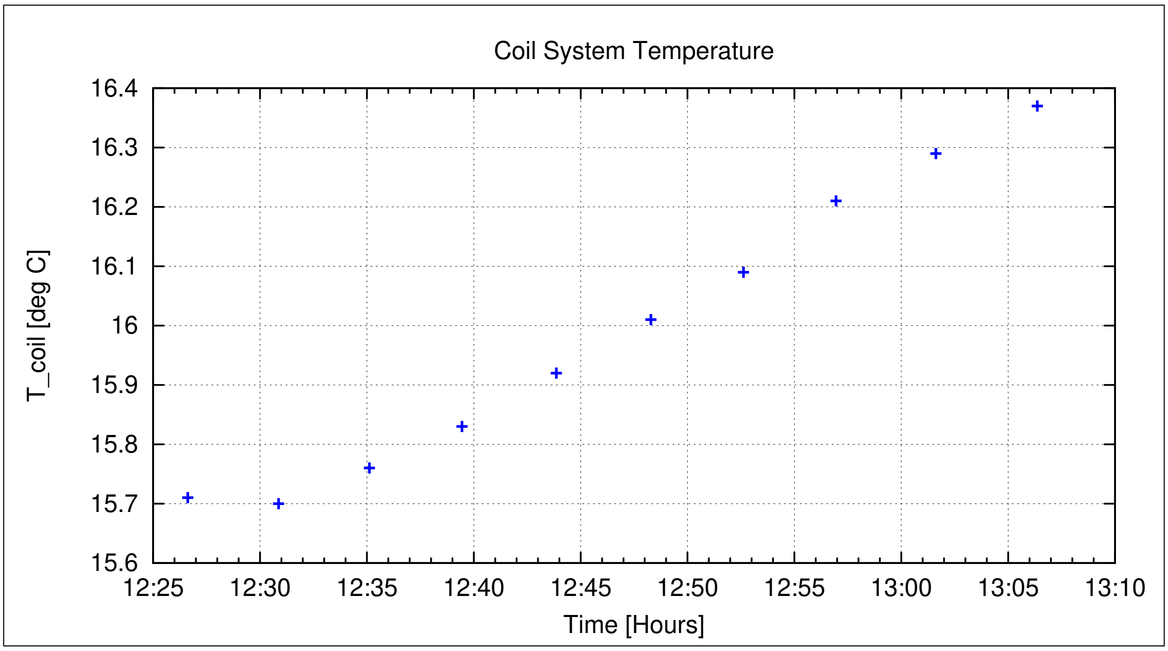

Figure 44: Coil System Temperature

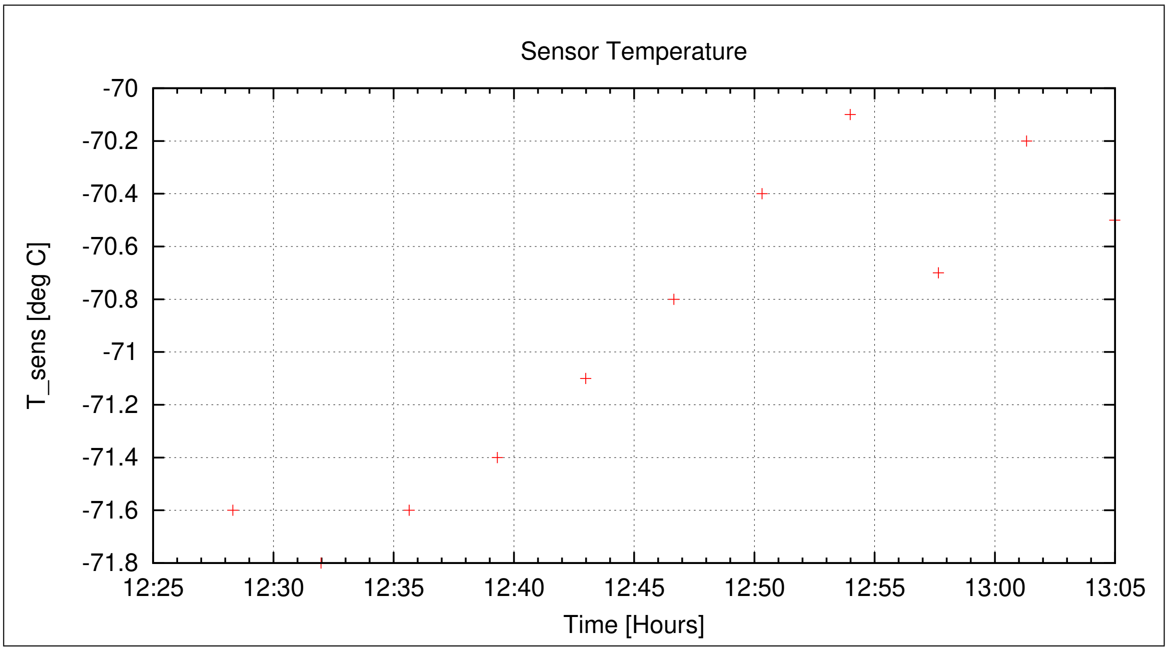

Figure 45: Sensor Temperature

9.6 AC-Analysis at very low Temperature - IB Sensor, cal mode 4

A frequency measurement was performed at -70°C.

Setup:

- Sensor mounted in thermal box. CoC. Box vertical.
- Sensor rotated to:
  Elevation= 45°
  Azimuth= 126°
- Field applied on Y_c.
- No attenuator

9.6.1 Frequency Measurements

This section is dedicated to the frequency behavior of the instrument. The analysis of the performed AC measurements allows to calculate the actual sampling frequency f_s of the instrument and the frequency response (amplitude vs. frequency). The measurements have been performed with the sensor placed at CoC in a diagonal in space orientation. The AC-fields have been applied on the Y_c axis only. Using this setup it can be guaranteed that only one frequency is applied at a time and no beat effects occur.

Used Frequency Measurements:

CCD File	Configuration File	Remark
`13-04-09\13-27-51.CCR`	`FREQ2000.MAG`	

Parameter File: `FREQ_PARAMETER__13-04-09-13-27-51.FPF`

Calibration Parameter:

Sampling Frequency:

Component	f_s [Hz]	Standard deviation [Hz]
X	127.9989	0.000082
Y	127.9985	0.000084
Z	127.9989	0.000075
Mean Sampling Frequency	127.9988	0.000263

3 dB Corner Frequency:

Component	$f_{3\text{dB}}$ [Hz]
X	58.25
Y	58.38
Z	54.46

Applied Frequencies and Measured Amplitudes

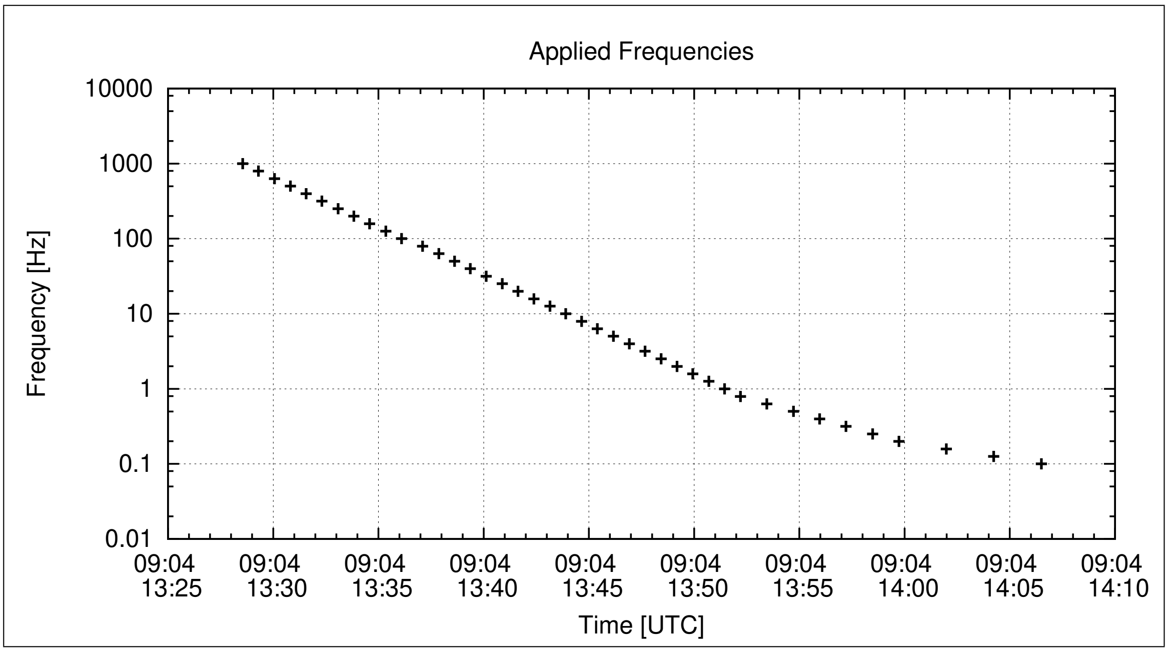

Figure 46: Applied Frequencies for AC Analysis

Applied Frequency [Hz]	Bx [enT]	By [enT]	Bz [enT]
1000.000	1.81	1.87	0.67
794.000	9.91	10.20	4.04
631.000	16.17	16.60	7.32
501.000	24.15	24.69	12.07
398.000	19.53	19.89	10.72
316.000	36.29	36.82	21.76
251.000	49.52	50.07	32.29
199.000	104.41	105.27	73.73
158.000	54.73	55.04	41.53
126.000	66.51	66.77	53.69
100.000	152.14	152.01	129.35
79.400	339.62	340.05	300.02
63.100	440.17	440.43	399.99
50.100	513.53	513.25	475.90
39.800	563.29	563.11	529.00
31.600	596.19	595.86	564.80
25.100	618.32	617.90	589.09
19.900	633.19	632.69	605.47
15.800	641.46	640.91	614.80
12.600	646.25	645.68	620.31
10.000	646.92	646.33	621.55
7.900	651.80	651.18	626.62
6.310	650.84	650.22	625.95
5.010	652.41	651.77	627.62
3.980	654.41	651.36	629.71
3.160	653.65	653.00	629.01
2.510	653.75	653.09	629.16
1.990	654.21	653.54	629.65
1.580	656.19	655.53	631.58
1.260	652.68	651.99	628.23
1.000	653.78	653.08	629.30
0.790	656.51	655.82	631.99
0.631	655.29	654.60	630.85
0.501	657.59	656.91	633.03
0.398	657.66	656.97	633.08
0.316	654.58	653.90	630.12
0.251	656.20	655.49	631.65
0.199	656.72	655.98	632.18
0.158	656.96	655.70	632.46
0.126	657.43	656.68	632.95
0.100	658.19	657.42	633.70

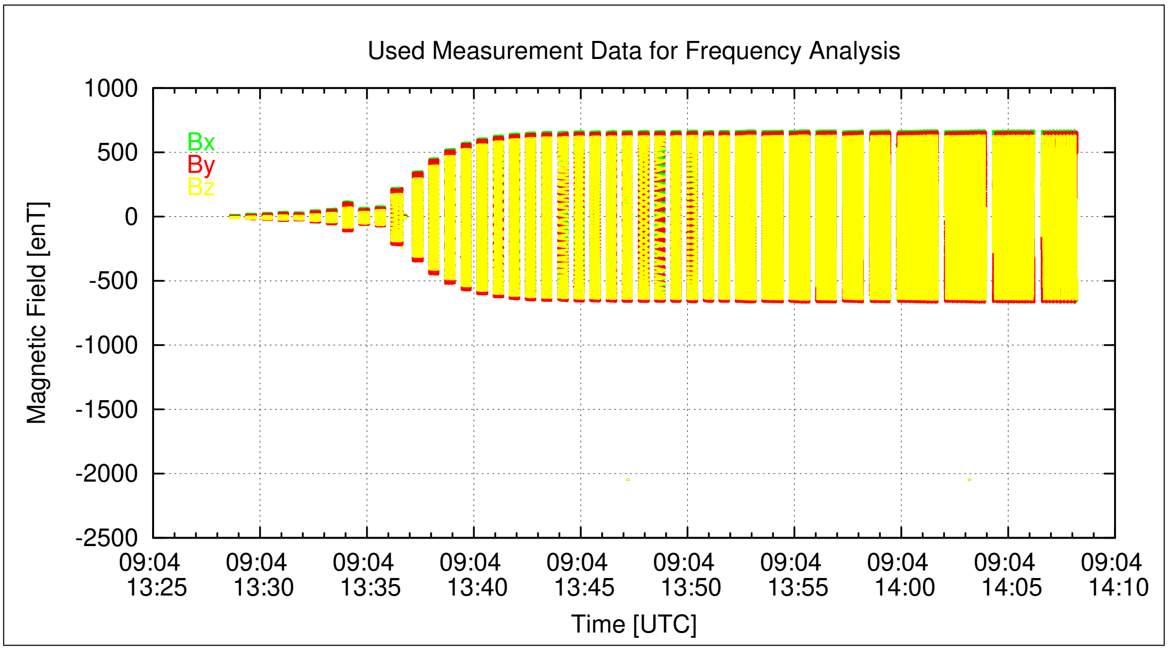

Figure 47: Used packets of Measured data for the Frequency analysis

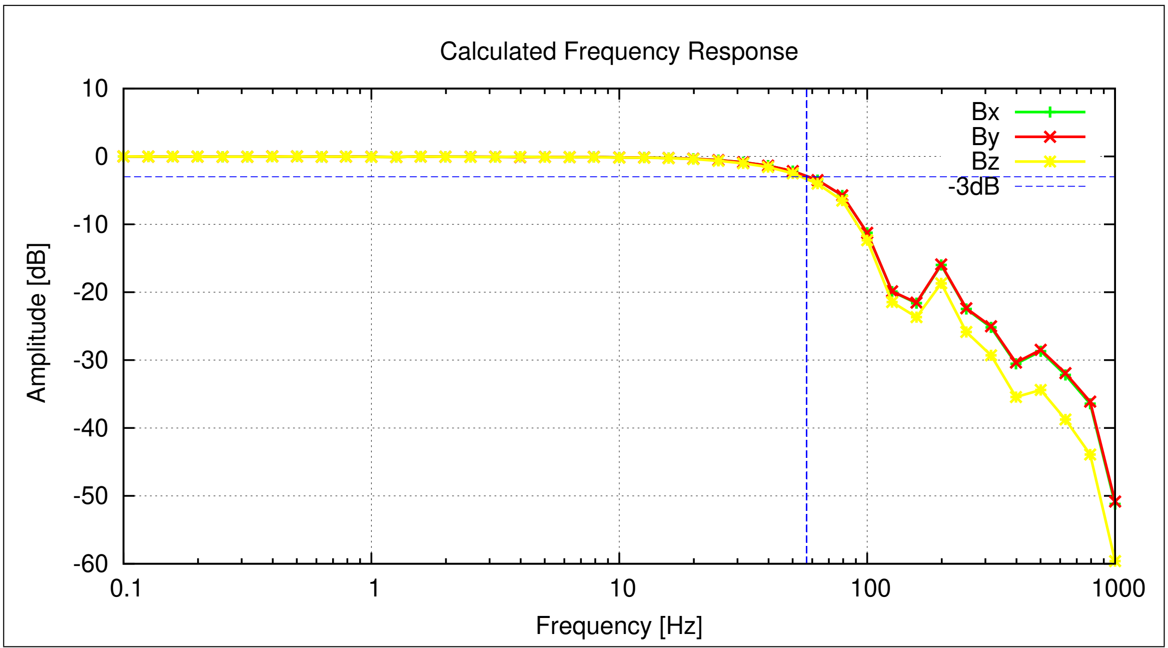

Figure 48: Calculated Frequency Response

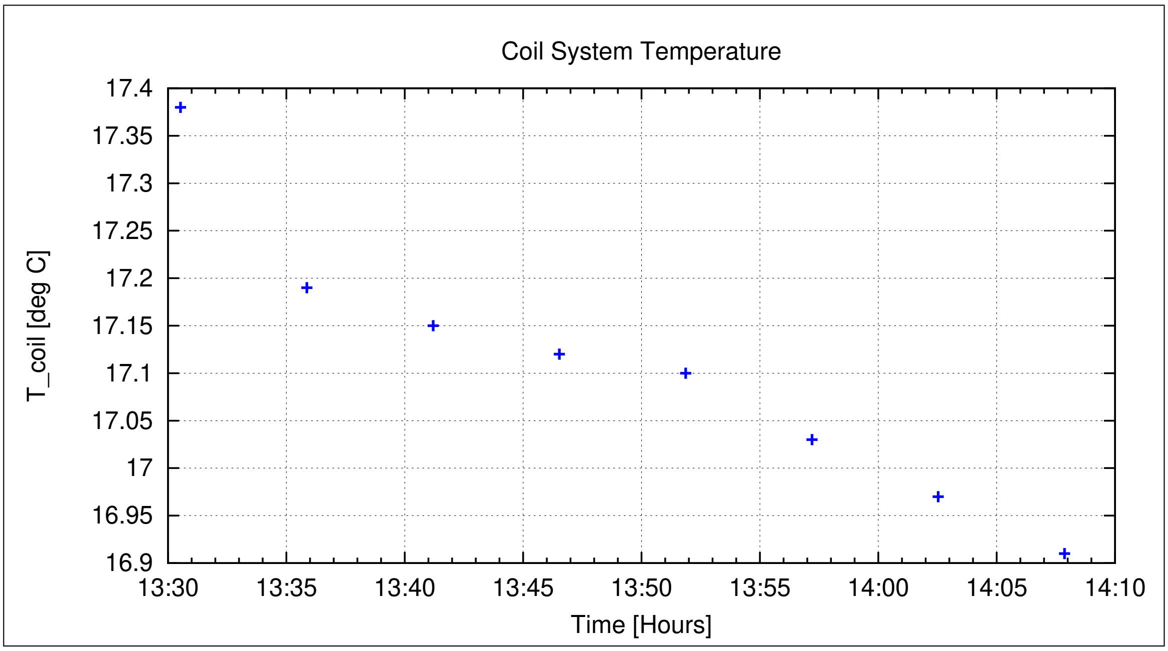

Figure 49: Coil System Temperature

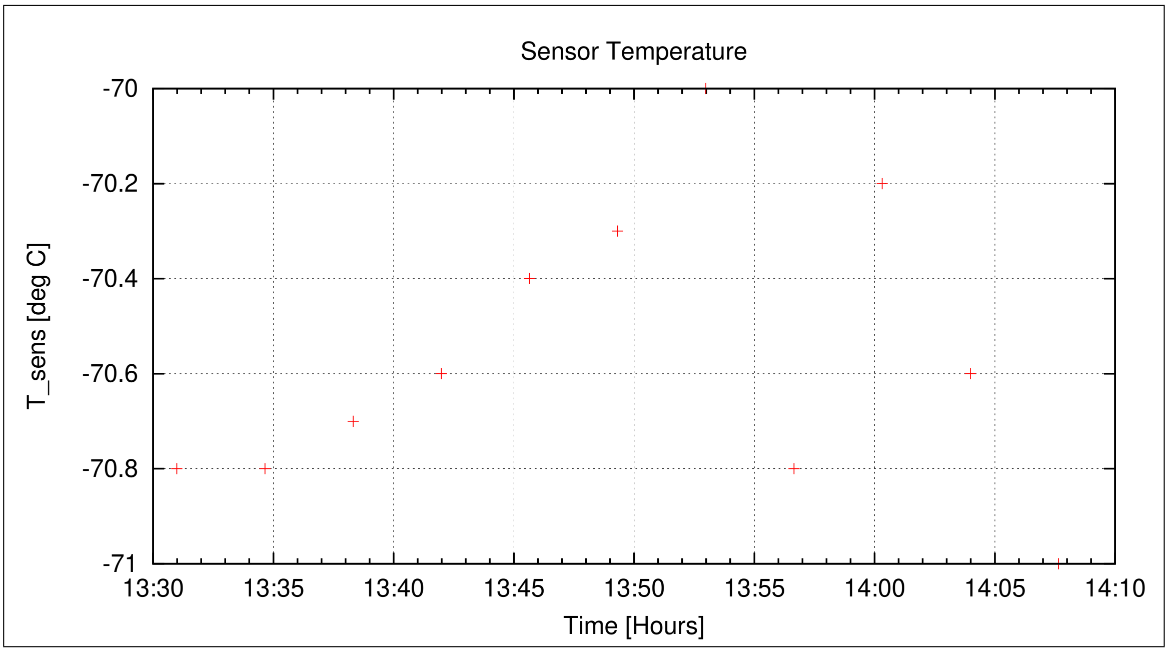

Figure 50: Sensor Temperature

After finishing these measurements the sensor was rotated back to normal orientation and the thermal system was switched off. The temperature will increase smoothly over night.

Over night zerofield measurements in dynamically compensated earthfield conditions were conducted. The IB sensor (at CoC) was operated in the fixed 64 nT range, the OB sensor (in the μ-metal shield outside the coilsystem) was set to the 512 nT range.

Measurements started at 14:53.

10 Measurements on April 10, 2013

At 06:28 the system was inspected. The measurements have been performing flawlessly during the night. The box temperature has reached a level of −14°C.

The measurements were stopped and the thermal system was reactivated.
Temperature goal: $T_{59} = +30°C$.

The operating range of the magnetometer has been set back to 2048 nT.

10.1 Data

CCD File	Configuration File	Remark
13-04-10\02-54-22.CCR	NULL.MAG	
13-04-10\06-27-43.CCR	NULL.MAG	
13-04-10\06-28-37.CCR	LIN2000XYZE.MAG	
13-04-10\06-58-41.CCR	LIN2000XYZE.MAG	
13-04-10\07-28-44.CCR	LIN2000XYZE.MAG	
13-04-10\07-59-38.CCR	OFFSET_200.MAG	
13-04-10\08-09-57.CCR	OFFSET_200.MAG	
13-04-10\08-18-43.CCR	LIN2000XYZE.MAG	
13-04-10\10-16-52.CCR	LIN2000XYZE.MAG	
13-04-10\10-46-56.CCR	LIN2000XYZE.MAG	
13-04-10\11-17-00.CCR	LIN2000XYZE.MAG	
13-04-10\11-47-03.CCR	LIN2000XYZE.MAG	
13-04-10\12-16-47.CCR	LIN2000XYZE.MAG	
13-04-10\12-17-18.CCR	OFFSET_200.MAG	
13-04-10\12-26-40.CCR	FREQ2000.MAG	
13-04-10\13-11-42.CCR	LIN2000XYZE.MAG	
13-04-10\13-47-06.CCR	OFFSET_200.MAG	
13-04-10\13-56-47.CCR	FREQ2000.MAG	
13-04-10\14-44-30.CCR	NULL_STATISCH.MAG	

10.2 DC-Analysis at moderate Temperature - IB Sensor

Linearity and offset measurements were performed at $T_{59} = +30°C$ in cal mode 4 and cal mode 0.

Thermal Analysis: refer to section 13.

It turned out that the magnetometer thermistor T_SENS_2 shows temperatures being a few degrees to high. Furthermore the value is not stable and jumps by a few degrees. While T_SENS_1 showed stable 22°C, T_SENS_2 showed values between 39 and 48 °C.

The instrument was switched off, connectors were swapped, and electronics was rebooted. It showed up that the suspicious value belongs physically to the thermistor T_SENS_2 and does not be influenced by the electronics. The sensors were toggled to the nominal connection state. Probably there is a connection problem in the test cable leading from the sensor to the electronics. As this does not really hamper the calibration we decided to proceed with the measurements and to investigate the cable in the institute later.

Afterwards the system was heated up to $T_{59} = +80°$ starting at 10:16.

10.3 DC-Analysis at high Temperature - IB Sensor

Linearity and offset measurements were performed at $T_{59} = +80°C$ in cal mode 4 and cal mode 0.
Thermal Analysis: refer to section 13.

10.4 AC-Analysis at high Temperature - IB Sensor

The sensor was rotated to the diagonal in space orientation and the usual AC measurements were conducted at at $T_{59} = +80°C$ in cal mode 4 and cal mode 0.
Thermal Analysis: refer to section 13.

Afterward the sensor was rotated back to the standard orientation (POS1).

The thermal system was switched off for smooth cooling during the night. Measurements in fixed compensated zerofield conditions, starting at 14:44, were conducted during the night in cal mode 0. Data were sampled with 128 Hz.

11 Measurements on April 11, 2013

At 06:30 the system was inspected. The measurements have been performing flawlessly during the night. The box temperature has dropped to $T_{59} = +39.4°C$.

The measurements were stopped and the thermal system was reactivated.
Temperature goal $T_{59} = +130°C$.

11.1 Data

CCD File	Configuration File	Remark
13-04-11\06-36-24.CCR	LIN2000XYZE.MAG	
13-04-11\07-06-27.CCR	LIN2000XYZE.MAG	
13-04-11\07-36-30.CCR	LIN2000XYZE.MAG	
13-04-11\08-06-33.CCR	LIN2000XYZE.MAG	
13-04-11\08-37-21.CCR	OFFSET_200.MAG	
13-04-11\08-46-10.CCR	FREQ2000.MAG	
13-04-11\09-31-53.CCR	LIN2000XYZE.MAG	
13-04-11\10-11-50.CCR	OFFSET_200.MAG	
13-04-11\10-20-53.CCR	FREQ2000.MAG	
13-04-11\11-05-33.CCR	LIN2000XYZE.MAG	
13-04-11\11-35-36.CCR	LIN2000XYZE.MAG	
13-04-11\12-05-40.CCR	LIN2000XYZE.MAG	
13-04-11\12-35-43.CCR	LIN2000XYZE.MAG	
13-04-11\13-06-41.CCR	LIN2000XYZE.MAG	
13-04-11\13-37-03.CCR	OFFSET_200.MAG	
13-04-11\13-45-45.CCR	FREQ2000.MAG	
13-04-11\14-42-54.CCR	LIN2000XYZE.MAG	
13-04-11\14-47-36.CCR	LIN2000XYZE.MAG	
13-04-11\15-18-03.CCR	OFFSET_200.MAG	
13-04-11\15-26-22.CCR	FREQ2000.MAG	

11.2 DC-Analysis at very high Temperature - IB Sensor

Linearity and offset measurements were performed at $T_{59} = +130°C$ in cal mode 4 and cal mode 0 starting at 08:06.

Thermal Analysis: refer to section 13.

11.3 AC-Analysis at very high Temperature - IB Sensor

The sensor was rotated to the diagonal in space orientation and the usual AC measurements were conducted at $T_{59} = +130°C$ in cal mode 4 and cal mode 0.

Thermal Analysis: refer to section 13.

Afterwards the thermal box was heated up to the final temperature of +180°C.

11.4 DC-Analysis at highest Temperature - IB Sensor

Linearity and offset measurements were performed at $T_{59} = +180°C$ in cal mode 4 and cal mode 0 starting at 13:06.

Thermal Analysis: refer to section 13.

11.5 AC-Analysis at highest Temperature - IB Sensor

The sensor was rotated to the diagonal in space orientation and the usual AC measurements were conducted at at $T_{59} = +180°C$ in cal mode 4 and cal mode 0.

Thermal Analysis: refer to section 13.

Afterwards the thermal system was switched off to let the temperature fall smoothly. Over night and for thee next days zerofield measurements in fixed compensated earthfield conditions were conducted in science mode.
Sensor alignment: Standard, Azimuth =180°, Elevation=0°.
Data collection by EGSE only.
The measurements started at 16:16.

From the calibration point of view the campaign for the IB sensor is finished now.

12 Combined Measurements from April 3 – 9, 2013

12.1 Thermal-Analysis - OB Sensor, cal mode 0

12.1.1 Temperature Calibration on Linear Axes

Used Temperature Measurements:

Calibration Parameter File	Remark
PARAMETER_TEMPLIN__13-04-03_09-22-38.CPF	
PARAMETER_TEMPLIN__13-04-03_12-16-15.CPF	
PARAMETER_TEMPLIN__13-04-04_08-08-11.CPF	
PARAMETER_TEMPLIN__13-04-04_09-51-19.CPF	
PARAMETER_TEMPLIN__13-04-04_14-55-20.CPF	
PARAMETER_TEMPLIN__13-04-08_08-29-20.CPF	
PARAMETER_TEMPLIN__13-04-08_15-06-16.CPF	

Thermal Parameter File: THERMAL_PARAMETER__13-04-03-09-22-38.TPF

Facility Parameter:

Nominal Sensor Setup $\underline{B}_{\mathrm{DUT}} = \underline{\underline{R}}_{\mathrm{nom}} \underline{B}_{\mathrm{c}}$

$$\underline{\underline{R}}_{\mathrm{nom}} = \begin{pmatrix} +1.000000 & +0.000000 & +0.000000 \\ +0.000000 & +1.000000 & +0.000000 \\ +0.000000 & +0.000000 & +1.000000 \end{pmatrix}$$

Calculated Initial Sensor Rotation:

$$\underline{\underline{R}} = \begin{pmatrix} +0.999800 & +0.018895 & +0.006519 \\ -0.018810 & +0.999740 & -0.012858 \\ -0.006760 & +0.012733 & +0.999896 \end{pmatrix}$$

Initial Rotation Angles:

$$\begin{array}{rrl} \text{Rotation @ X:} & \lambda_{\mathrm{x}} = & +1^\circ\ 8'43'' \\ \text{Rotation @ Y:} & \mu_{\mathrm{y}} = & +1^\circ\ 18'20'' \\ \text{Rotation @ Z:} & \nu_{\mathrm{z}} = & +0^\circ\ 49'34'' \end{array}$$

Determinant of Rotation Matrix: 1.0000

Nominal Field Source: FLDS

Automatic Coil correction: used

Used Sensor-Temperature-Channel: T_{59}

Temperature Profile

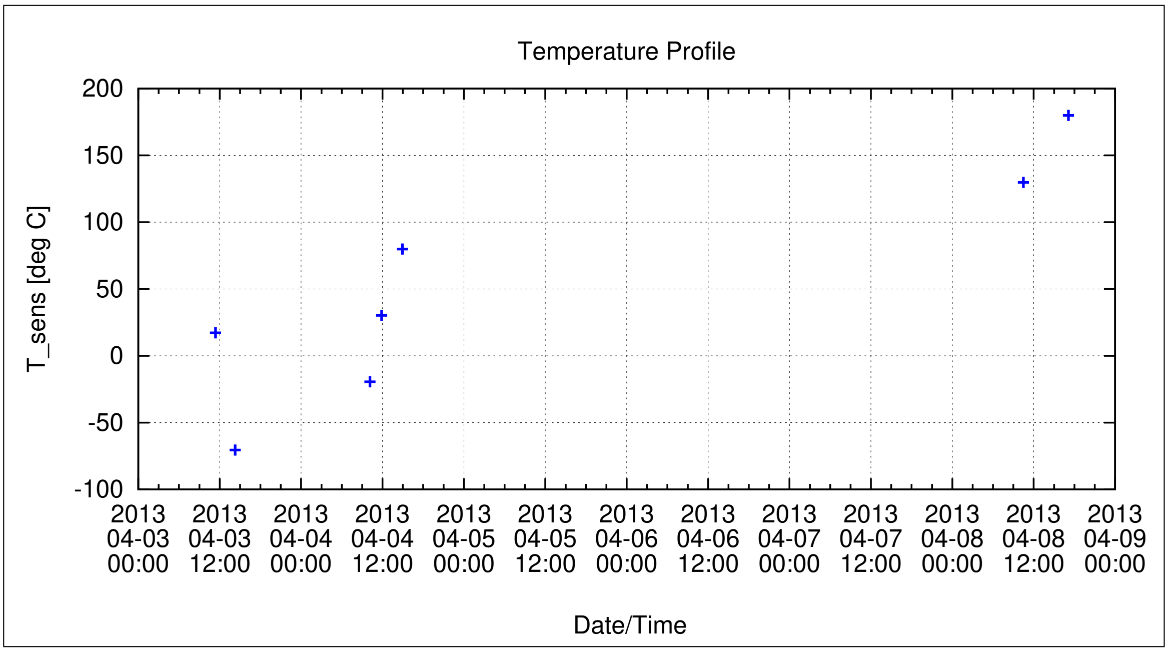

Figure 51: Temperature Profile

Calibration Parameter:

Sensitivity σ_i vs. Temperature:

$$\sigma_i(T) = \sum_{k=0}^{n} \sigma_{k,i} T^k \qquad [1,\ ^\circ C],\ i=\{x,y,z\}$$

	$\sigma_{0,i}$	$\sigma_{1,i}$	$\sigma_{2,i}$	$\sigma_{3,i}$	$\sigma_{4,i}$	$\sigma_{5,i}$
σ_x	9.72692E-1	-1.80180E-5				
σ_y	9.96420E-1	-1.56674E-5				
σ_z	9.89066E-1	-1.96816E-5				

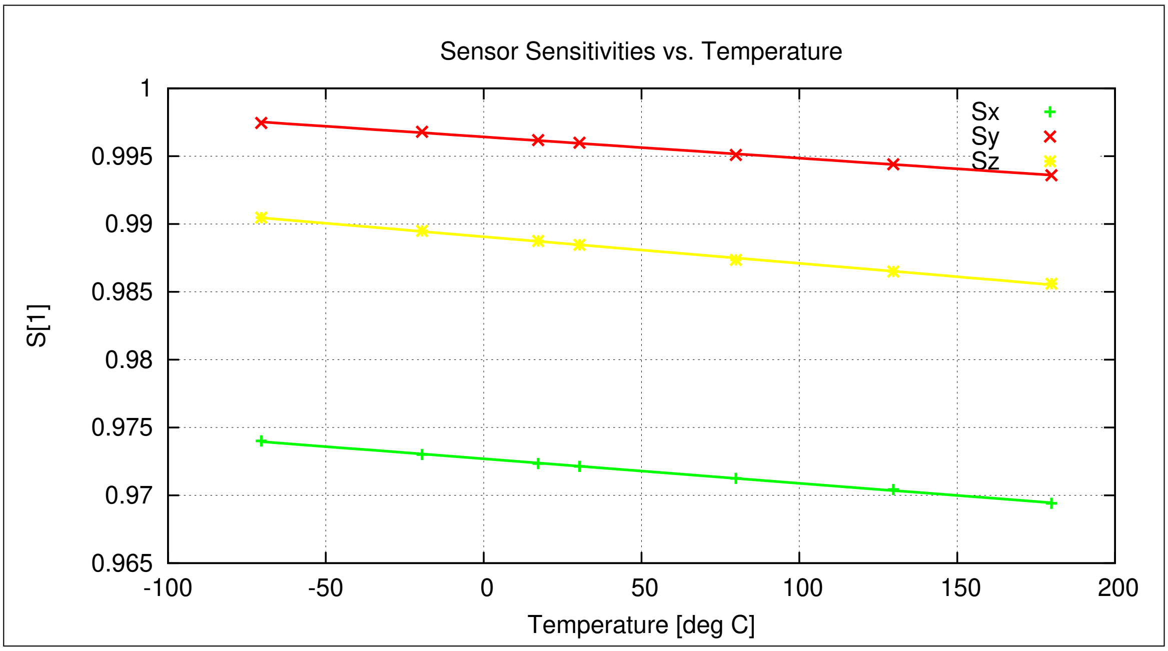

Figure 52: Temperature dependence of Sensitivities

Misalignment Angles ξ_{ij} vs. Temperature:

$$\xi_{ij}(T) = \sum_{k=0}^{n} \xi_{k,ij} T^k \qquad [\text{deg}, \ ^\circ\text{C}], \ \text{ij}= \{\text{xy,xz,yz}\}$$

	$\xi_{0,ij}$	$\xi_{1,ij}$	$\xi_{2,ij}$	$\xi_{3,ij}$	$\xi_{4,ij}$	$\xi_{5,ij}$
ξ_{xy}	8.9789E+1	-1.7948E-5				
ξ_{xz}	9.0056E+1	4.5473E-5				
ξ_{yz}	9.0013E+1	-1.1504E-4				

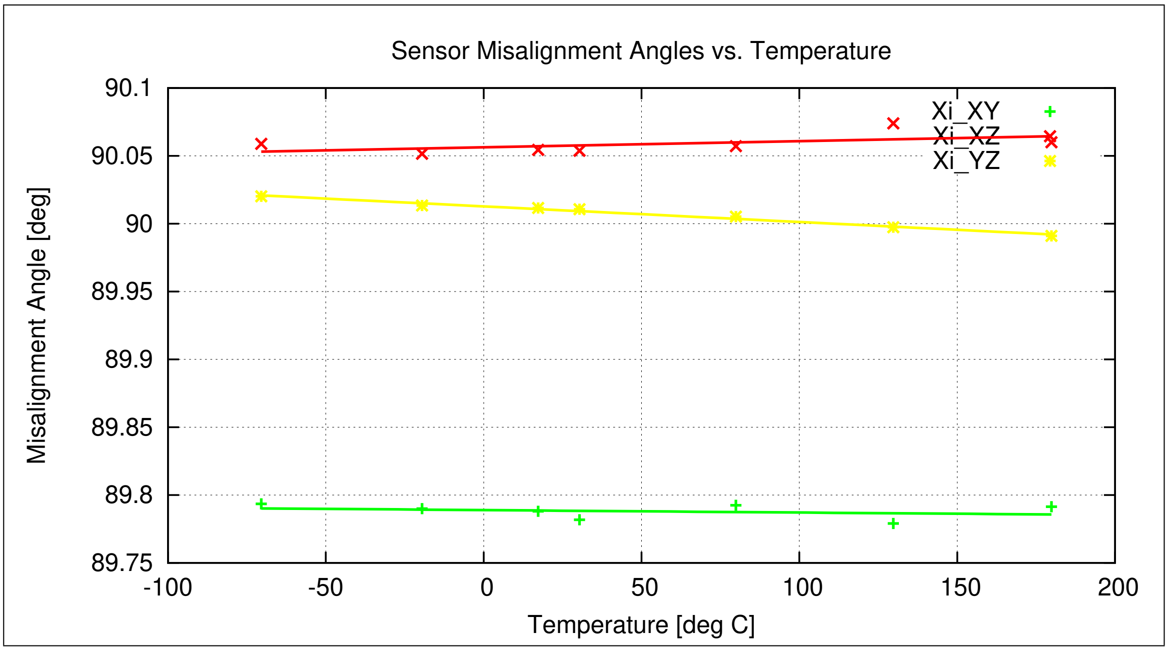

Figure 53: Temperature dependence of Misalignment Angles

Offset & Residual MCF Field $\underline{B}^{or} = \underline{B}^{off} + \underline{B}^{res}$ vs. Temperature:

$$\underline{B}^{or}(T) = \sum_{k=0}^{n} \underline{B}_k^{or} T^k \qquad [\text{enT}, {}^\circ\text{C}]$$

	$\underline{B}_0^{or}$	$\underline{B}_1^{or}$	$\underline{B}_2^{or}$	$\underline{B}_3^{or}$	$\underline{B}_4^{or}$	$\underline{B}_5^{or}$
B_x^{or}	-1.038E+0	5.086E-3	1.028E-4	-8.062E-7		
B_y^{or}	4.990E-1	4.459E-4	2.056E-4	-9.631E-7		
B_z^{or}	-9.215E+0	-4.711E-3	-1.042E-4	8.416E-7		

Model Quality:

Minimum and maximum errors of the calculated Model vs. Temperature:

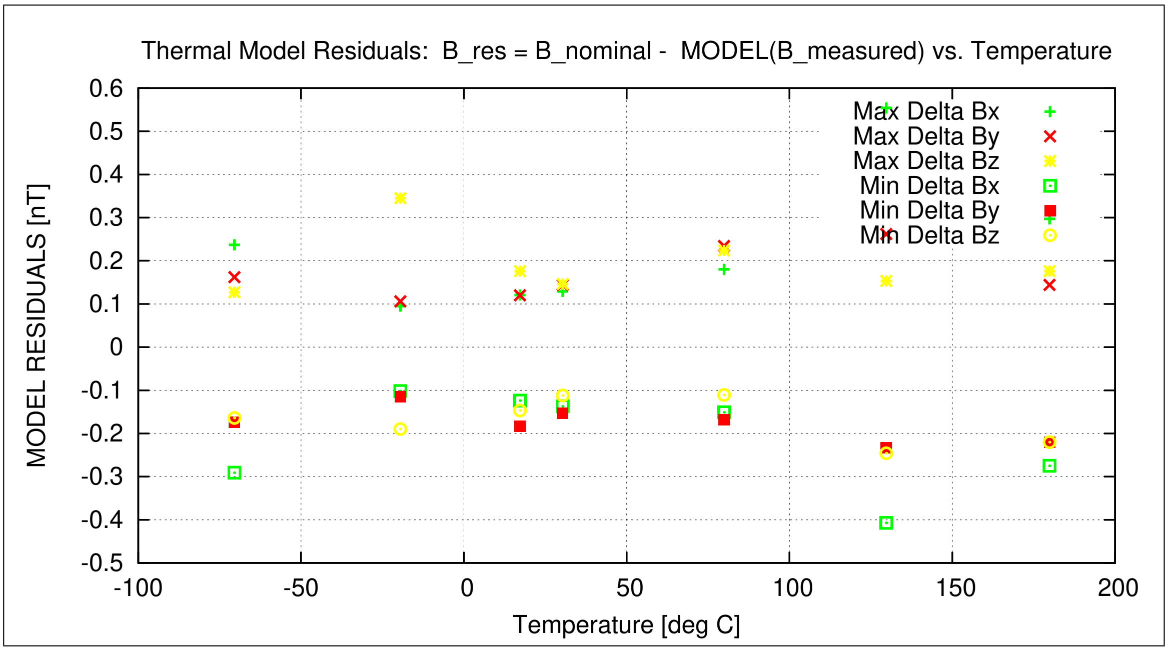

Figure 54: Residuals of Thermal Model

Sensor Rotation during Test:

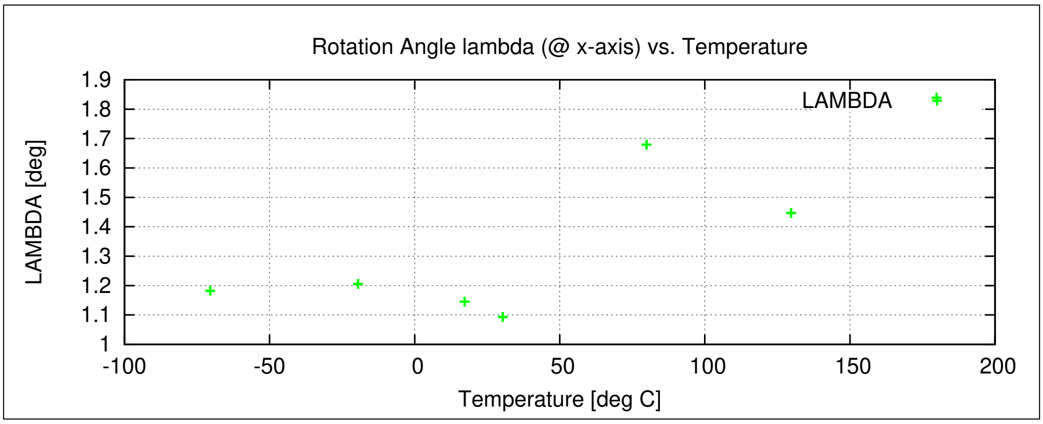

Figure 55: Rotation @ X-Axis

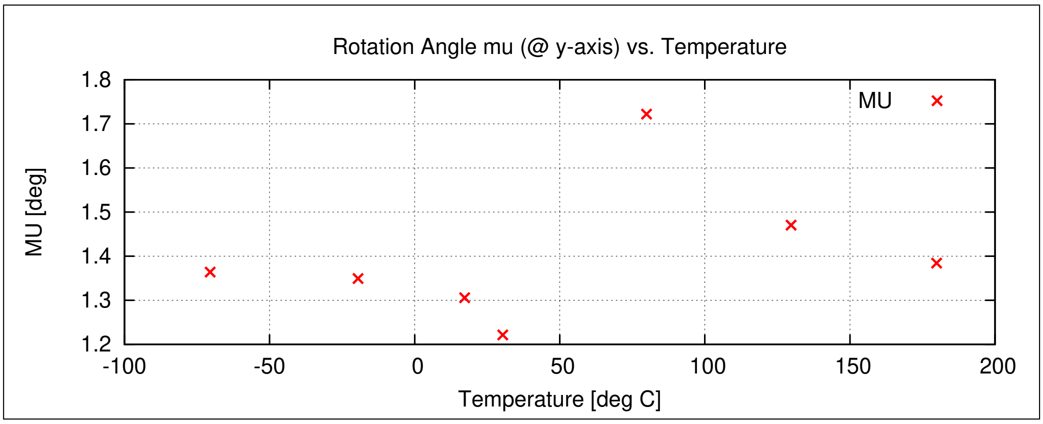

Figure 56: Rotation @ Y-Axis

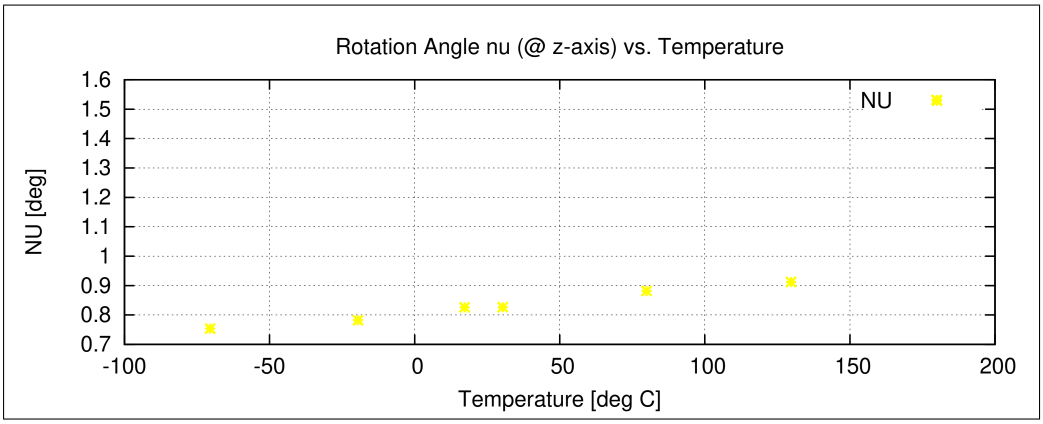

Figure 57: Rotation @ Z-Axis

12.1.2 Temperature Calibration of the Sensor Offset

Used Temperature Measurements:

Calibration Parameter File	Remark
OFF_PARAMETER__13-04-03-09-53-35.OPF	
OFF_PARAMETER__13-04-03-12-47-57.OPF	
OFF_PARAMETER__13-04-04-08-39-48.OPF	
OFF_PARAMETER__13-04-04-10-26-52.OPF	
OFF_PARAMETER__13-04-04-15-26-56.OPF	
OFF_PARAMETER__13-04-08-09-30-44.OPF	
OFF_PARAMETER__13-04-08-15-36-36.OPF	

Thermal Parameter File: THERMAL_OFF_PARAMETER__13-04-03-09-53-35.TOF

Facility Parameter:

Nominal Sensor Setup $\underline{B}_{\mathrm{DUT}} = \underline{\underline{R}}_{\mathrm{nom}} \underline{B}_{\mathrm{c}}$

$$\underline{\underline{R}}_{\mathrm{nom}} = \begin{pmatrix} +1.000000 & +0.000000 & +0.000000 \\ +0.000000 & +1.000000 & +0.000000 \\ +0.000000 & +0.000000 & +1.000000 \end{pmatrix}$$

Sensor Temperature Channel: T_{59}

Coil System Temperature Channel: T_{29}

<u>**Temperature Profile**</u>

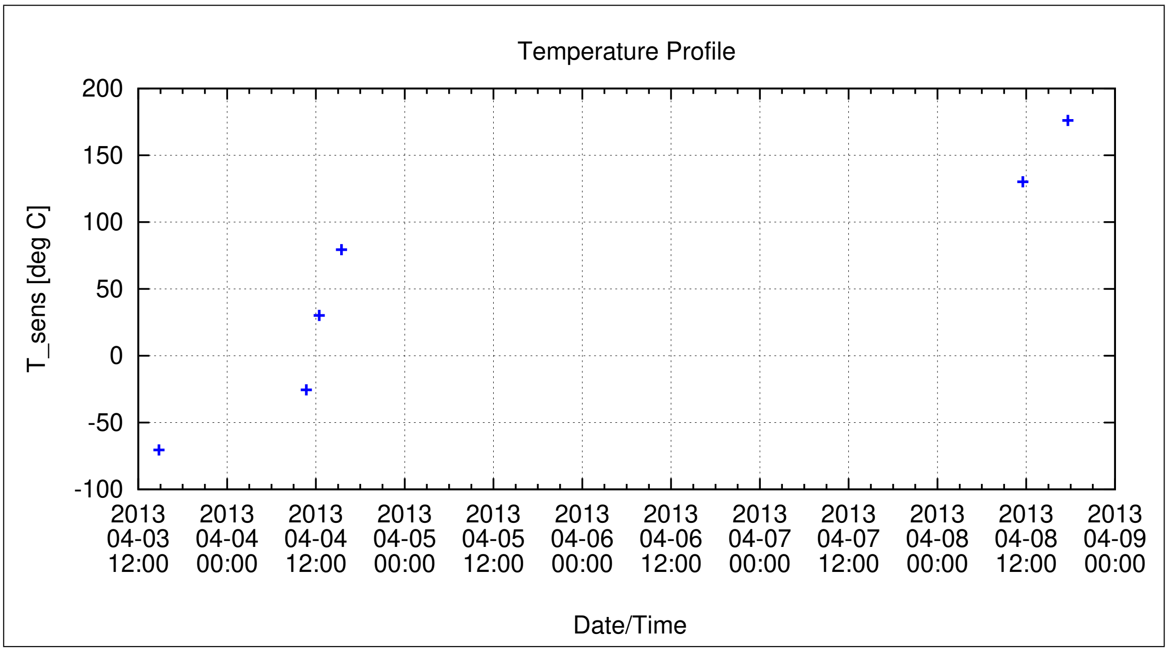

Figure 58: Temperature Profile

Calibration Parameter:

Sensor Offset $\underline{B_{\rm off}}$ vs. Temperature:

$$B_{\rm off,i}(T) = \sum_{k=0}^{n} B_{\rm off,k,i} T^k \qquad [\text{enT}, \ ^\circ\text{C}], \ \text{i}=\{\text{x,y,z}\}$$

	$B_{\rm off,0,i}$	$B_{\rm off,1,i}$	$B_{\rm off,2,i}$	$B_{\rm off,3,i}$	$B_{\rm off,4,i}$	$B_{\rm off,5,i}$
$B_{\rm off,x}$	-1.81567E-1	2.66715E-3	6.76985E-5	-4.57147E-7		
$B_{\rm off,y}$	1.12886E+0	-2.66713E-3	8.93650E-5	-2.48924E-7		
$B_{\rm off,z}$	1.32950E+0	1.18837E-3	-1.17584E-5	1.39437E-7		

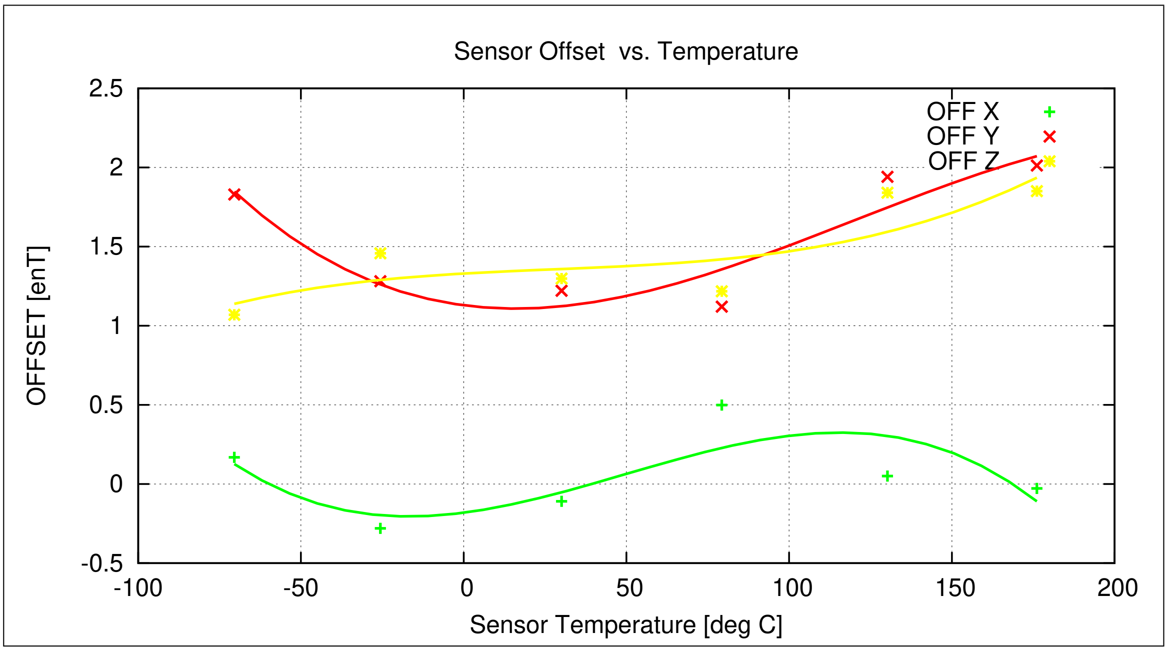

Figure 59: Temperature dependence of Sensor Offsets

Coil System Temperature

The following graph shows the mean Coil System temperature during the complete thermal cycle for the offset measurements.

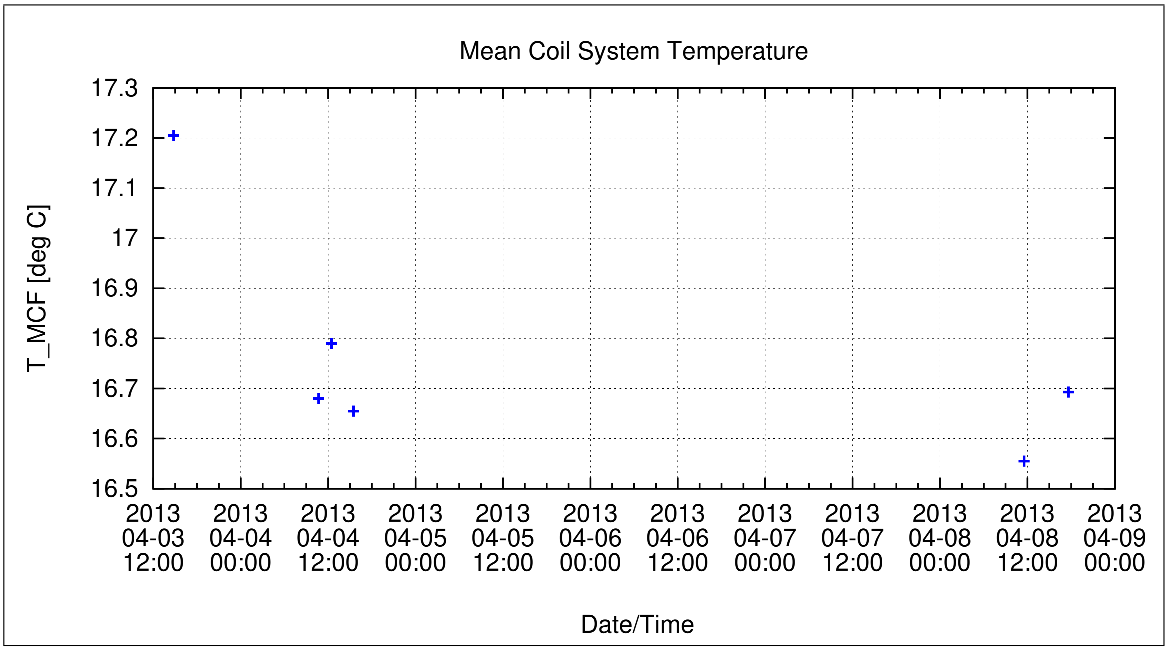

Figure 60: Coil System Temperature during Thermal Measurements

Coil System Residual Field:

The following graph shows the three components of the Coil System Residual field during the whole measurement. Axes designators are related to the actual DUT coordinate system and NOT to Coil System coordinates.

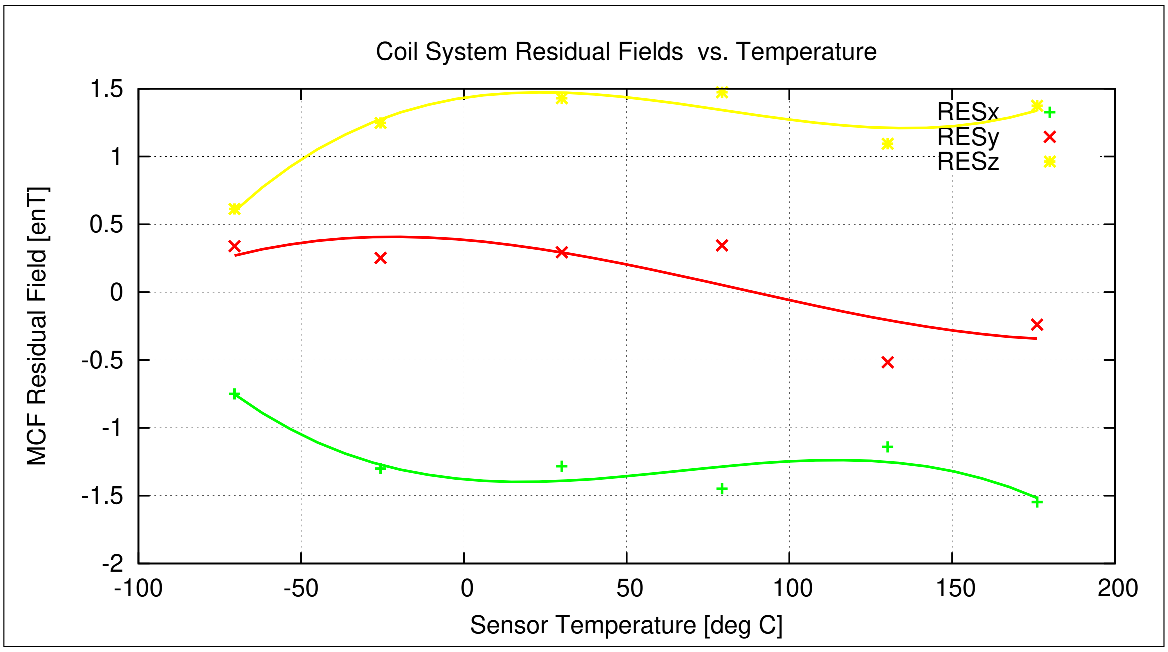

Figure 61: Coil System Residual Fields during Thermal Measurements

Remark:

The axes designation for this graph is given as follows (rf. to setup defined in chapter 1):

$$X_m = X_c$$
$$Y_m = Y_c$$
$$Z_m = -X_c$$

12.1.3 Temperature Calibration of the AC Transfer Function

Used Temperature Measurements:

Calibration Parameter File	Remark
FREQ_PARAMETER__13-04-03-12-59-48.FPF	
FREQ_PARAMETER__13-04-04-14-11-50.FPF	
FREQ_PARAMETER__13-04-08-09-40-37.FPF	
FREQ_PARAMETER__13-04-08-15-46-19.FPF	

Thermal Parameter File: THERMAL_AC_PARAMETER__13-04-03-12-59-48.TAF

Facility Parameter:

Nominal Sensor Setup: Diagonal in Space inside Thermal Box.

Sensor Temperature Channel: T_{59}

Coil System Temperature Channel: T_{29}

Temperature Profile

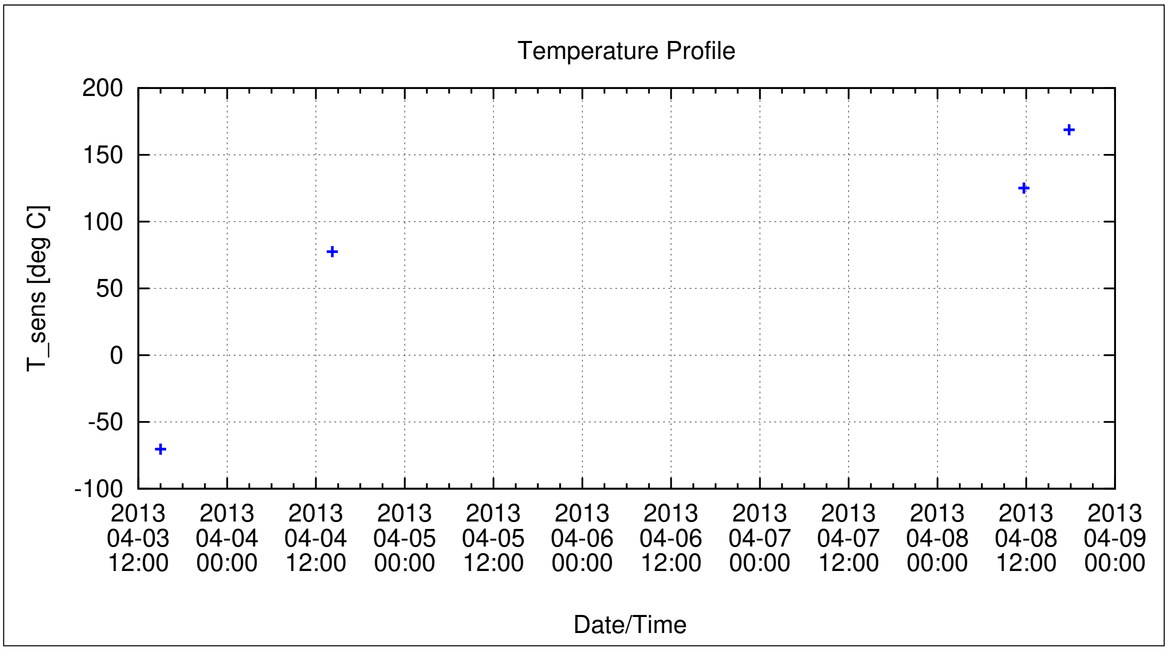

Figure 62: Temperature Profile

Coil System Temperature

The following graph shows the mean Coil System temperature during the complete thermal cycle for the AC measurements.

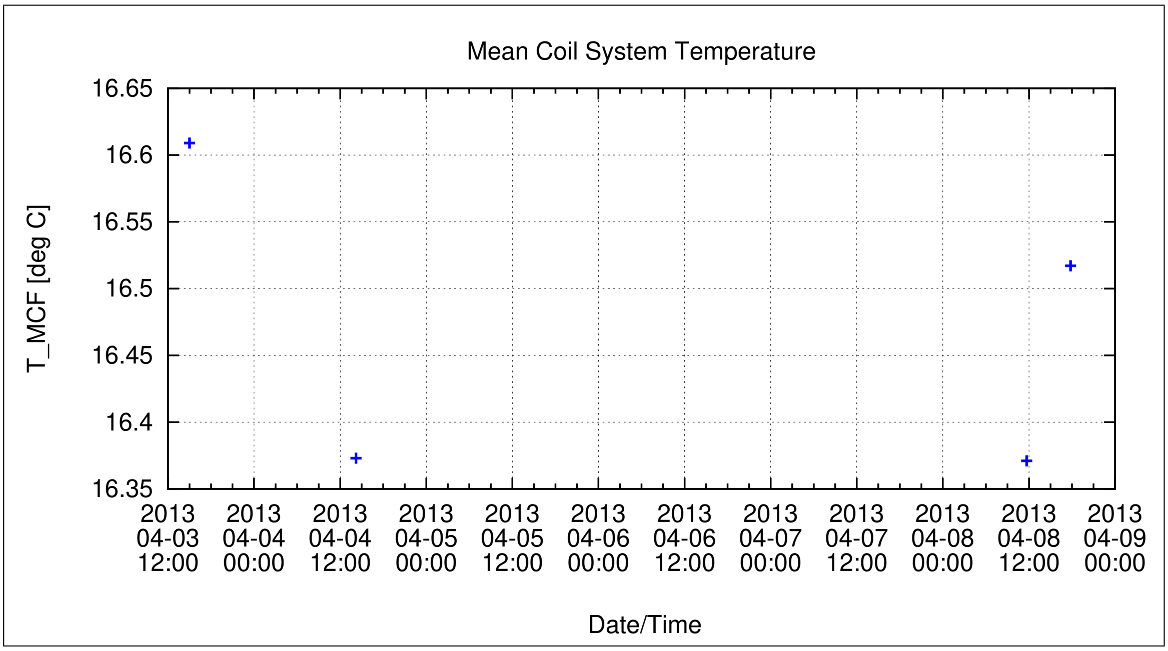

Figure 63: Coil System Temperature during Thermal AC Measurements

Calibration Parameter:

-3dB Corner Frequency f_{3dB} vs. Temperature:

$$f_{3dB,i}(T) = \sum_{k=0}^{n} f_{3dB,k,i} T^k \qquad [Hz,\ ^\circ C],\ i=\{x,y,z\}$$

	$f_{3dB,0,i}$	$f_{3dB,1,i}$	$f_{3dB,2,i}$	$f_{3dB,3,i}$	$f_{3dB,4,i}$	$f_{3dB,5,i}$
$f_{3dB,x}$	5.82762E+1	-7.55338E-2				
$f_{3dB,y}$	5.67012E+1	-9.12999E-2				
$f_{3dB,z}$	5.37114E+1	-2.50266E-2				

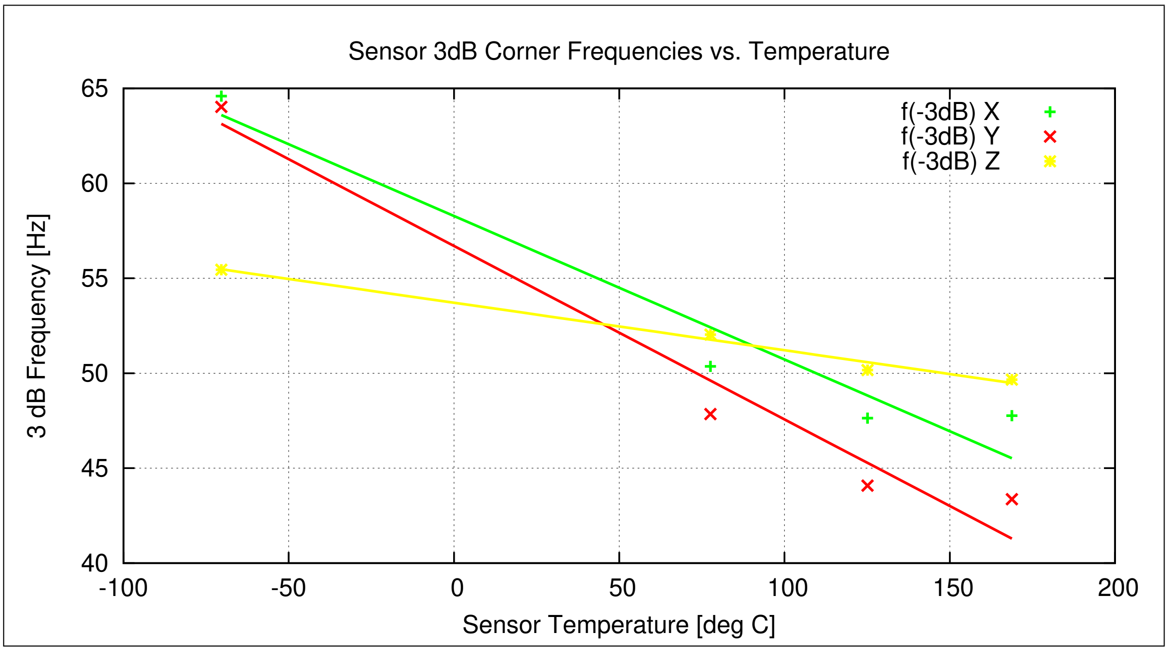

Figure 64: Temperature dependence of 3dB Corner Frequency

Instrument Sampling Frequency:

The following graph shows the calculated sampling frequencies vs. the actual sensor temperature.

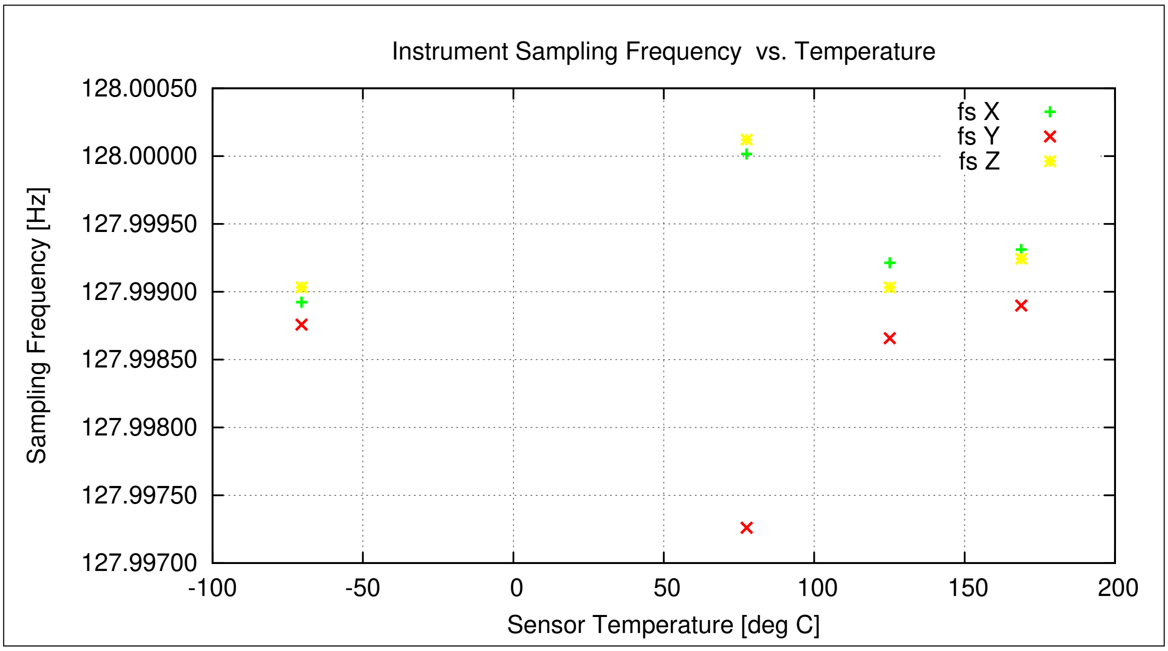

Figure 65: Instrument Sampling Frequency versus Sensor Temperature

Mean Samplerate: 127.999039 Hz.
Mean Standard Deviation of Samplerate: 0.000122 Hz.

12.2 Thermal-Analysis - OB Sensor, cal mode 4

12.2.1 Temperature Calibration on Linear Axes

Used Temperature Measurements:

Calibration Parameter File	Remark
PARAMETER_TEMPLIN__13-04-03_15-24-42.CPF	
PARAMETER_TEMPLIN__13-04-04_07-18-40.CPF	
PARAMETER_TEMPLIN__13-04-04_10-51-43.CPF	
PARAMETER_TEMPLIN__13-04-04_12-34-10.CPF	
PARAMETER_TEMPLIN__13-04-08_11-15-40.CPF	
PARAMETER_TEMPLIN__13-04-08_13-25-22.CPF	

Thermal Parameter File: `THERMAL_PARAMETER__13-04-03-15-24-42.TPF`

Facility Parameter:

Nominal Sensor Setup $\underline{B}_{\mathrm{DUT}} = \underline{\underline{R}}_{\mathrm{nom}} \underline{B}_{\mathrm{c}}$

$$\underline{\underline{R}}_{\mathrm{nom}} = \begin{pmatrix} +1.000000 & +0.000000 & +0.000000 \\ +0.000000 & +1.000000 & +0.000000 \\ +0.000000 & +0.000000 & +1.000000 \end{pmatrix}$$

Calculated Initial Sensor Rotation:

$$\underline{\underline{R}} = \begin{pmatrix} +0.999400 & +0.033623 & +0.008371 \\ -0.033527 & +0.999374 & -0.011332 \\ -0.008747 & +0.011044 & +0.999901 \end{pmatrix}$$

Initial Rotation Angles:

$$\begin{aligned} &\text{Rotation @ X:} \quad \lambda_{\mathrm{x}} = && +1^\circ\ 59'8'' \\ &\text{Rotation @ Y:} \quad \mu_{\mathrm{y}} = && +2^\circ\ 1'41'' \\ &\text{Rotation @ Z:} \quad \nu_{\mathrm{z}} = && +0^\circ\ 48'26'' \end{aligned}$$

Determinant of Rotation Matrix: 1.0000

Nominal Field Source: SOLARTRON

Automatic Coil correction: used

Used Sensor-Temperature-Channel: T_{59}

Temperature Profile

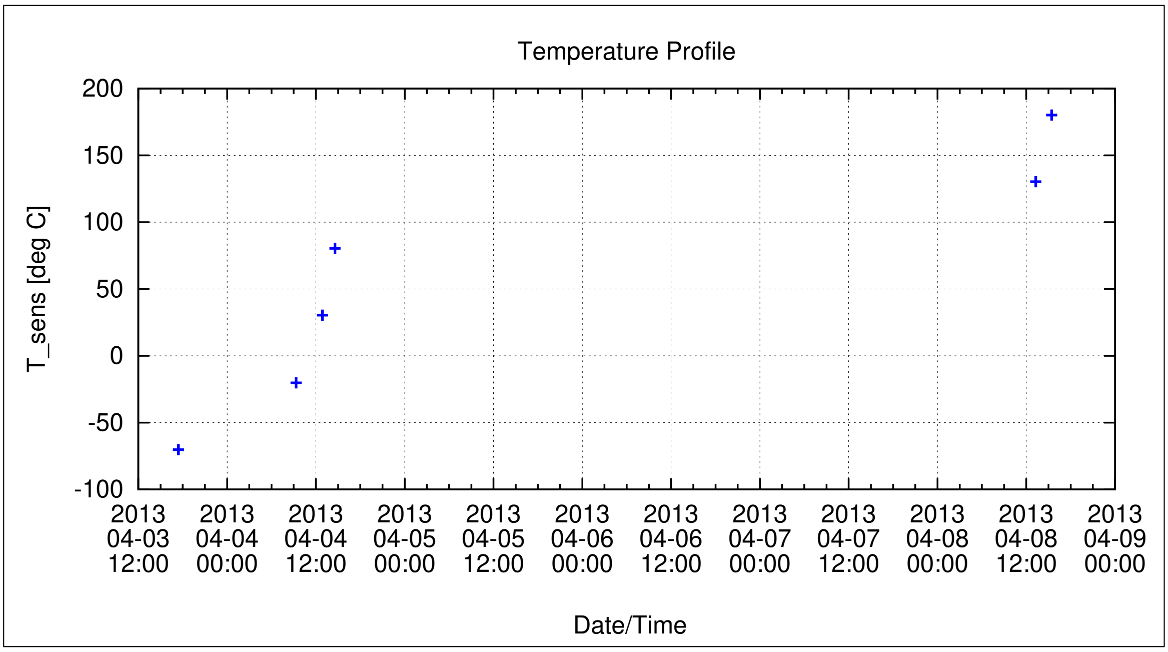

Figure 66: Temperature Profile

Calibration Parameter:

Sensitivity σ_i vs. Temperature:

$$\sigma_i(T) = \sum_{k=0}^{n} \sigma_{k,i} T^k \qquad [1,\ ^\circ\mathrm{C}],\ \mathrm{i=\{x,y,z\}}$$

	$\sigma_{0,i}$	$\sigma_{1,i}$	$\sigma_{2,i}$	$\sigma_{3,i}$	$\sigma_{4,i}$	$\sigma_{5,i}$
σ_x	9.97312E-1	8.41537E-4	-2.34026E-6			
σ_y	1.01904E+0	9.92588E-4	-2.21768E-6			
σ_z	9.81879E-1	6.63730E-4	-1.40862E-6			

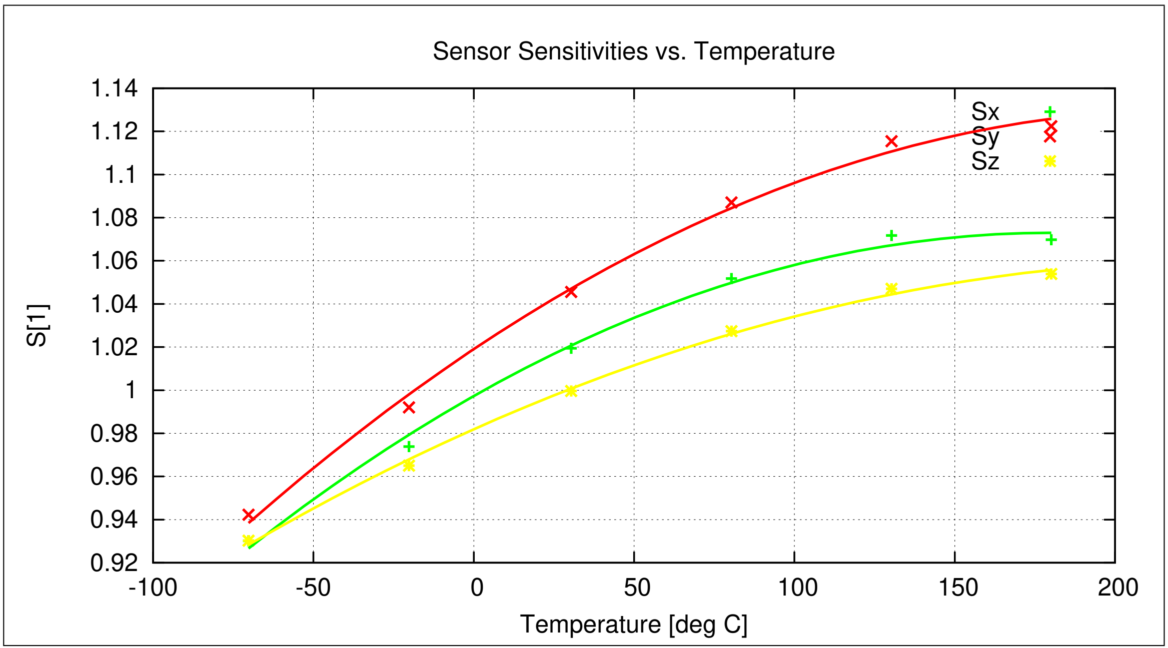

Figure 67: Temperature dependence of Sensitivities

Misalignment Angles ξ_{ij} vs. Temperature:

$$\xi_{ij}(T) = \sum_{k=0}^{n} \xi_{k,ij} T^k \qquad [\text{deg}, \ ^\circ\text{C}], \ \text{ij}= \{\text{xy,xz,yz}\}$$

	$\xi_{0,ij}$	$\xi_{1,ij}$	$\xi_{2,ij}$	$\xi_{3,ij}$	$\xi_{4,ij}$	$\xi_{5,ij}$
ξ_{xy}	9.0578E+1	1.4757E-3	-5.1834E-6			
ξ_{xz}	8.9782E+1	-4.0098E-4	2.5339E-6			
ξ_{yz}	9.0109E+1	-4.8477E-4	5.5736E-7			

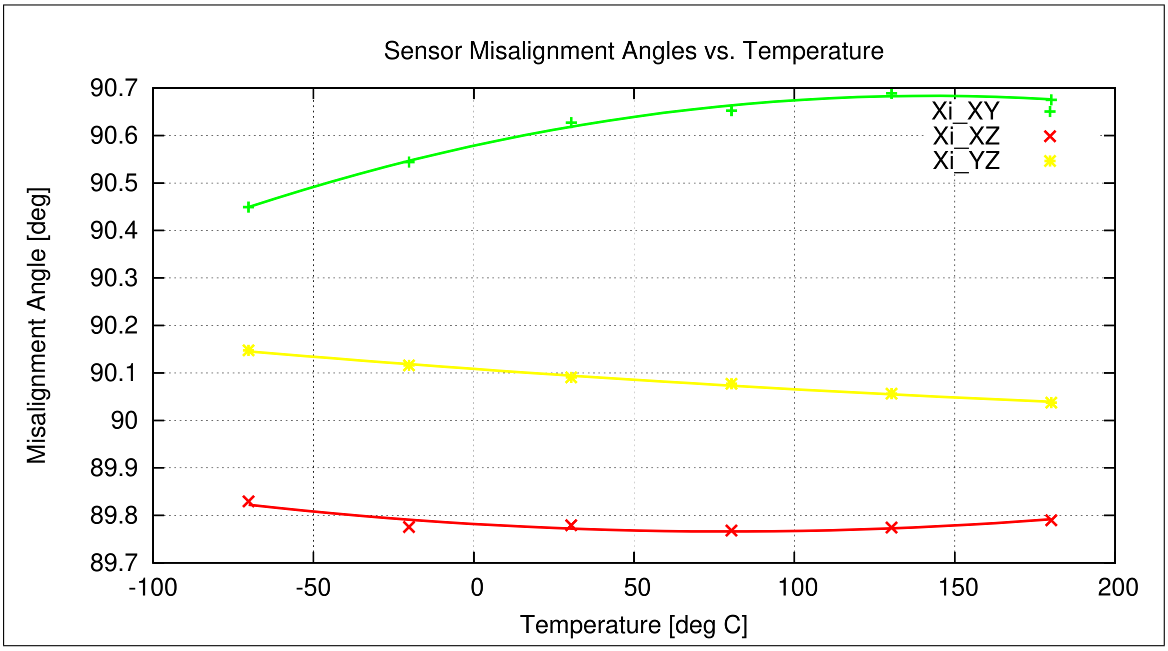

Figure 68: Temperature dependence of Misalignment Angles

Offset & Residual MCF Field $\underline{B}^{or} = \underline{B}^{off} + \underline{B}^{res}$ vs. Temperature:

$$\underline{B}^{or}(T) = \sum_{k=0}^{n} \underline{B}_k^{or} T^k \qquad [\text{enT}, {}^\circ\text{C}]$$

	$\underline{B}_0^{or}$	$\underline{B}_1^{or}$	$\underline{B}_2^{or}$	$\underline{B}_3^{or}$	$\underline{B}_4^{or}$	$\underline{B}_5^{or}$
B_x^{or}	-1.154E+0	4.076E-3	5.321E-5	-5.044E-7		
B_y^{or}	9.191E-1	-4.584E-3	1.387E-4	-5.106E-7		
B_z^{or}	-9.347E+0	9.076E-3	-7.507E-5	3.609E-7		

Model Quality:

Minimum and maximum errors of the calculated Model vs. Temperature:

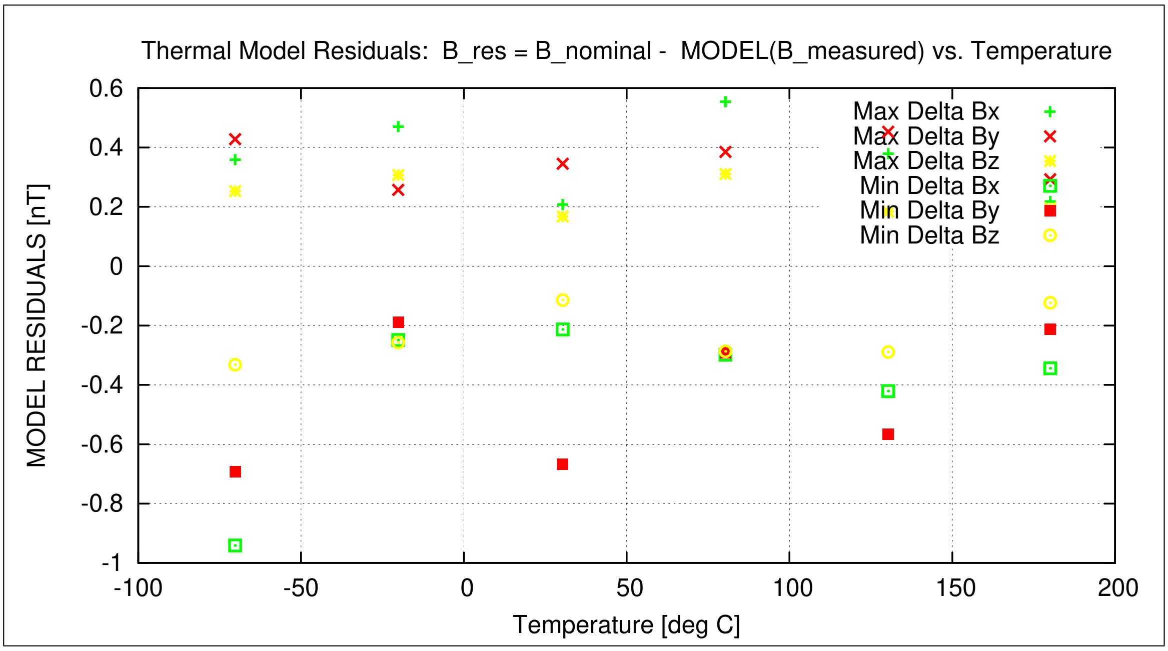

Figure 69: Residuals of Thermal Model

Sensor Rotation during Test:

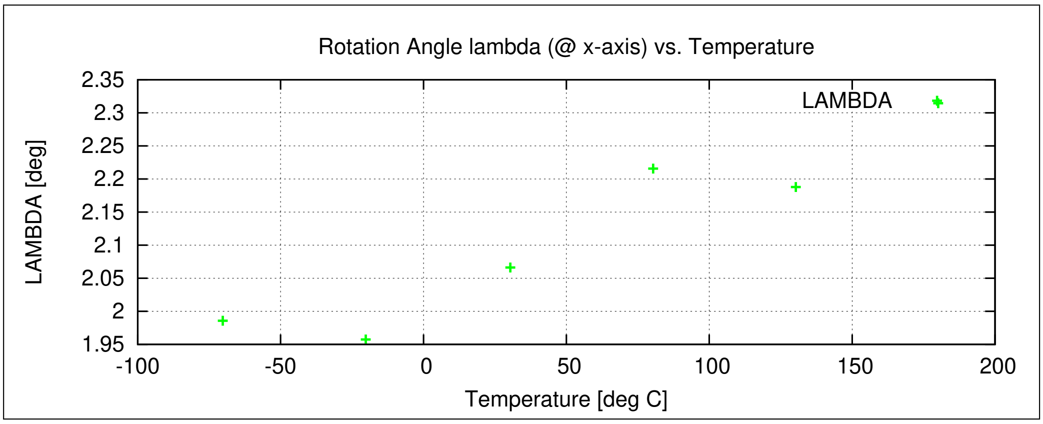

Figure 70: Rotation @ X-Axis

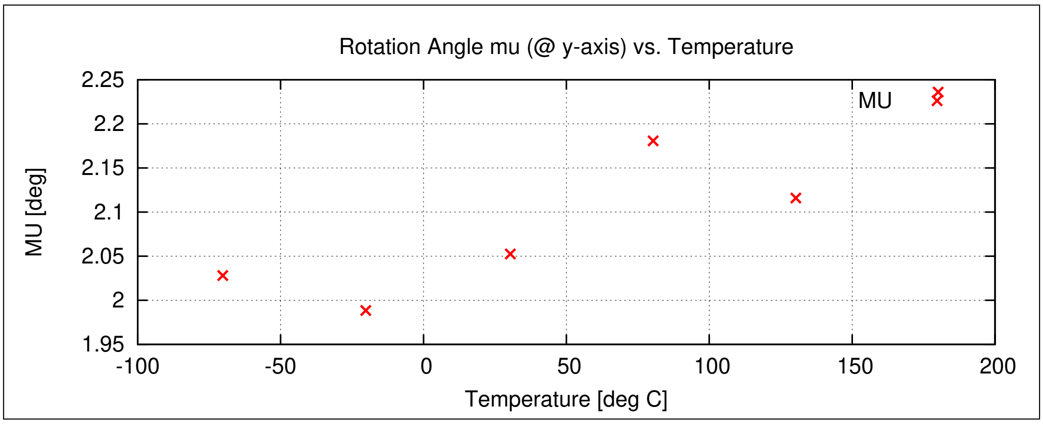

Figure 71: Rotation @ Y-Axis

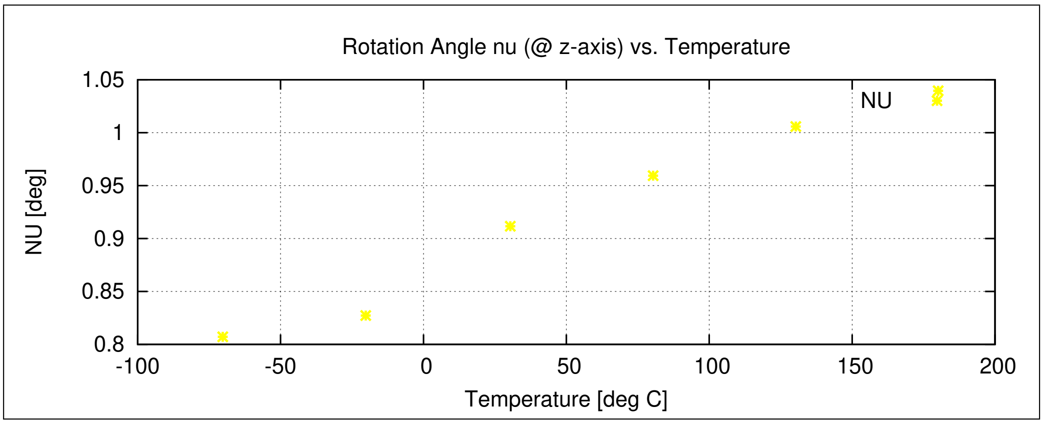

Figure 72: Rotation @ Z-Axis

12.2.2 Temperature Calibration of the Sensor Offset

Used Temperature Measurements:

Calibration Parameter File	Remark
OFF_PARAMETER__13-04-03-15-55-48.OPF	
OFF_PARAMETER__13-04-04-07-54-10.OPF	
OFF_PARAMETER__13-04-04-11-22-26.OPF	
OFF_PARAMETER__13-04-04-13-05-27.OPF	
OFF_PARAMETER__13-04-08-11-46-06.OPF	
OFF_PARAMETER__13-04-08-13-56-15.OPF	

Thermal Parameter File: THERMAL_OFF_PARAMETER__13-04-03-15-55-48.TOF

Facility Parameter:

Nominal Sensor Setup $\underline{B}_{\mathrm{DUT}} = \underline{\underline{R}}_{\mathrm{nom}} \underline{B}_{\mathrm{C}}$

$$\underline{\underline{R}}_{\mathrm{nom}} = \begin{pmatrix} +1.000000 & +0.000000 & +0.000000 \\ +0.000000 & +1.000000 & +0.000000 \\ +0.000000 & +0.000000 & +1.000000 \end{pmatrix}$$

Sensor Temperature Channel: T_{59}

Coil System Temperature Channel: T_{29}

Temperature Profile

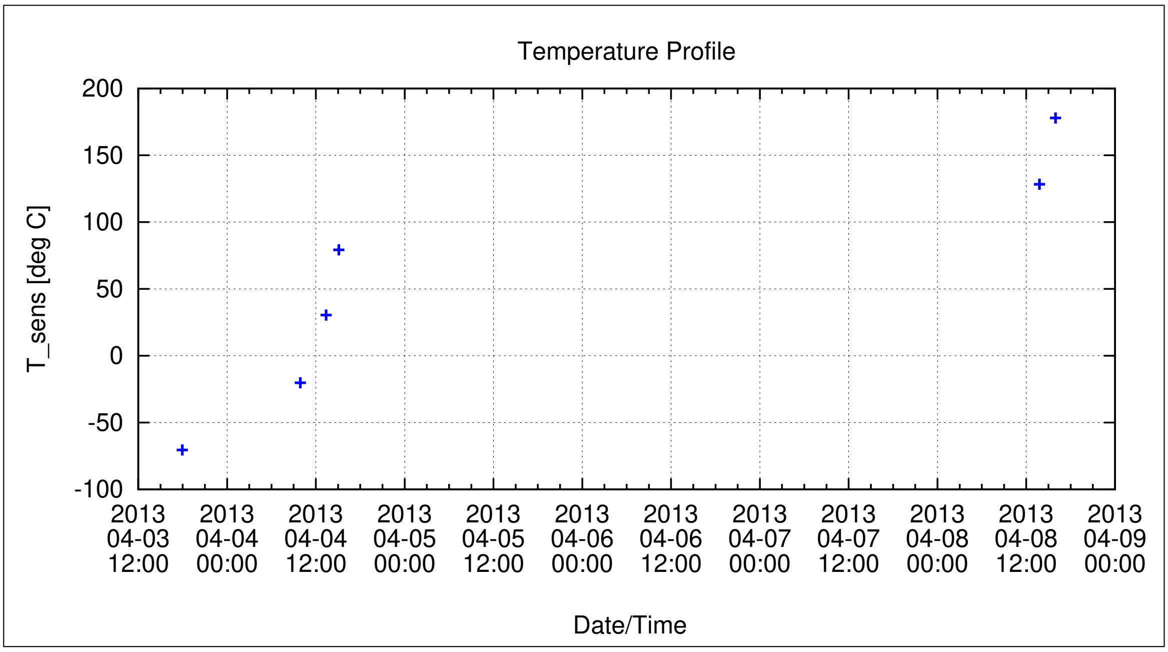

Figure 73: Temperature Profile

Calibration Parameter:

Sensor Offset $\underline{B}_{\text{off}}$ vs. Temperature:

$$B_{\text{off,i}}(T) = \sum_{k=0}^{n} B_{\text{off,k,i}} T^k \qquad [\text{enT}, \ ^\circ\text{C}], \ \text{i}=\{\text{x,y,z}\}$$

	$B_{\text{off,0,i}}$	$B_{\text{off,1,i}}$	$B_{\text{off,2,i}}$	$B_{\text{off,3,i}}$	$B_{\text{off,4,i}}$	$B_{\text{off,5,i}}$
$B_{\text{off,x}}$	-2.11499E-1	3.43452E-3	3.65776E-5	-3.04488E-7		
$B_{\text{off,y}}$	9.20378E-1	-4.22661E-3	1.35052E-4	-4.54142E-7		
$B_{\text{off,z}}$	1.60582E+0	1.55047E-3	-5.85991E-5	3.47774E-7		

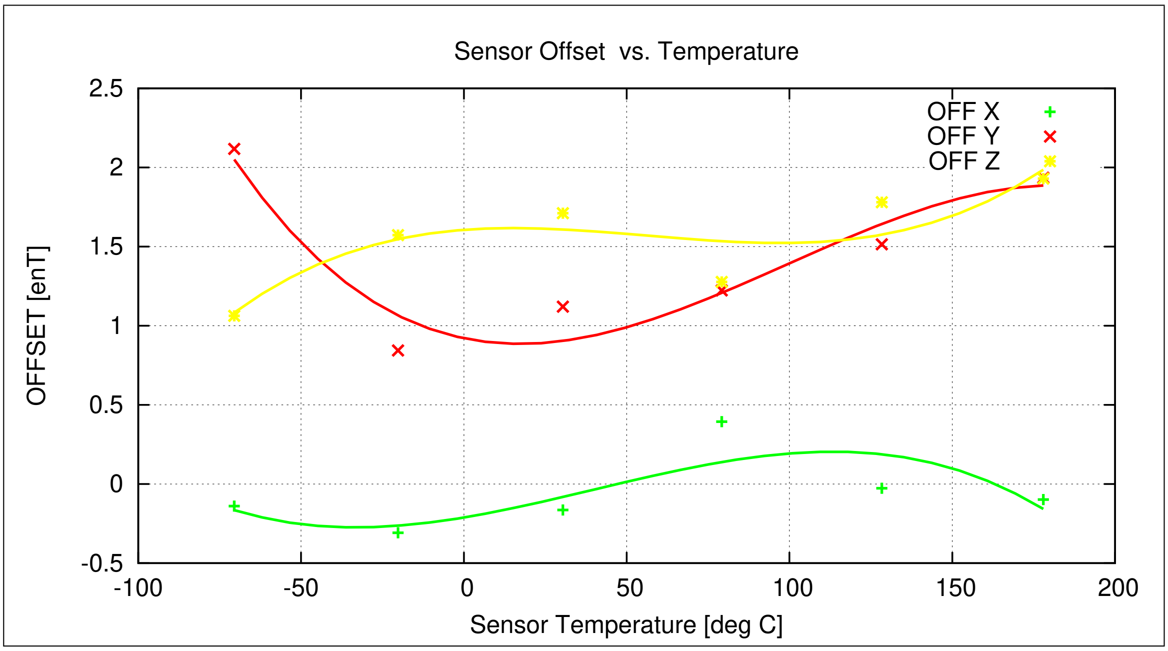

Figure 74: Temperature dependence of Sensor Offsets

Coil System Temperature

The following graph shows the mean Coil System temperature during the complete thermal cycle for the offset measurements.

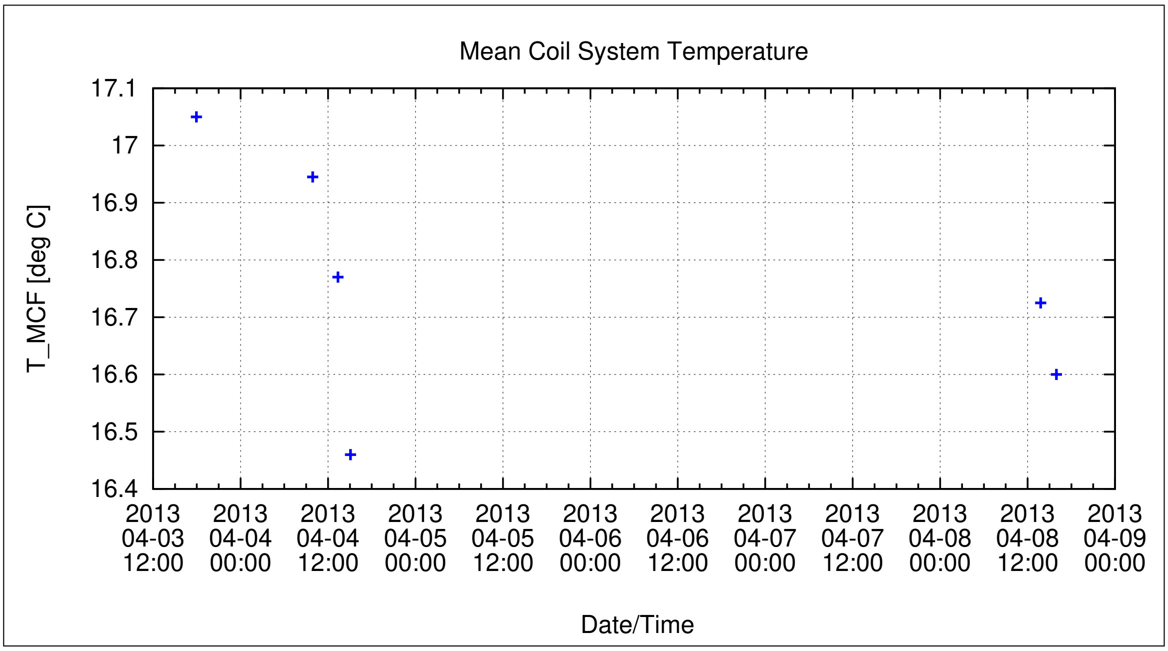

Figure 75: Coil System Temperature during Thermal Measurements

Coil System Residual Field:

The following graph shows the three components of the Coil System Residual field during the whole measurement. Axes designators are related to the actual DUT coordinate system and NOT to Coil System coordinates.

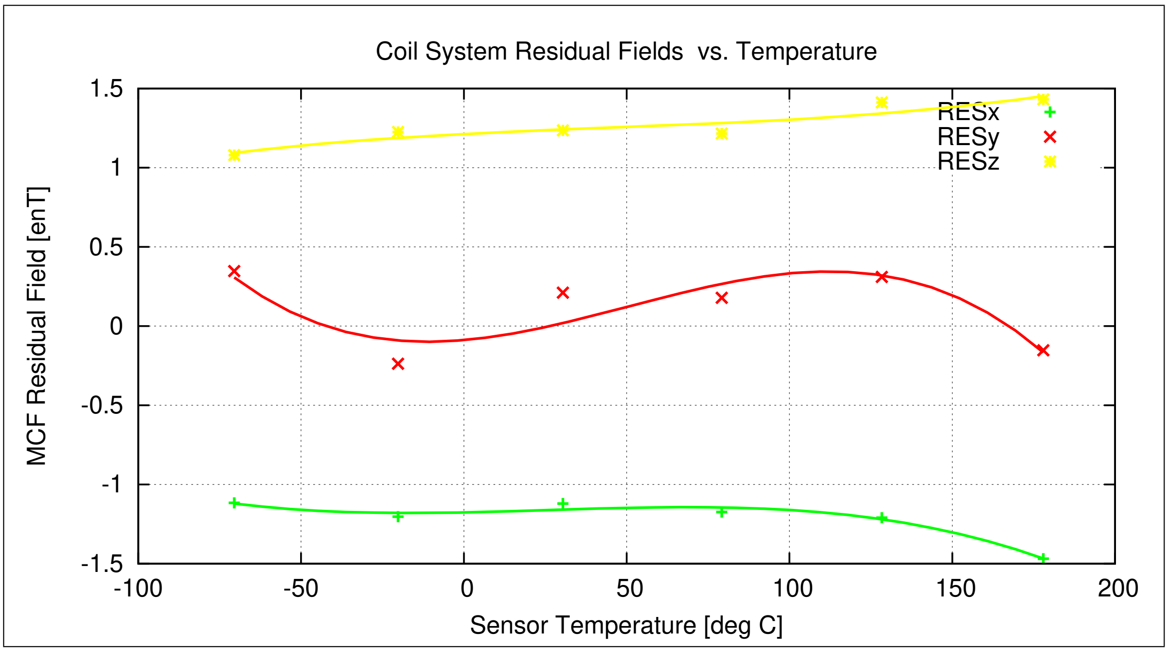

Figure 76: Coil System Residual Fields during Thermal Measurements

Remark:

The axes designation for this graph is given as follows (rf. to setup defined in chapter 1):

$$X_m = X_c$$
$$Y_m = Y_c$$
$$Z_m = -X_c$$

12.2.3 Temperature Calibration of the AC Transfer Function

Used Temperature Measurements:

Calibration Parameter File	Remark
FREQ_PARAMETER__13-04-03-14-41-31.FPF	
FREQ_PARAMETER__13-04-04-13-14-59.FPF	
FREQ_PARAMETER__13-04-08-10-31-48.FPF	
FREQ_PARAMETER__13-04-08-14-06-16.FPF	

Thermal Parameter File: THERMAL_AC_PARAMETER__13-04-03-14-41-31.TAF

Facility Parameter:

Nominal Sensor Setup: Diagonal in Space inside Thermal Box.

Sensor Temperature Channel: T_{59}

Coil System Temperature Channel: T_{29}

Temperature Profile

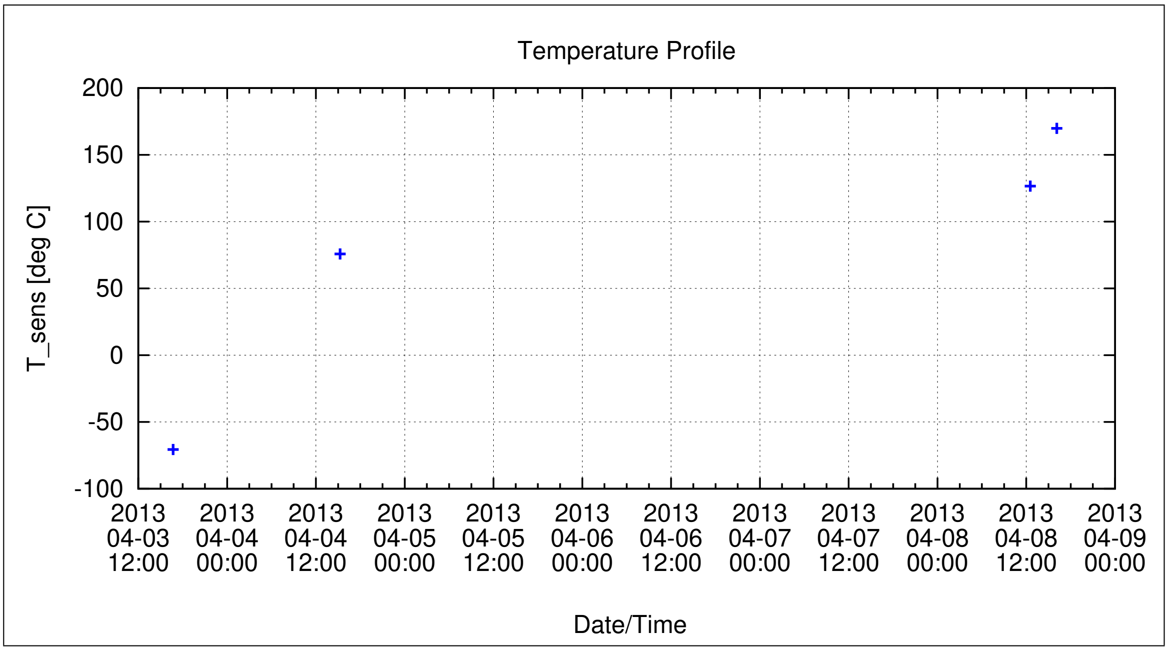

Figure 77: Temperature Profile

Coil System Temperature

The following graph shows the mean Coil System temperature during the complete thermal cycle for the AC measurements.

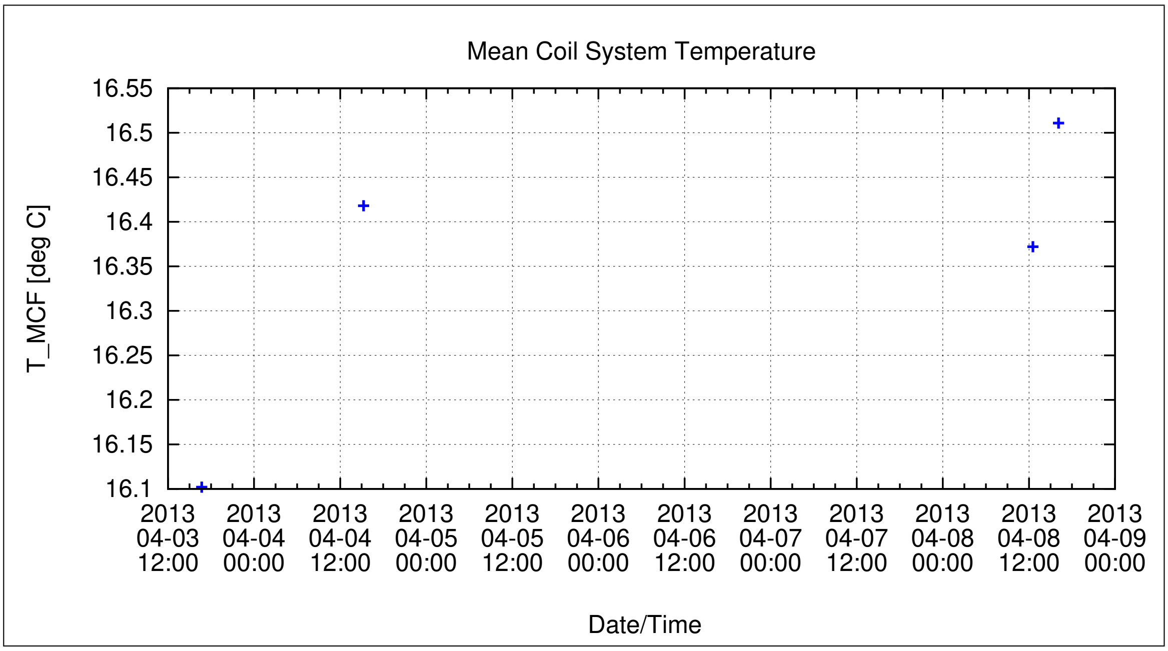

Figure 78: Coil System Temperature during Thermal AC Measurements

Calibration Parameter:

-3dB Corner Frequency f_{3dB} vs. Temperature:

$$f_{3dB,i}(T) = \sum_{k=0}^{n} f_{3dB,k,i} T^k \qquad [Hz,\ °C],\ i=\{x,y,z\}$$

	$f_{3dB,0,i}$	$f_{3dB,1,i}$	$f_{3dB,2,i}$	$f_{3dB,3,i}$	$f_{3dB,4,i}$	$f_{3dB,5,i}$
$f_{3dB,x}$	5.91894E+1	9.13759E-3				
$f_{3dB,y}$	5.91557E+1	1.06586E-2				
$f_{3dB,z}$	5.61646E+1	2.16322E-2				

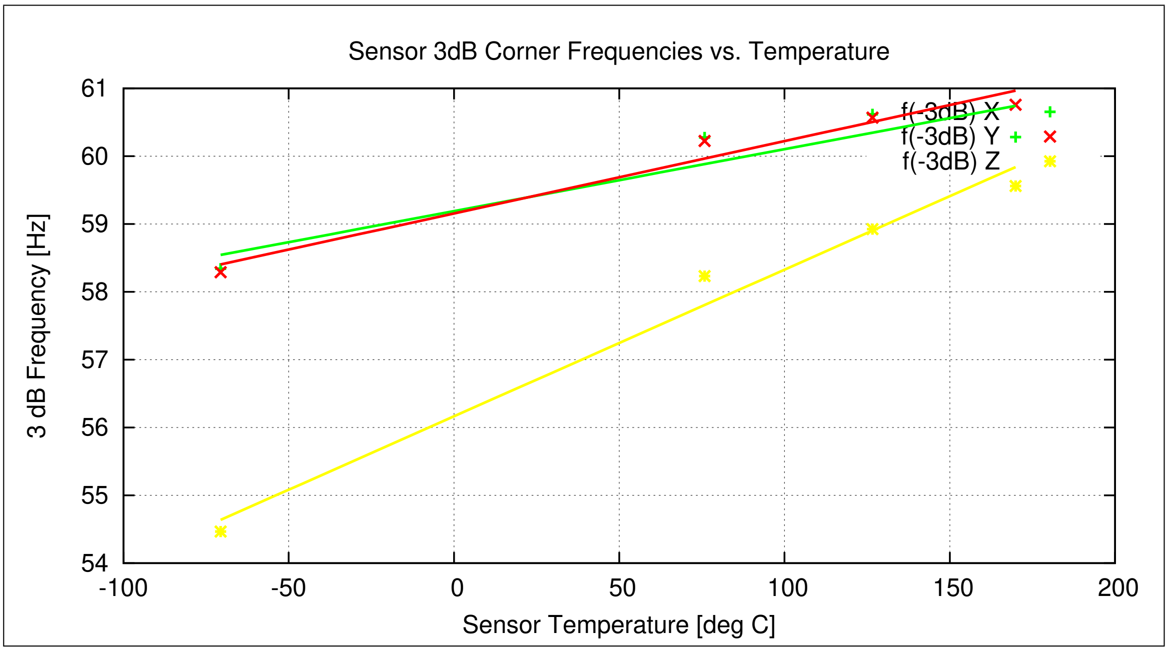

Figure 79: Temperature dependence of 3dB Corner Frequency

Instrument Sampling Frequency:

The following graph shows the calculated sampling frequencies vs. the actual sensor temperature.

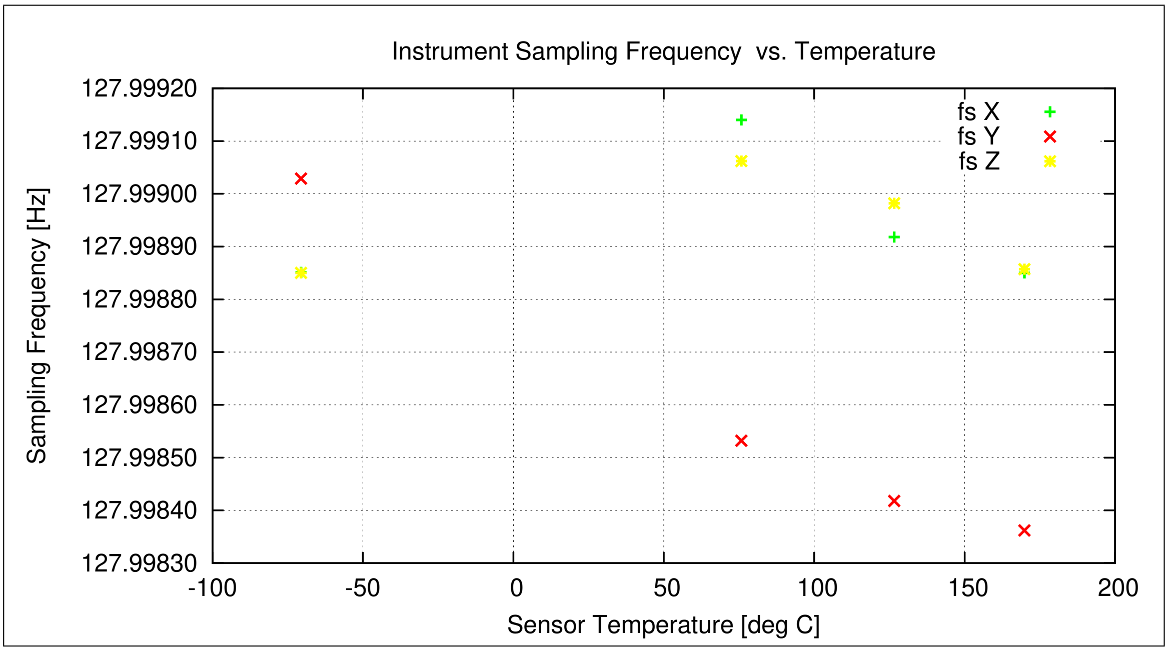

Figure 80: Instrument Sampling Frequency versus Sensor Temperature

Mean Samplerate: 127.998821 Hz.
Mean Standard Deviation of Samplerate: 0.000109 Hz.

13 Combined Measurements from April 09 – 11, 2013

13.1 Thermal-Analysis - IB Sensor, cal mode 0

13.1.1 Temperature Calibration on Linear Axes

Used Temperature Measurements:

Calibration Parameter File	Remark
PARAMETER_TEMPLIN__13-04-09_09-52-27.CPF	
PARAMETER_TEMPLIN__13-04-09_11-54-15.CPF	
PARAMETER_TEMPLIN__13-04-10_08-18-43.CPF	
PARAMETER_TEMPLIN__13-04-10_11-47-03.CPF	
PARAMETER_TEMPLIN__13-04-11_08-06-33.CPF	
PARAMETER_TEMPLIN__13-04-11_14-47-36.CPF	

Thermal Parameter File: THERMAL_PARAMETER__13-04-09-09-52-27.TPF

Facility Parameter:

Nominal Sensor Setup $\underline{B}_{\mathrm{DUT}} = \underline{\underline{R}}_{\mathrm{nom}} \underline{B}_{\mathrm{c}}$

$$\underline{\underline{R}}_{\mathrm{nom}} = \begin{pmatrix} +1.000000 & +0.000000 & +0.000000 \\ +0.000000 & +1.000000 & +0.000000 \\ +0.000000 & +0.000000 & +1.000000 \end{pmatrix}$$

Calculated Initial Sensor Rotation:

$$\underline{\underline{R}} = \begin{pmatrix} +0.999974 & +0.003127 & +0.006434 \\ -0.003132 & +0.999995 & +0.000706 \\ -0.006432 & -0.000726 & +0.999979 \end{pmatrix}$$

Initial Rotation Angles:

$$\begin{aligned} \text{Rotation @ X:} \quad \lambda_{\mathrm{x}} &= +0^\circ\ 24'36'' \\ \text{Rotation @ Y:} \quad \mu_{\mathrm{y}} &= +0^\circ\ 11'2'' \\ \text{Rotation @ Z:} \quad \nu_{\mathrm{z}} &= +0^\circ\ 22'15'' \end{aligned}$$

Determinant of Rotation Matrix: 1.0000

Nominal Field Source: SOLARTRON

Automatic Coil correction: used

Used Sensor-Temperature-Channel: T_{59}

Temperature Profile

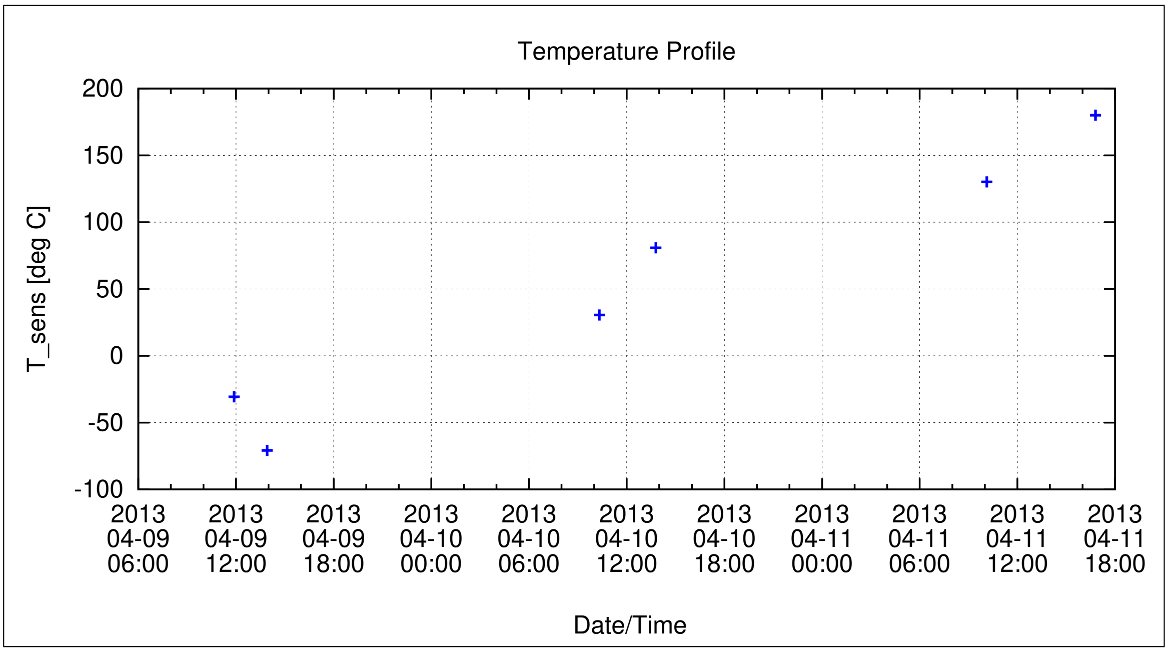

Figure 81: Temperature Profile

Calibration Parameter:

Sensitivity σ_i vs. Temperature:

$$\sigma_i(T) = \sum_{k=0}^{n} \sigma_{k,i} T^k \qquad [1,\ ^\circ\mathrm{C}],\ \mathrm{i}=\{\mathrm{x,y,z}\}$$

	$\sigma_{0,i}$	$\sigma_{1,i}$	$\sigma_{2,i}$	$\sigma_{3,i}$	$\sigma_{4,i}$	$\sigma_{5,i}$
σ_x	9.75788E-1	-1.59695E-5				
σ_y	9.88057E-1	-1.44024E-5				
σ_z	9.85916E-1	-1.77112E-5				

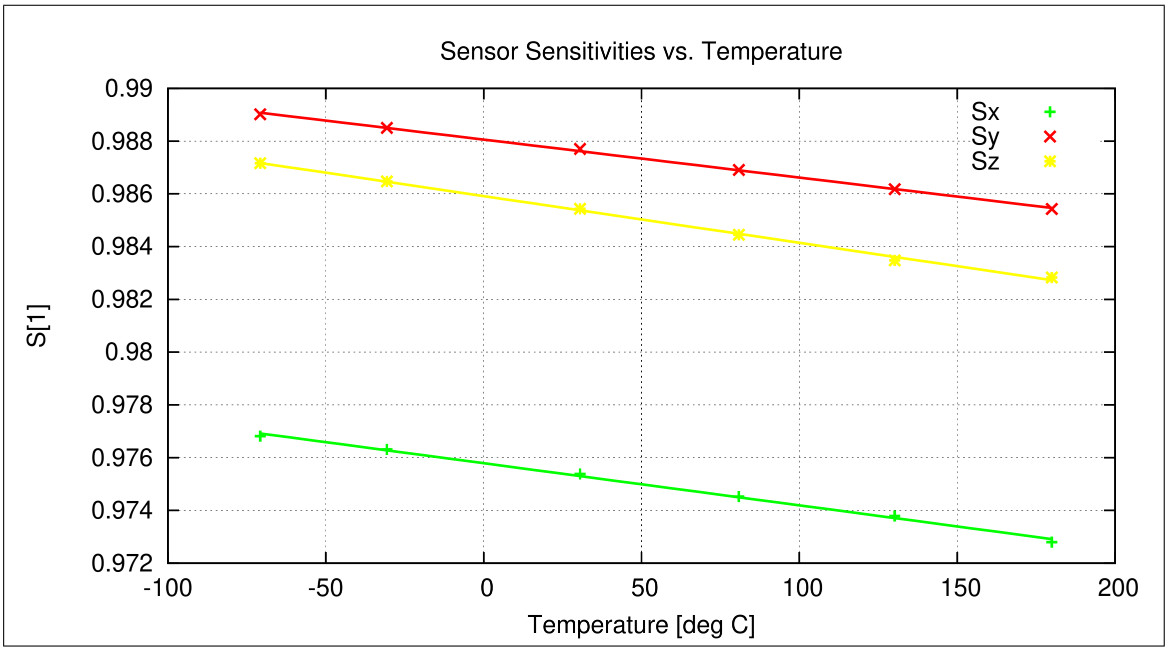

Figure 82: Temperature dependence of Sensitivities

Misalignment Angles ξ_{ij} vs. Temperature:

$$\xi_{ij}(T) = \sum_{k=0}^{n} \xi_{k,ij} T^k \qquad [\text{deg}, \ ^\circ\text{C}], \ \text{ij}= \{\text{xy,xz,yz}\}$$

	$\xi_{0,ij}$	$\xi_{1,ij}$	$\xi_{2,ij}$	$\xi_{3,ij}$	$\xi_{4,ij}$	$\xi_{5,ij}$
ξ_{xy}	8.9575E+1	5.8946E-5				
ξ_{xz}	8.9942E+1	4.1061E-5				
ξ_{yz}	9.0345E+1	-1.6514E-5				

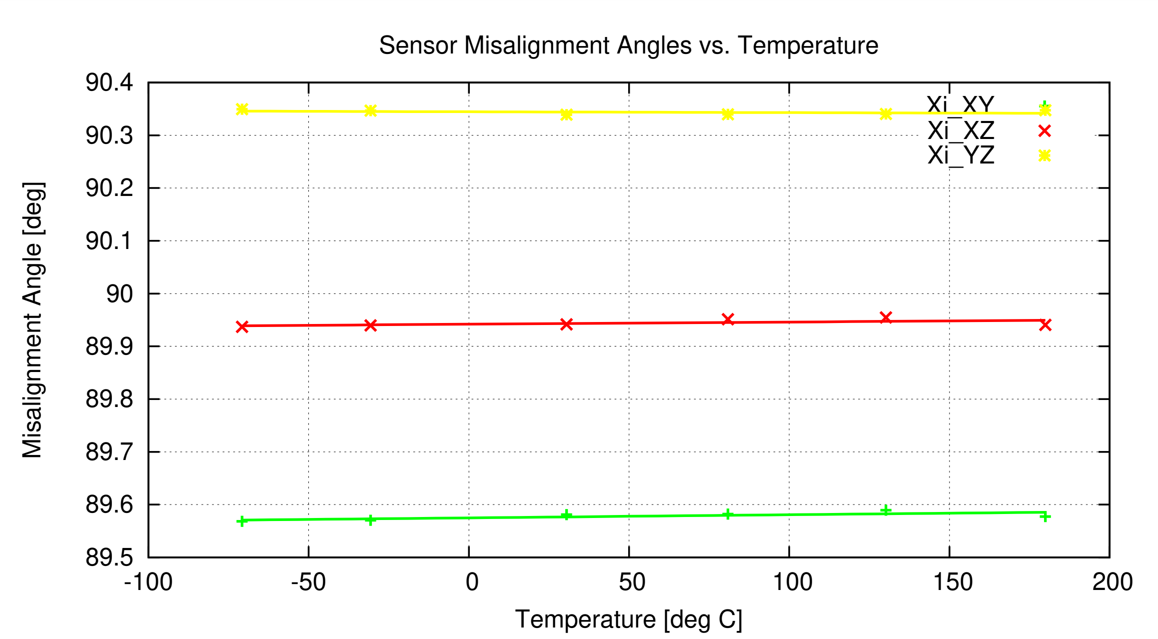

Figure 83: Temperature dependence of Misalignment Angles

Offset & Residual MCF Field $\underline{B}^{or} = \underline{B}^{off} + \underline{B}^{res}$ vs. Temperature:

$$\underline{B}^{or}(T) = \sum_{k=0}^{n} \underline{B}_k^{or} T^k \qquad [\text{enT}, {}^\circ\text{C}]$$

	$\underline{B}_0^{or}$	$\underline{B}_1^{or}$	$\underline{B}_2^{or}$	$\underline{B}_3^{or}$	$\underline{B}_4^{or}$	$\underline{B}_5^{or}$
B_x^{or}	-3.543E+0	1.981E-3	1.637E-4	-7.621E-7		
B_y^{or}	-1.315E+0	-5.537E-3	-1.109E-4	6.784E-7		
B_z^{or}	-1.075E+1	6.562E-3	9.510E-6	-6.083E-8		

Model Quality:

Minimum and maximum errors of the calculated Model vs. Temperature:

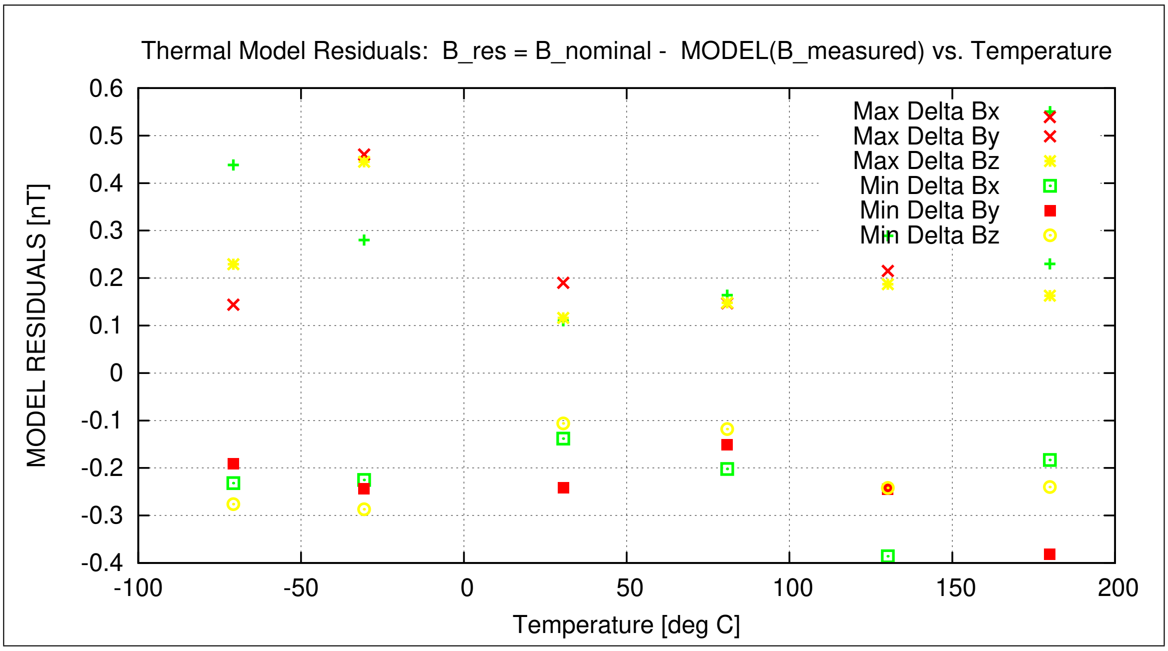

Figure 84: Residuals of Thermal Model

Sensor Rotation during Test:

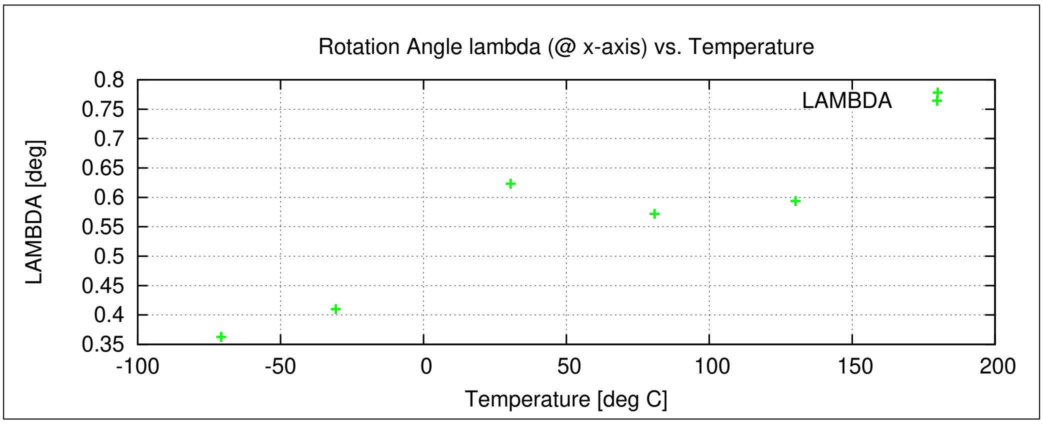

Figure 85: Rotation @ X-Axis

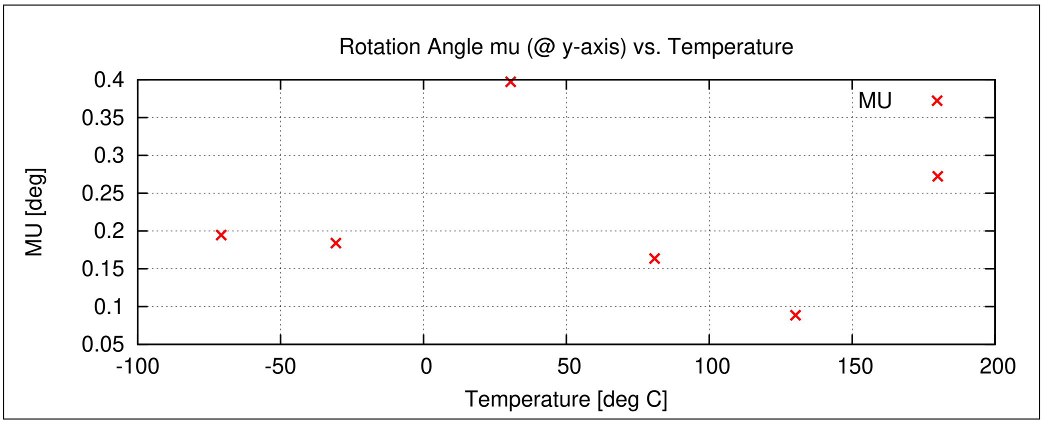

Figure 86: Rotation @ Y-Axis

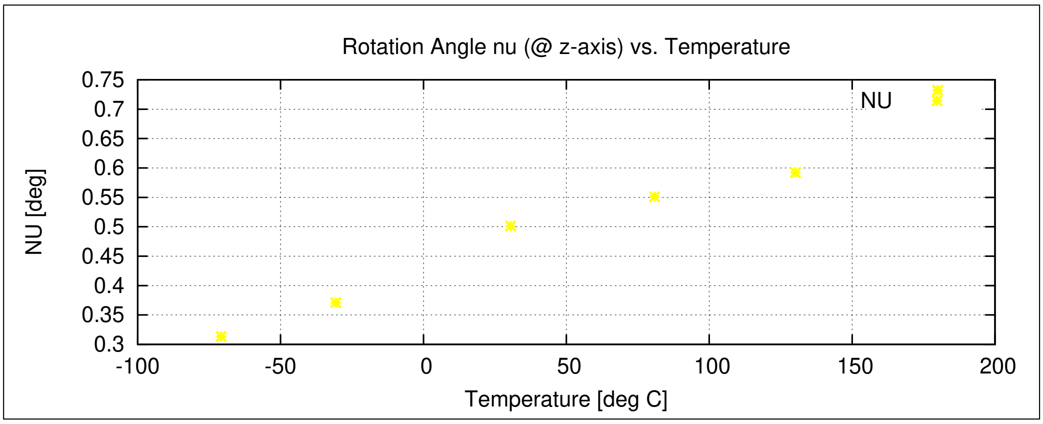

Figure 87: Rotation @ Z-Axis

13.1.2 Temperature Calibration of the Sensor Offset

Used Temperature Measurements:

Calibration Parameter File	Remark
OFF_PARAMETER__13-04-09-11-14-46.OPF	
OFF_PARAMETER__13-04-09-13-08-27.OPF	
OFF_PARAMETER__13-04-10-08-09-57.OPF	
OFF_PARAMETER__13-04-10-12-17-18.OPF	
OFF_PARAMETER__13-04-11-08-37-21.OPF	
OFF_PARAMETER__13-04-11-15-18-03.OPF	

Thermal Parameter File: `THERMAL_OFF_PARAMETER__13-04-09-11-14-46.TOF`

Facility Parameter:

Nominal Sensor Setup $\underline{B}_{\mathrm{DUT}} = \underline{\underline{R}}_{\mathrm{nom}} \underline{B}_{\mathrm{c}}$

$$\underline{\underline{R}}_{\mathrm{nom}} = \begin{pmatrix} +1.000000 & +0.000000 & +0.000000 \\ +0.000000 & +1.000000 & +0.000000 \\ +0.000000 & +0.000000 & +1.000000 \end{pmatrix}$$

Sensor Temperature Channel: T_{59}

Coil System Temperature Channel: T_{29}

Temperature Profile

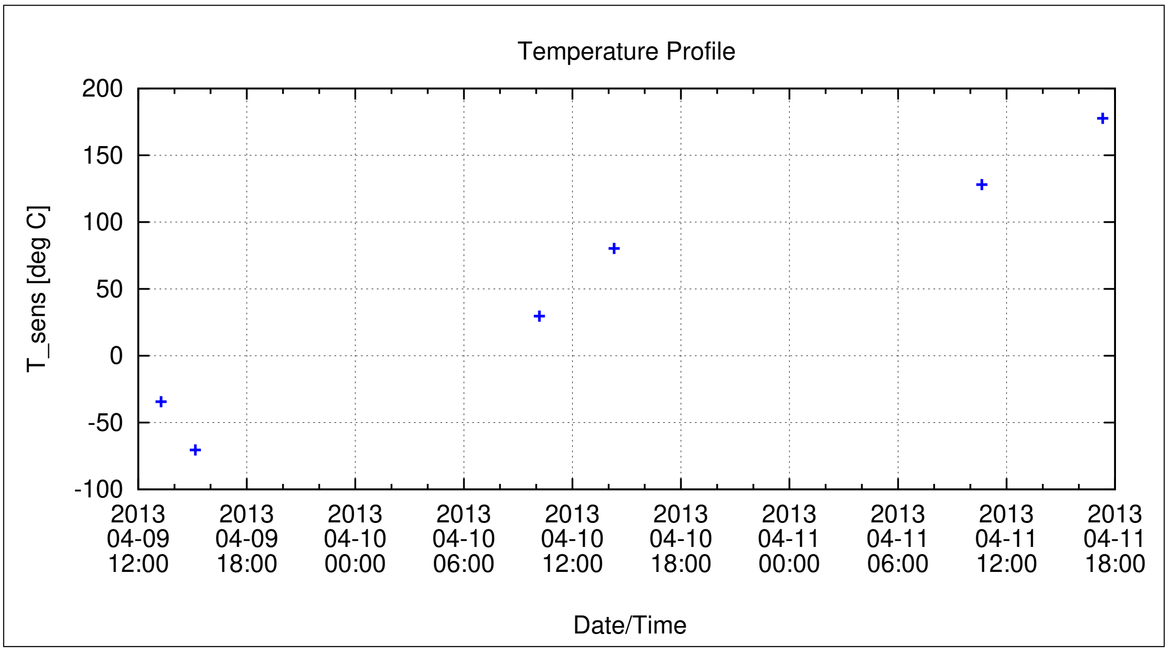

Figure 88: Temperature Profile

Calibration Parameter:

Sensor Offset $\underline{B}_{\rm off}$ vs. Temperature:

$$B_{\rm off,i}(T) = \sum_{k=0}^{n} B_{\rm off,k,i} T^k \qquad [\text{enT},\ ^\circ\text{C}],\ \text{i}=\{\text{x,y,z}\}$$

	$B_{\rm off,0,i}$	$B_{\rm off,1,i}$	$B_{\rm off,2,i}$	$B_{\rm off,3,i}$	$B_{\rm off,4,i}$	$B_{\rm off,5,i}$
$B_{\rm off,x}$	-2.92971E-1	-3.69506E-3	4.77003E-5			
$B_{\rm off,y}$	-1.05443E+0	-1.72164E-3	1.51567E-5			
$B_{\rm off,z}$	1.46463E-1	3.34259E-3	-2.31102E-5			

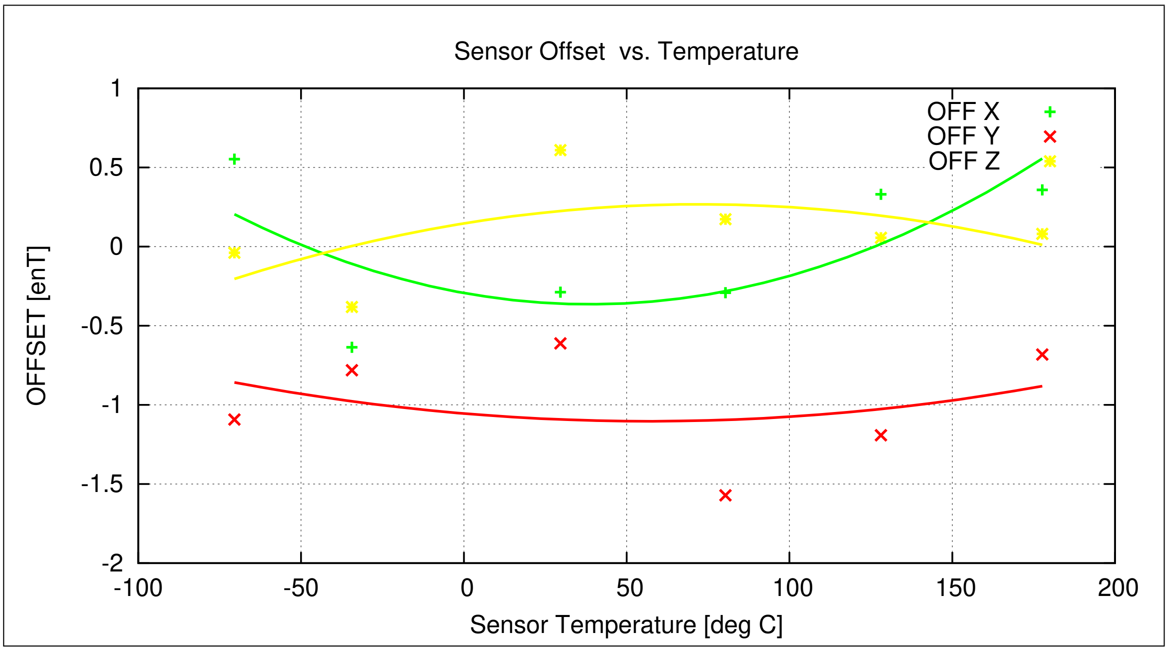

Figure 89: Temperature dependence of Sensor Offsets

Coil System Temperature

The following graph shows the mean Coil System temperature during the complete thermal cycle for the offset measurements.

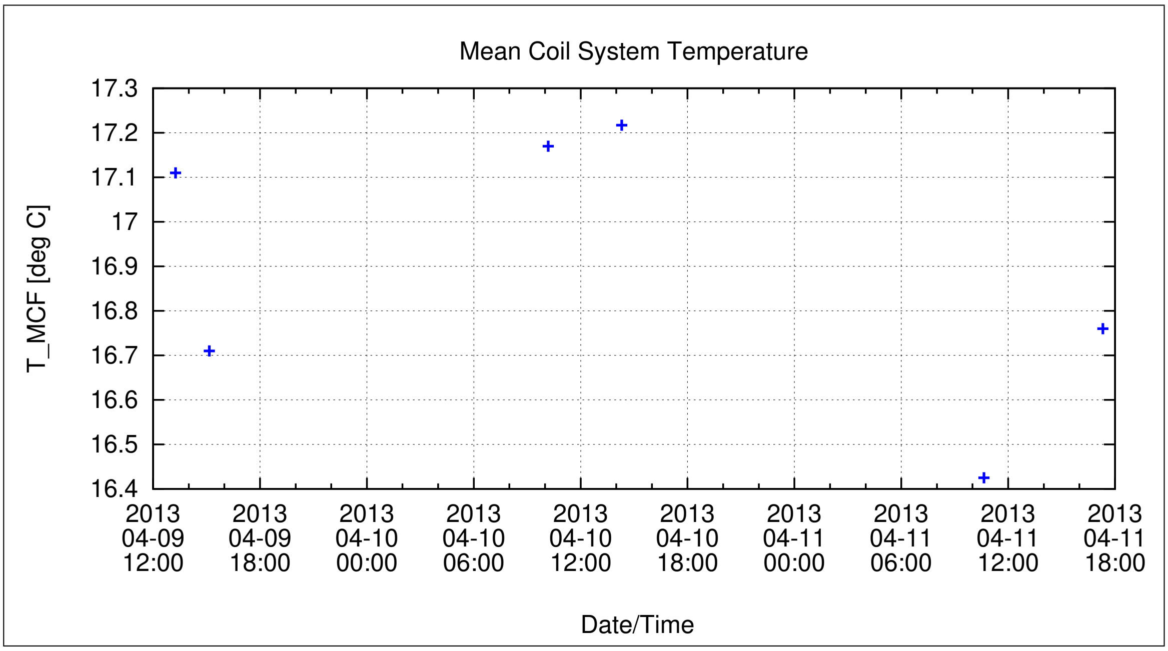

Figure 90: Coil System Temperature during Thermal Measurements

Coil System Residual Field:

The following graph shows the three components of the Coil System Residual field during the whole measurement. Axes designators are related to the actual DUT coordinate system and NOT to Coil System coordinates.

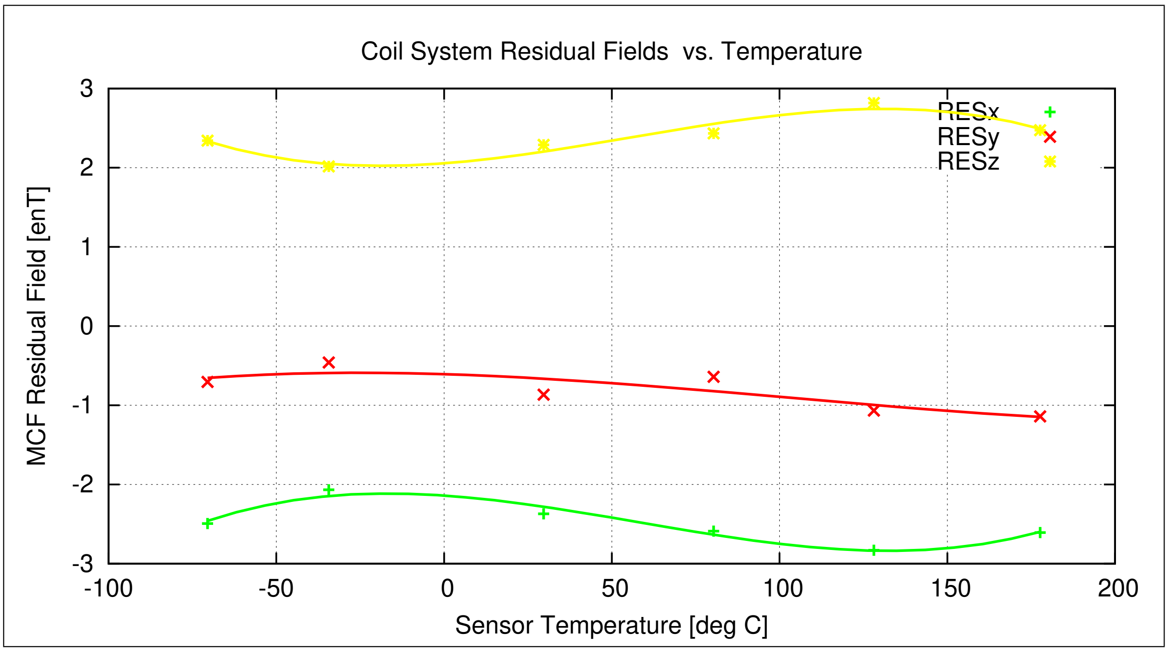

Figure 91: Coil System Residual Fields during Thermal Measurements

Remark:

The axes designation for this graph is given as follows (rf. to setup defined in chapter 1):

$$\begin{array}{|rcr|} X_m & = & X_c \\ Y_m & = & Y_c \\ Z_m & = & -X_c \end{array}$$

13.1.3 Temperature Calibration of the AC Transfer Function

Used Temperature Measurements:

Calibration Parameter File	Remark
FREQ_PARAMETER__13-04-09-12-26-36.FPF	
FREQ_PARAMETER__13-04-10-12-26-40.FPF	
FREQ_PARAMETER__13-04-11-08-46-10.FPF	
FREQ_PARAMETER__13-04-11-15-26-22.FPF	

Thermal Parameter File: THERMAL_AC_PARAMETER__13-04-09-12-26-36.TAF

Facility Parameter:

Nominal Sensor Setup: Diagonal in Space inside Thermal Box.

Sensor Temperature Channel: T_{59}

Coil System Temperature Channel: T_{29}

Temperature Profile

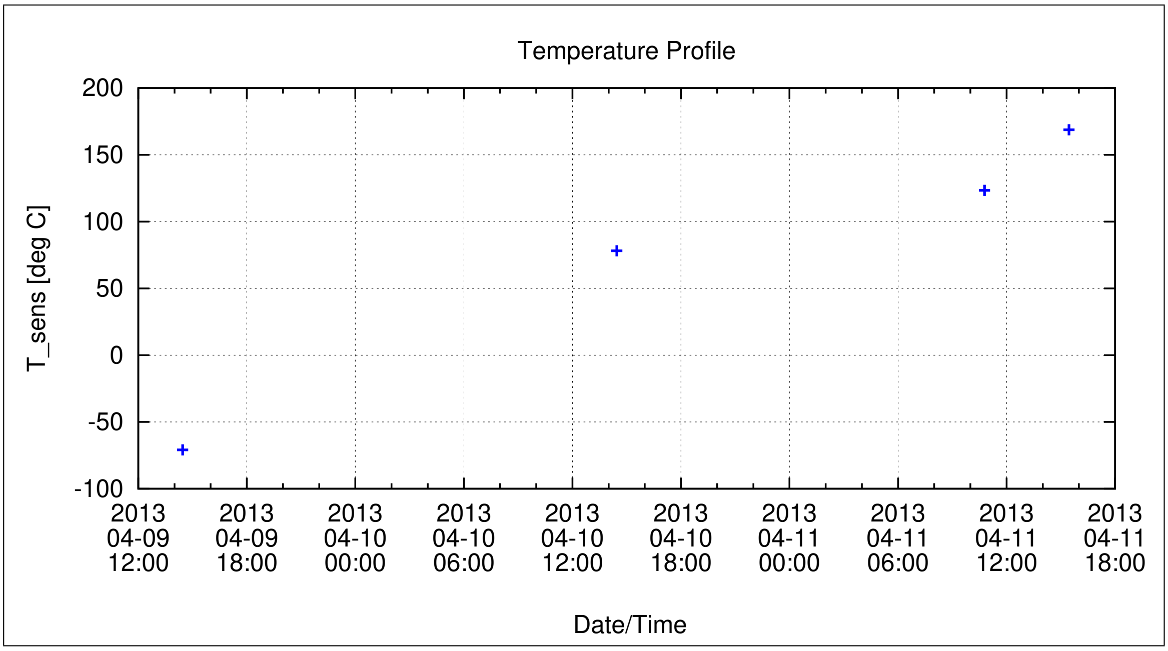

Figure 92: Temperature Profile

Coil System Temperature

The following graph shows the mean Coil System temperature during the complete thermal cycle for the AC measurements.

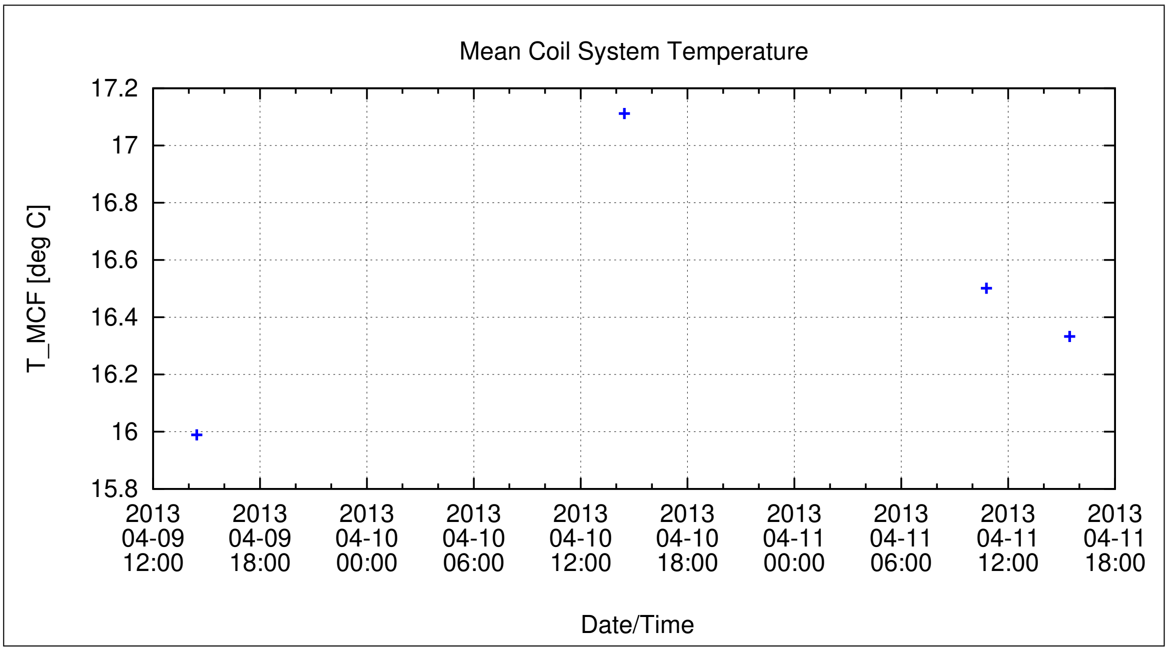

Figure 93: Coil System Temperature during Thermal AC Measurements

Calibration Parameter:

-3dB Corner Frequency $f_{3\text{dB}}$ vs. Temperature:

$$f_{3\text{dB,i}}(T) = \sum_{k=0}^{n} f_{3\text{dB,k,i}} T^k \qquad [\text{Hz}, \ ^\circ\text{C}], \ \text{i}=\{\text{x,y,z}\}$$

	$f_{3\text{dB,0,i}}$	$f_{3\text{dB,1,i}}$	$f_{3\text{dB,2,i}}$	$f_{3\text{dB,3,i}}$	$f_{3\text{dB,4,i}}$	$f_{3\text{dB,5,i}}$
$f_{3\text{dB,x}}$	5.23089E+1	-1.76236E-1	4.32362E-4			
$f_{3\text{dB,y}}$	4.80020E+1	-2.09909E-1	5.51143E-4			
$f_{3\text{dB,z}}$	5.28160E+1	-3.41876E-2	8.18077E-5			

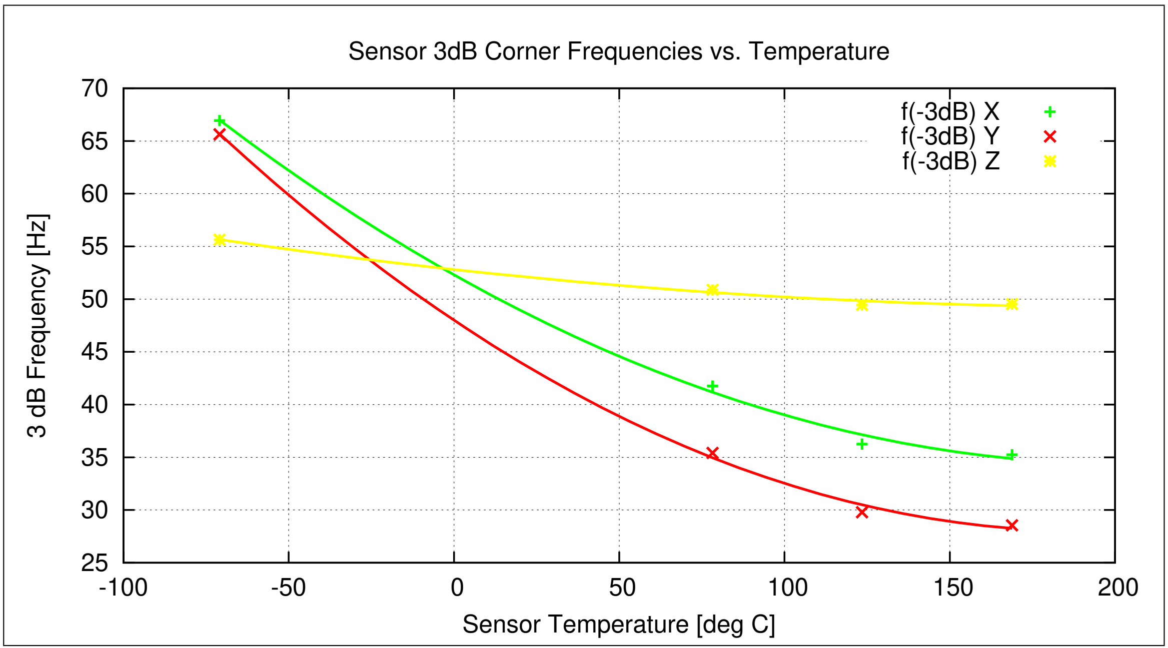

Figure 94: Temperature dependence of 3dB Corner Frequency

Instrument Sampling Frequency:

The following graph shows the calculated sampling frequencies vs. the actual sensor temperature.

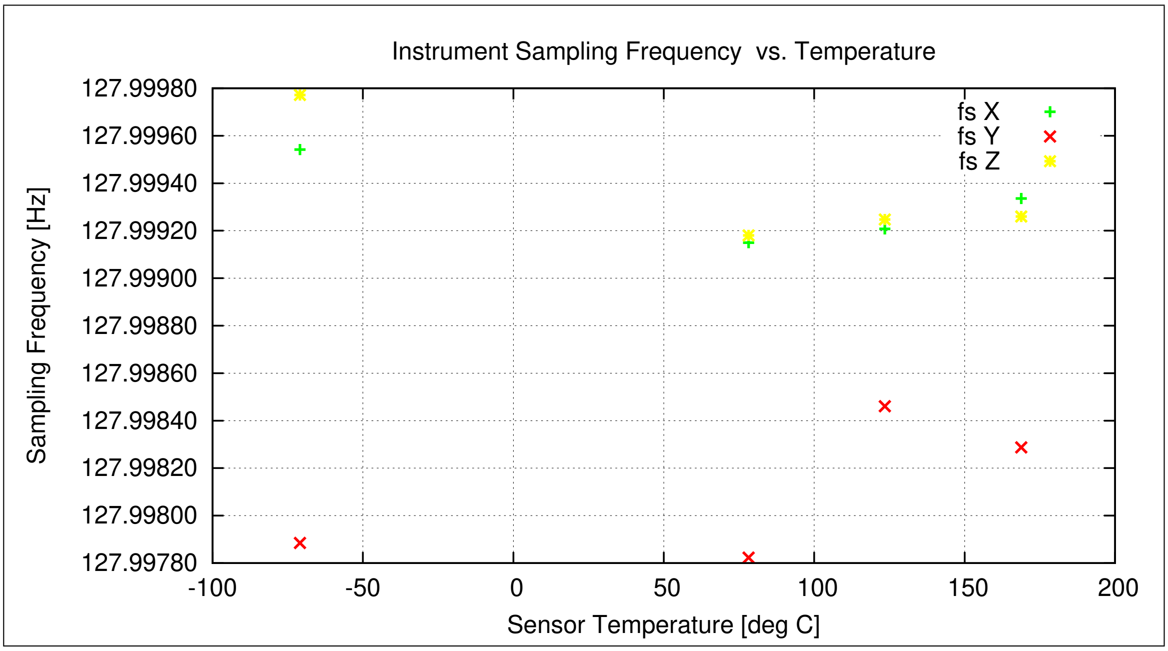

Figure 95: Instrument Sampling Frequency versus Sensor Temperature

Mean Samplerate: 127.998929 Hz.
Mean Standard Deviation of Samplerate: 0.000149 Hz.

13.2 Thermal-Analysis - IB Sensor, cal mode 4

13.2.1 Temperature Calibration on Linear Axes

Used Temperature Measurements:

Calibration Parameter File	Remark
PARAMETER_TEMPLIN__13-04-09_10-34-40.CPF	
PARAMETER_TEMPLIN__13-04-09_14-12-36.CPF	
PARAMETER_TEMPLIN__13-04-10_07-28-44.CPF	
PARAMETER_TEMPLIN__13-04-10_13-11-42.CPF	
PARAMETER_TEMPLIN__13-04-11_09-31-53.CPF	
PARAMETER_TEMPLIN__13-04-11_12-35-43.CPF	
PARAMETER_TEMPLIN__13-04-11_13-06-41.CPF	

Thermal Parameter File: THERMAL_PARAMETER__13-04-09-10-34-40.TPF

Facility Parameter:

Nominal Sensor Setup $\underline{B}_{\mathrm{DUT}} = \underline{\underline{R}}_{\mathrm{nom}} \underline{B}_{\mathrm{C}}$

$$\underline{\underline{R}}_{\mathrm{nom}} = \begin{pmatrix} +1.000000 & +0.000000 & +0.000000 \\ +0.000000 & +1.000000 & +0.000000 \\ +0.000000 & +0.000000 & +1.000000 \end{pmatrix}$$

Calculated Initial Sensor Rotation:

$$\underline{\underline{R}} = \begin{pmatrix} +0.999707 & +0.023539 & +0.005617 \\ -0.023561 & +0.999715 & +0.003876 \\ -0.005524 & -0.004007 & +0.999977 \end{pmatrix}$$

Initial Rotation Angles:

$$\begin{aligned} \text{Rotation @ X:} \quad & \lambda_{\mathrm{x}} = && +1^\circ\ 23'12'' \\ \text{Rotation @ Y:} \quad & \mu_{\mathrm{y}} = && +1^\circ\ 22'6'' \\ \text{Rotation @ Z:} \quad & \nu_{\mathrm{z}} = && +0^\circ\ 23'28'' \end{aligned}$$

Determinant of Rotation Matrix: 1.0000

Nominal Field Source: FLDS

Automatic Coil correction: used

Used Sensor-Temperature-Channel: T_{59}

Temperature Profile

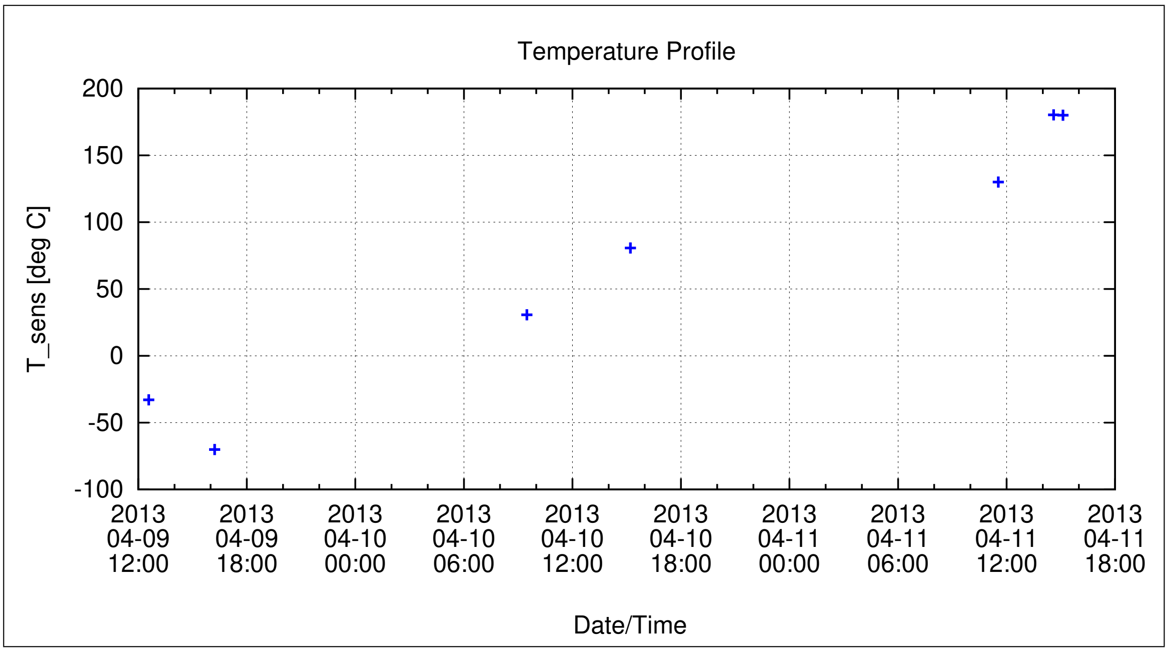

Figure 96: Temperature Profile

Calibration Parameter:

Sensitivity σ_i vs. Temperature:

$$\sigma_i(T) = \sum_{k=0}^{n} \sigma_{k,i} T^k \qquad [1,\ ^\circ\mathrm{C}],\ \mathrm{i}=\{\mathrm{x,y,z}\}$$

	$\sigma_{0,i}$	$\sigma_{1,i}$	$\sigma_{2,i}$	$\sigma_{3,i}$	$\sigma_{4,i}$	$\sigma_{5,i}$
σ_x	1.01127E+0	1.13608E-3				
σ_y	1.02445E+0	1.39015E-3				
σ_z	9.74889E-1	4.76147E-4				

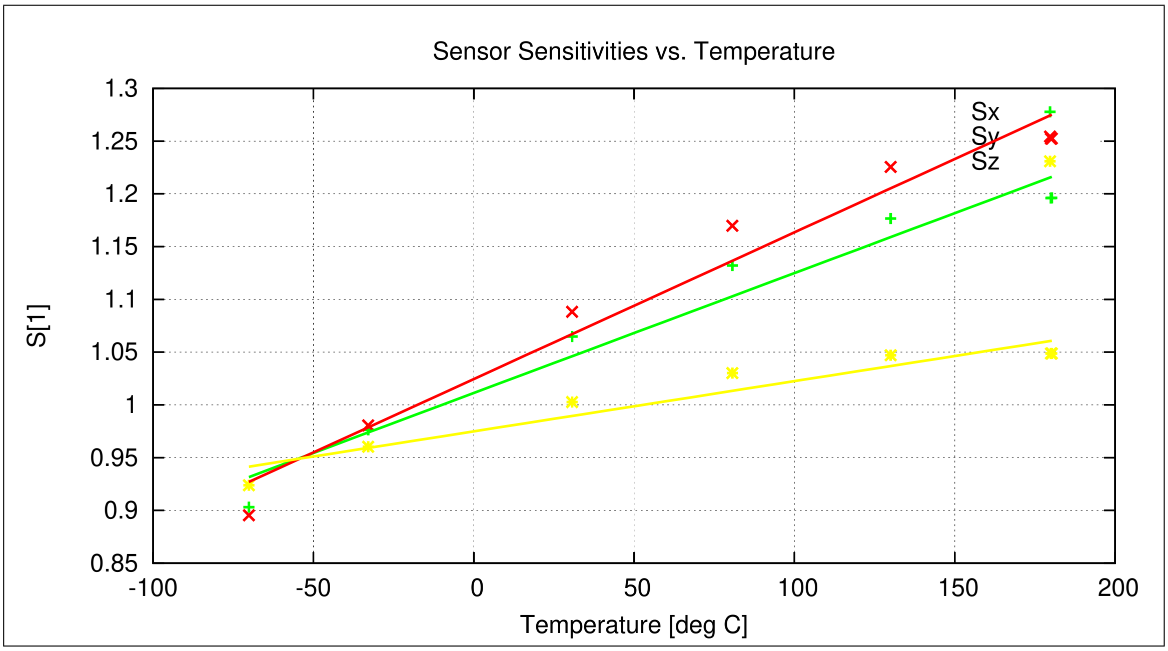

Figure 97: Temperature dependence of Sensitivities

Misalignment Angles ξ_{ij} vs. Temperature:

$$\xi_{ij}(T) = \sum_{k=0}^{n} \xi_{k,ij} T^k \qquad [\text{deg}, \ ^\circ\text{C}], \ \text{ij} = \{\text{xy,xz,yz}\}$$

	$\xi_{0,ij}$	$\xi_{1,ij}$	$\xi_{2,ij}$	$\xi_{3,ij}$	$\xi_{4,ij}$	$\xi_{5,ij}$
ξ_{xy}	9.0177E+1	1.0107E-3				
ξ_{xz}	8.9516E+1	-4.8192E-4				
ξ_{yz}	9.0554E+1	-1.7089E-3				

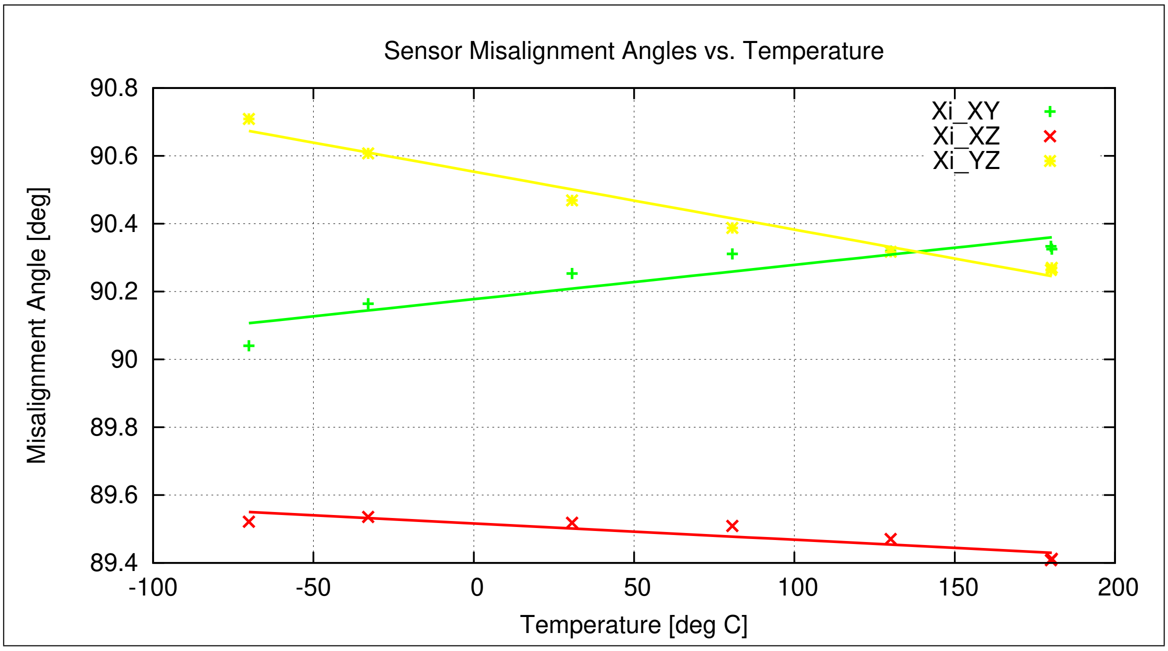

Figure 98: Temperature dependence of Misalignment Angles

Offset & Residual MCF Field $\underline{B}^{or} = \underline{B}^{off} + \underline{B}^{res}$ vs. Temperature:

$$\underline{B}^{or}(T) = \sum_{k=0}^{n} \underline{B}_k^{or} T^k \qquad [\text{enT}, {}^\circ\text{C}]$$

	$\underline{B}_0^{or}$	$\underline{B}_1^{or}$	$\underline{B}_2^{or}$	$\underline{B}_3^{or}$	$\underline{B}_4^{or}$	$\underline{B}_5^{or}$
B_x^{or}	-2.626E+0	1.250E-2	-7.866E-5	2.016E-7		
B_y^{or}	-1.160E+0	-5.595E-3	-7.993E-5	5.415E-7		
B_z^{or}	-1.065E+1	7.654E-3	8.301E-5	-4.486E-7		

Model Quality:

Minimum and maximum errors of the calculated Model vs. Temperature:

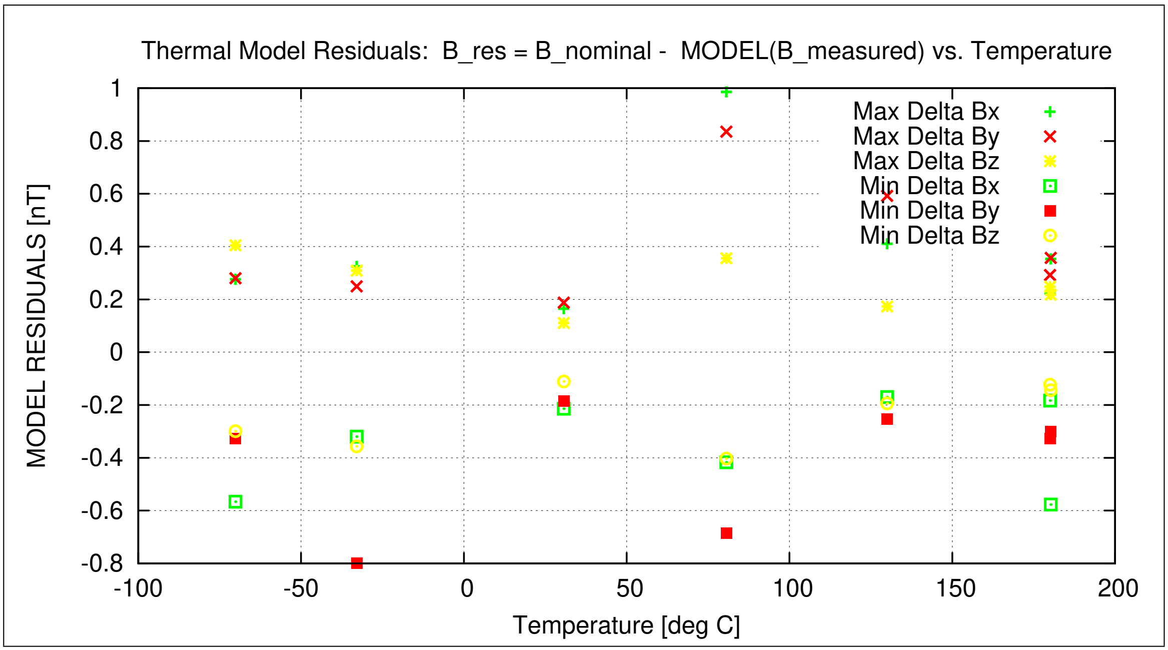

Figure 99: Residuals of Thermal Model

Sensor Rotation during Test:

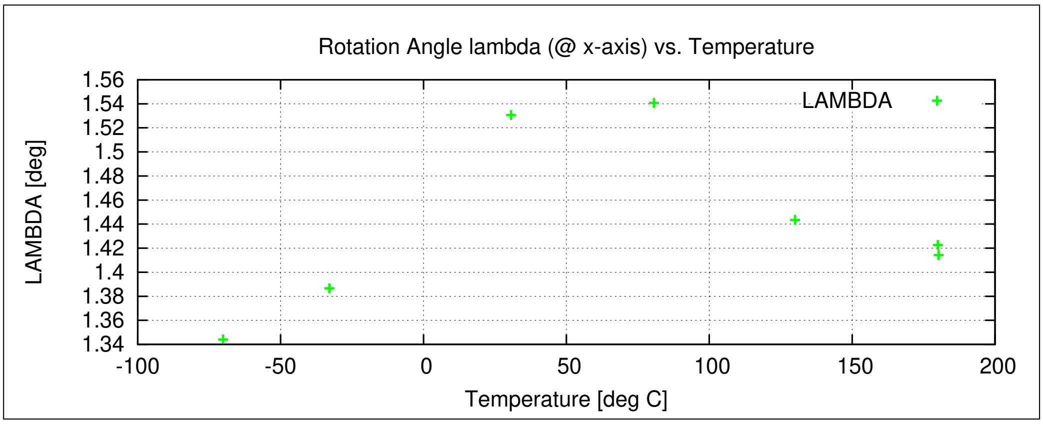

Figure 100: Rotation @ X-Axis

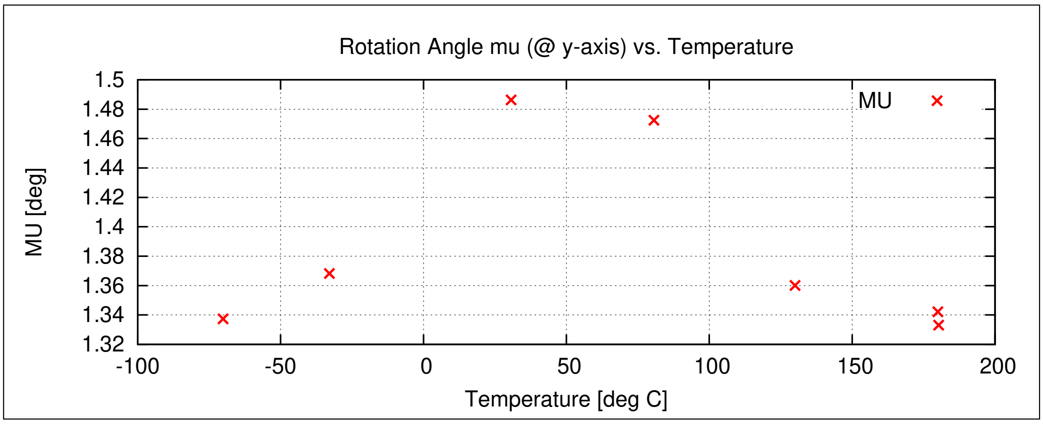

Figure 101: Rotation @ Y-Axis

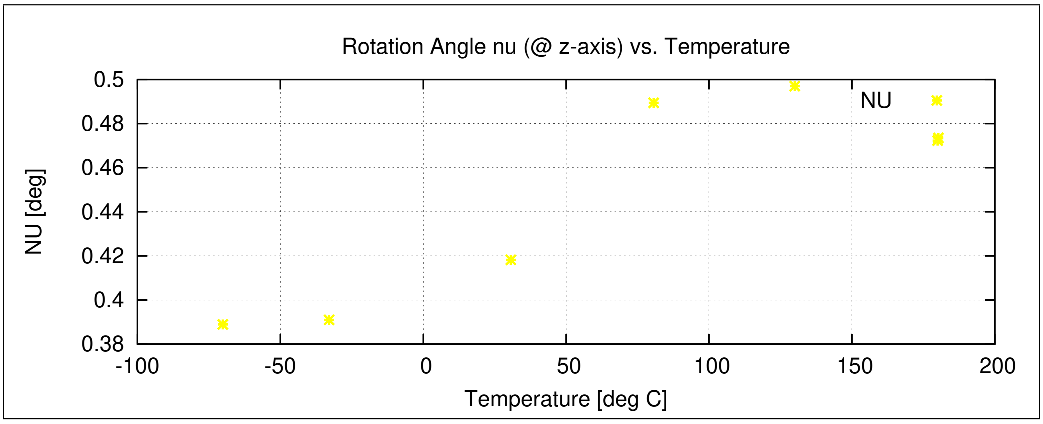

Figure 102: Rotation @ Z-Axis

13.2.2 Temperature Calibration of the Sensor Offset

Used Temperature Measurements:

Calibration Parameter File	Remark
OFF_PARAMETER__13-04-09-11-05-13.OPF	
OFF_PARAMETER__13-04-09-13-18-15.OPF	
OFF_PARAMETER__13-04-10-07-59-38.OPF	
OFF_PARAMETER__13-04-10-13-47-06.OPF	
OFF_PARAMETER__13-04-11-10-11-50.OPF	
OFF_PARAMETER__13-04-11-13-37-03.OPF	

Thermal Parameter File: THERMAL_OFF_PARAMETER__13-04-09-11-05-13.TOF

Facility Parameter:

Nominal Sensor Setup $\underline{B}_{\mathrm{DUT}} = \underline{\underline{R}}_{\mathrm{nom}} \underline{B}_{\mathrm{c}}$

$$\underline{\underline{R}}_{\mathrm{nom}} = \begin{pmatrix} +1.000000 & +0.000000 & +0.000000 \\ +0.000000 & +1.000000 & +0.000000 \\ +0.000000 & +0.000000 & +1.000000 \end{pmatrix}$$

Sensor Temperature Channel: T_{59}

Coil System Temperature Channel: T_{29}

Temperature Profile

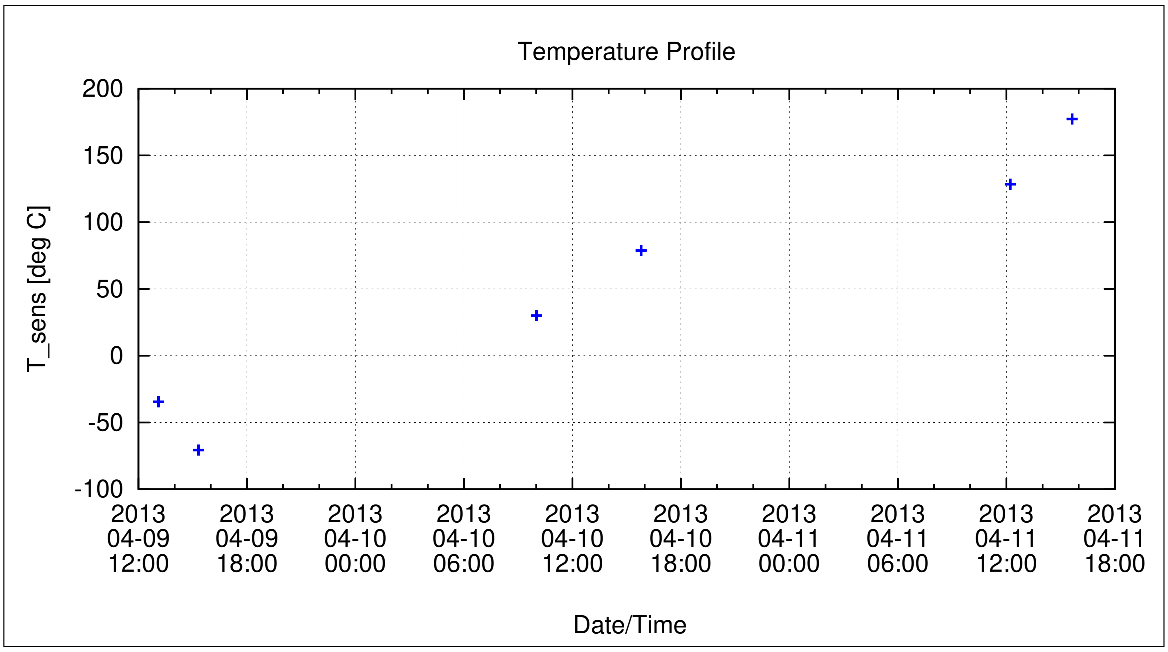

Figure 103: Temperature Profile

Calibration Parameter:

Sensor Offset $\underline{B}_{\rm off}$ vs. Temperature:

$$B_{\rm off,i}(T) = \sum_{k=0}^{n} B_{\rm off,k,i} T^k \qquad [\text{enT},\ ^\circ\text{C}],\ \text{i}=\{\text{x,y,z}\}$$

	$B_{\rm off,0,i}$	$B_{\rm off,1,i}$	$B_{\rm off,2,i}$	$B_{\rm off,3,i}$	$B_{\rm off,4,i}$	$B_{\rm off,5,i}$
$B_{\rm off,x}$	-5.68307E-1	4.08661E-3	6.45150E-5	-3.46324E-7		
$B_{\rm off,y}$	-5.22529E-1	-2.03202E-3	-6.13830E-5	3.69060E-7		
$B_{\rm off,z}$	-6.12748E-2	-3.29684E-6	8.06491E-5	-4.46246E-7		

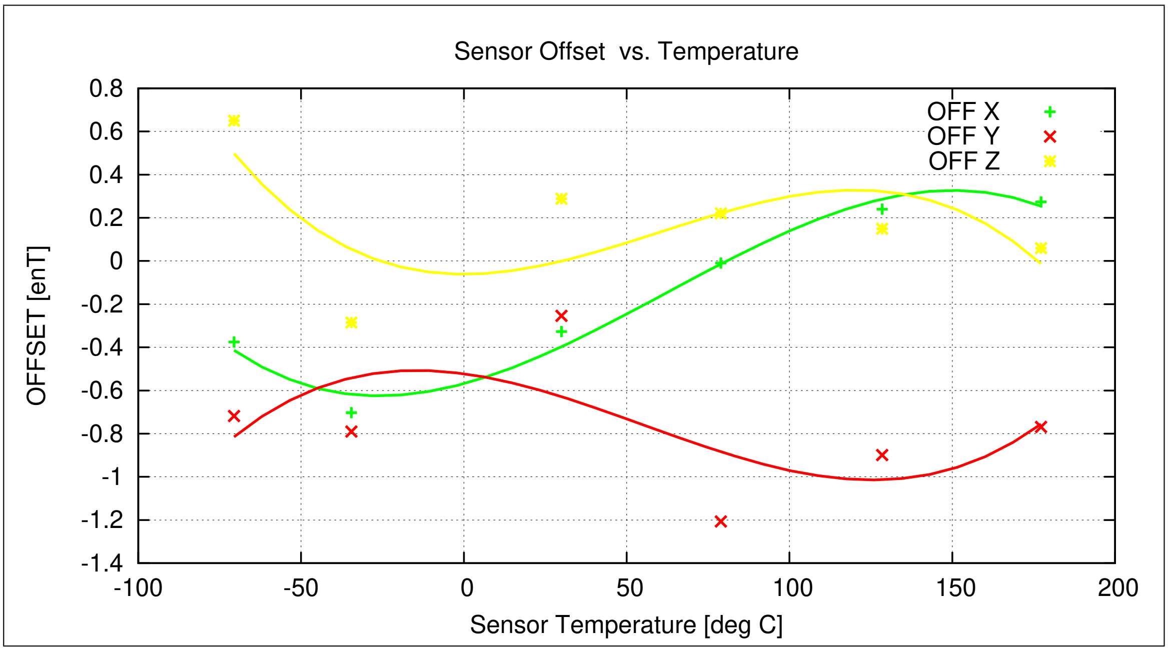

Figure 104: Temperature dependence of Sensor Offsets

Coil System Temperature

The following graph shows the mean Coil System temperature during the complete thermal cycle for the offset measurements.

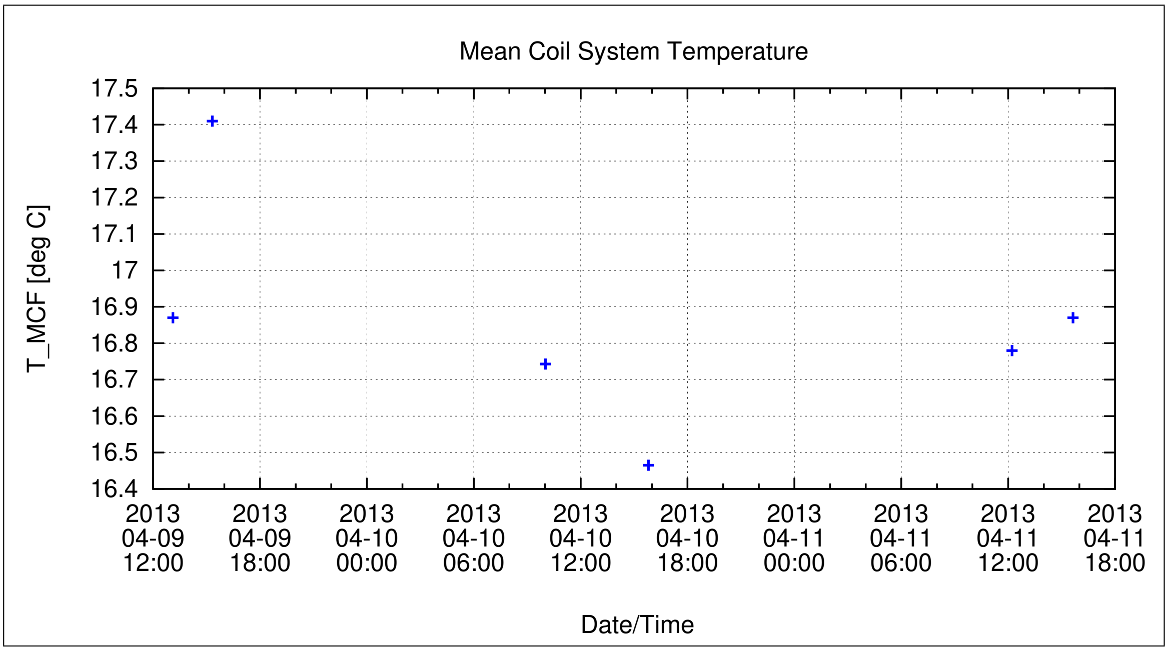

Figure 105: Coil System Temperature during Thermal Measurements

Coil System Residual Field:

The following graph shows the three components of the Coil System Residual field during the whole measurement. Axes designators are related to the actual DUT coordinate system and NOT to Coil System coordinates.

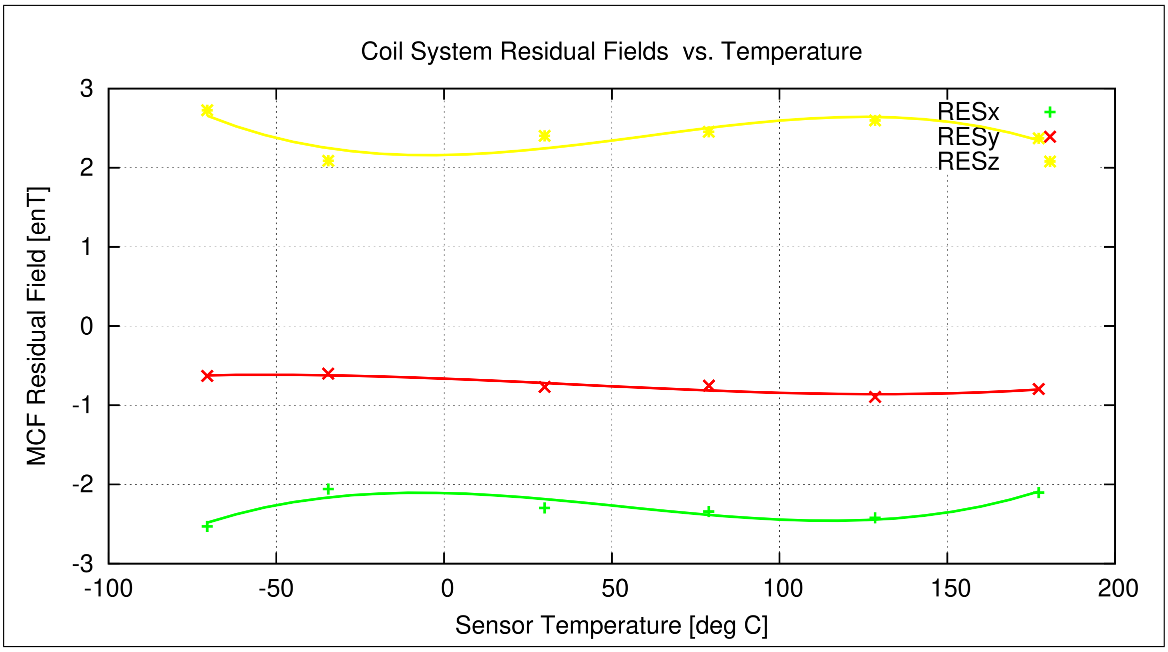

Figure 106: Coil System Residual Fields during Thermal Measurements

Remark:

The axes designation for this graph is given as follows (rf. to setup defined in chapter 1):

$$X_m = X_c$$
$$Y_m = Y_c$$
$$Z_m = -X_c$$

13.2.3 Temperature Calibration of the AC Transfer Function

Used Temperature Measurements:

Calibration Parameter File	Remark
FREQ_PARAMETER__13-04-09-13-27-51.FPF	
FREQ_PARAMETER__13-04-10-13-56-47.FPF	
FREQ_PARAMETER__13-04-11-10-20-53.FPF	
FREQ_PARAMETER__13-04-11-13-45-45.FPF	

Thermal Parameter File: THERMAL_AC_PARAMETER__13-04-09-13-27-51.TAF

Facility Parameter:

Nominal Sensor Setup: Diagonal in Space inside Thermal Box.

Sensor Temperature Channel: T_{59}

Coil System Temperature Channel: T_{29}

Temperature Profile

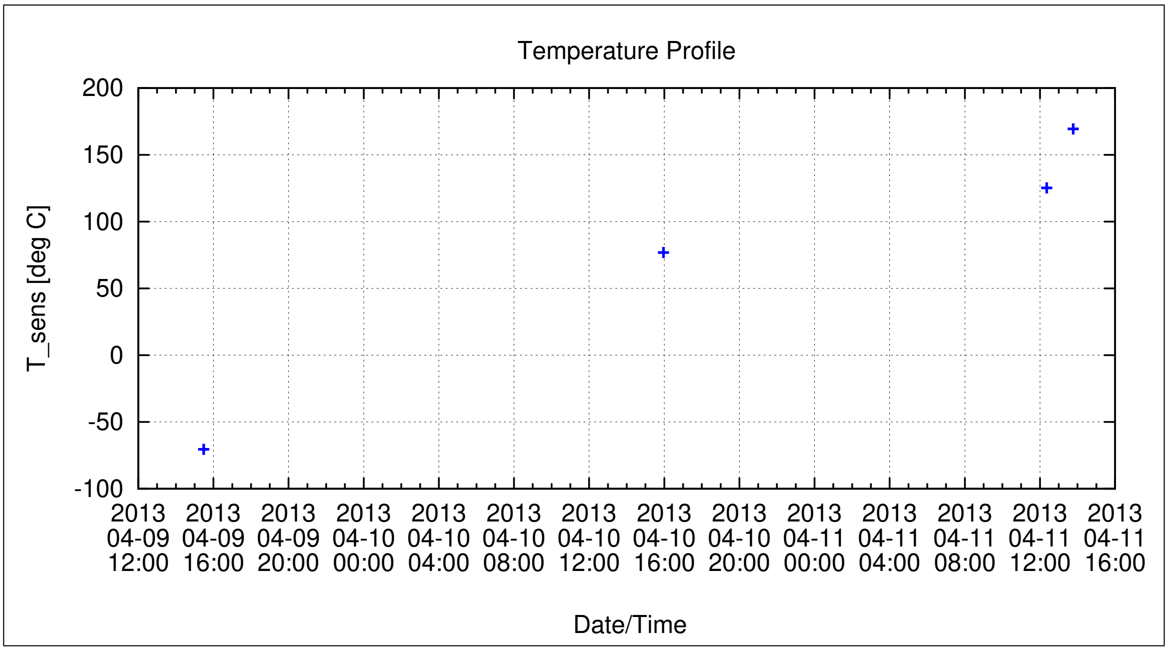

Figure 107: Temperature Profile

Coil System Temperature

The following graph shows the mean Coil System temperature during the complete thermal cycle for the AC measurements.

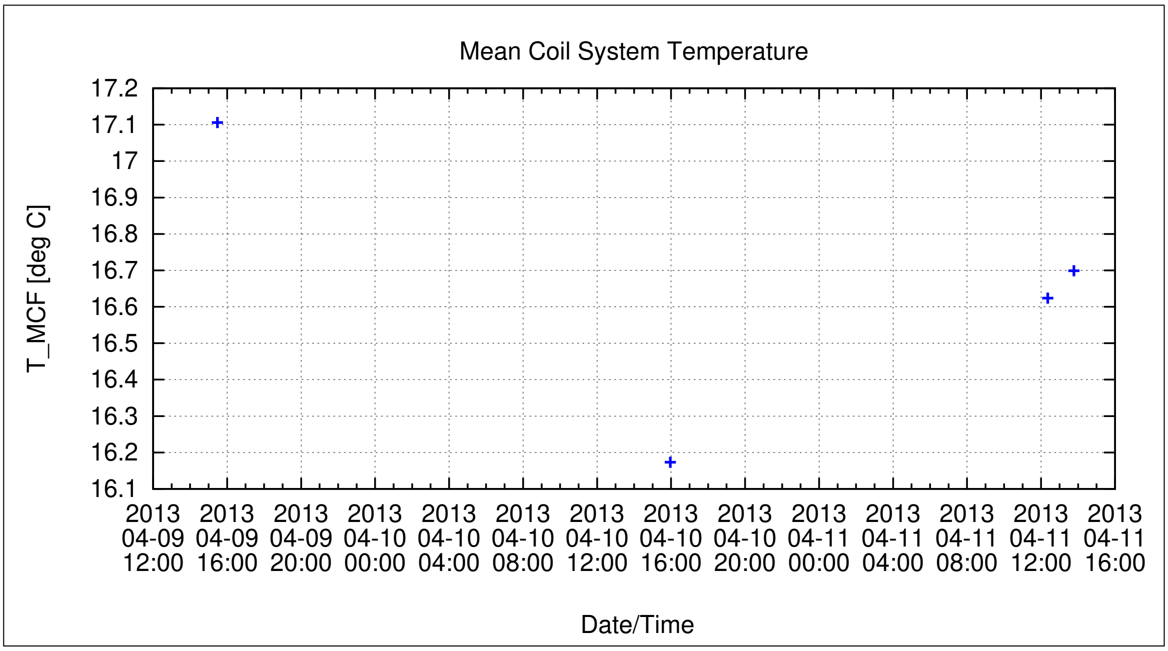

Figure 108: Coil System Temperature during Thermal AC Measurements

Calibration Parameter:

-3dB Corner Frequency f_{3dB} vs. Temperature:

$$f_{3dB,i}(T) = \sum_{k=0}^{n} f_{3dB,k,i} T^k \qquad [Hz,\ ^\circ C],\ i=\{x,y,z\}$$

	$f_{3dB,0,i}$	$f_{3dB,1,i}$	$f_{3dB,2,i}$	$f_{3dB,3,i}$	$f_{3dB,4,i}$	$f_{3dB,5,i}$
$f_{3dB,x}$	5.87823E+1	7.50885E-3				
$f_{3dB,y}$	5.88830E+1	7.81382E-3				
$f_{3dB,z}$	5.59134E+1	2.01382E-2				

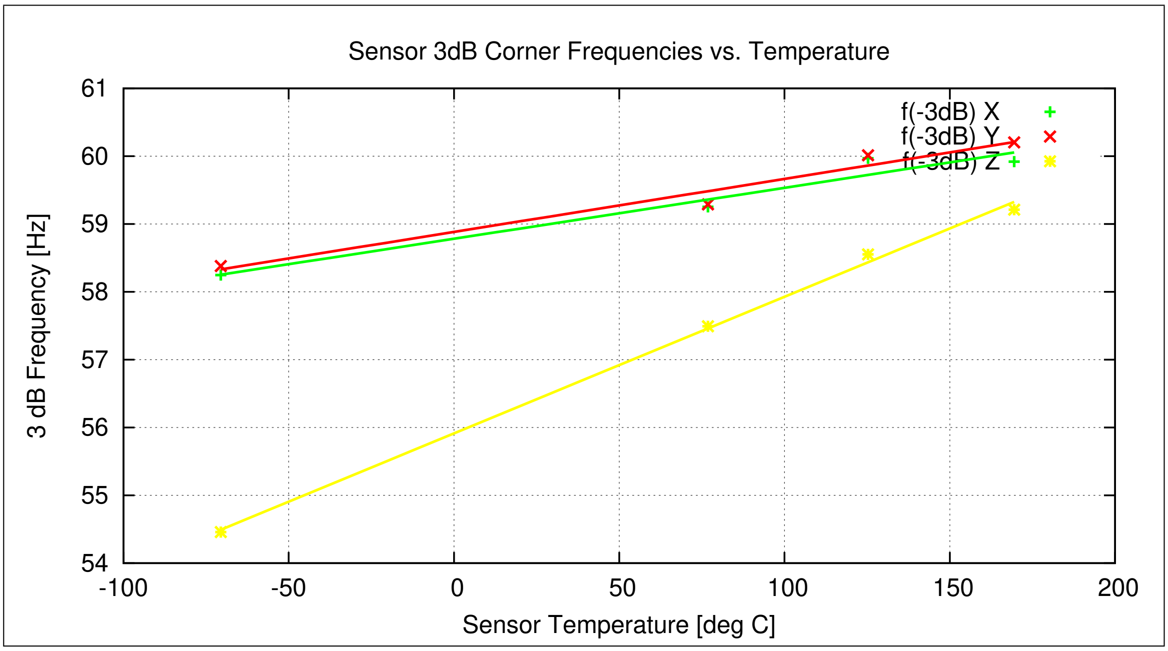

Figure 109: Temperature dependence of 3dB Corner Frequency

Instrument Sampling Frequency:

The following graph shows the calculated sampling frequencies vs. the actual sensor temperature.

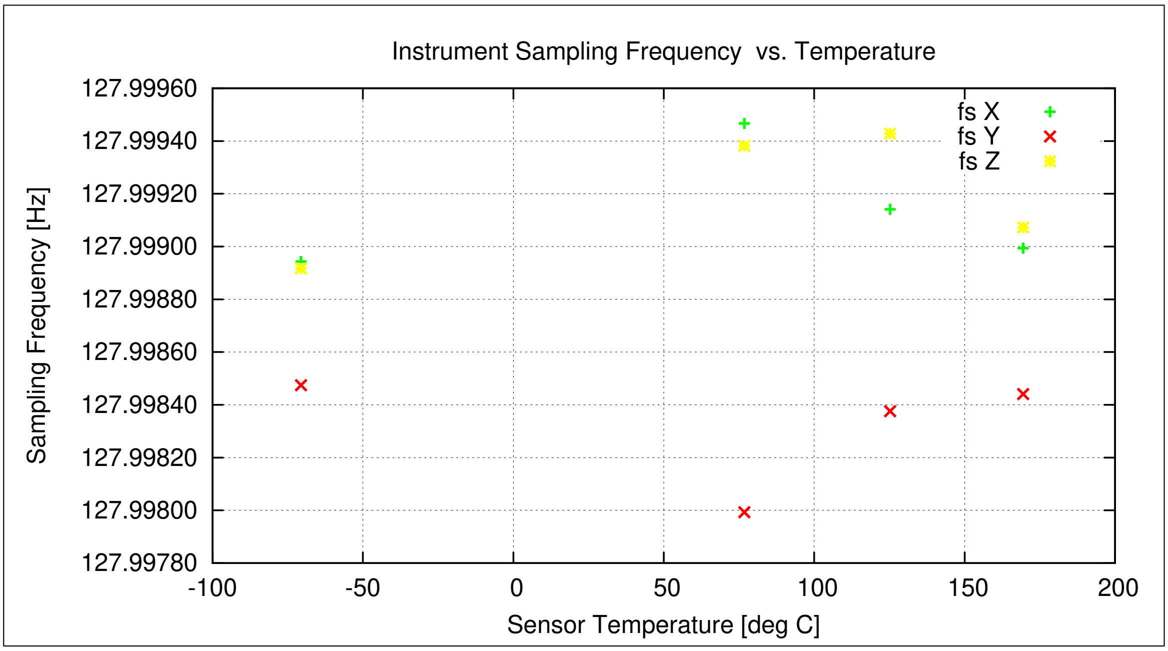

Figure 110: Instrument Sampling Frequency versus Sensor Temperature

Mean Samplerate: 127.998886 Hz.
Mean Standard Deviation of Samplerate: 0.000095 Hz.

14 Complete Temperature Profile

The following plot shows the complete thermal cycle of the sensor with all cooling and heating phases. The curves show the desired nominal temperatures in green and the actual measured temperatures in red.

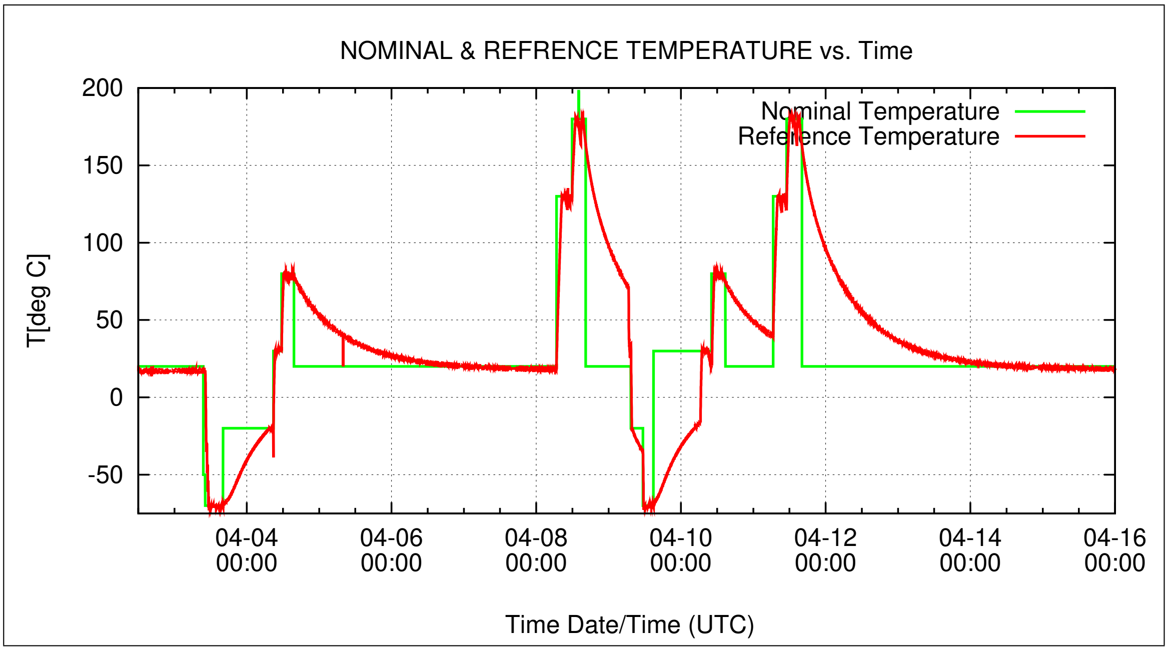

Figure 111: Complete thermal cycle

15 Mathematical Description of the Calibration

15.1 Basic Principle

The Magnetsrode Coil Facility (MCF) generates an artificial magnetic field $\underline{B}^{\mathrm{FLD}}$ that can be considered as a calibrated, orthogonal magnetic reference field[1] defined in coilsystem coordinates. For the calibration analysis this ideal coilsystem field is rotated to ideal orthogonal sensor coordinates using a nominal Rotation matrix $\underline{\underline{R}}_{\mathrm{nom}}$ at the first step. Nominal means that only rotations of ±90° or ±180° at any axis are considered here to get a coarse alignment of the applied field with the sensor-axes.

$$\underline{B}^{\mathrm{c}} = \underline{\underline{R}}_{\mathrm{nom}}\,\underline{B}^{\mathrm{FLD}}$$

For a standard calibration the matrix $\underline{\underline{R}}_{\mathrm{nom}}$ is just a $\underline{\underline{I}}$ - matrix - sensor coordinates and coilsystem coordinates have roughly the same direction. If the sensor coordinates are left-handed or the sensor is turned by about ±90° or ±180° at any axis $\underline{\underline{R}}_{\mathrm{nom}}$ will contain ±1-elements or 0-elements at any place. The rotated coil system field $\underline{B}^{\mathrm{c}}$ is the used reference field for the following analysis.

The magnetometer under test at the center of the coil system (CoC) generates magnetic raw data $\underline{B}^{\mathrm{r}}$. These data include an eventually existing residual field of the coil system $\underline{B}^{\mathrm{res}}$ and the magnetometer offset $\underline{B}^{\mathrm{off}}$. Both entities are combined in the offset & residual field $\underline{B}^{\mathrm{or}}$:

$$\underline{B}^{\mathrm{or}} = \underline{B}^{\mathrm{off}} + \underline{B}^{\mathrm{res}}$$

Therefore, the second step of the calibration is the generation of offset and residual field corrected measured field data $\underline{B}^{\mathrm{m}}$:

$$\underline{B}^{\mathrm{m}} = \underline{B}^{\mathrm{r}} - \underline{B}^{\mathrm{or}}$$

The actual offset and residual field is automatically taken into account during the calibration analysis. Either a constant field or - if needed - a linear trend of $\underline{B}^{\mathrm{or}}$ is subtracted from the raw data.

The relation between the calibration field and the magnetometer data is then defined by

$$\underline{B}^{\mathrm{c}} = \underline{\underline{\Phi}}\,\underline{B}^{\mathrm{m}}$$

where $\underline{\underline{\Phi}}$ is the complete calibration transfer matrix, defined by

$$\underline{\underline{\phi}} = \underline{\underline{R}}_{\mathrm{nom}}\;\underline{\underline{\rho}}\;\underline{\underline{\omega}}\;\underline{\underline{\sigma}}.$$

[1] During the calibration the temperature dependent sensitivity of the coil system is calculated every 3 minutes and taken into account as well as the static misalignment of the coil system to produce orthogonal, known fields.

$\underline{\underline{\sigma}}(T)$ represents the temperature dependent sensitivity.
$\underline{\underline{\omega}}(T)$ describes the temperature dependent internal sensor misalignment (orthogonalisation matrix).
$\underline{\underline{\rho}}(T)$ describes the real rotation of the sensor against the coil axes.[2]

Thus the calibration algorithms have to solve the following problem:

$$\begin{aligned} \underline{B}^{\mathrm{c}} &= \underline{\underline{\Phi}}\ \underline{B}^{\mathrm{m}} \\ &= \underline{\underline{R}}_{\mathrm{nom}}\ \underline{\underline{\rho}}\ \underline{\underline{\omega}}\ \underline{\underline{\sigma}}\ \underline{B}^{\mathrm{m}} \end{aligned} \qquad (1)$$

The separation into these submatrices and evaluation of their elements is done in subsequent steps:

- Calculation of the Sensitivity matrix $\underline{\underline{\sigma}}$
  The sensitivity matrix shall contain the on-axis sensitivity coefficients of the sensors. Therefore, $\underline{\underline{\sigma}}$ has to be a diagonal matrix of the following kind:

$$\underline{\underline{\sigma}} = \begin{pmatrix} \sigma_1 & 0 & 0 \\ 0 & \sigma_2 & 0 \\ 0 & 0 & \sigma_3 \end{pmatrix}$$

  The separation of matrix $\underline{\underline{\sigma}}$ from the transfer function $\underline{\underline{\phi}}$ yields

$$\underline{\underline{\phi}} = \begin{pmatrix} \frac{\phi_{11}}{\sigma_1} & \frac{\phi_{12}}{\sigma_2} & \frac{\phi_{13}}{\sigma_3} \\ \frac{\phi_{21}}{\sigma_1} & \frac{\phi_{22}}{\sigma_2} & \frac{\phi_{23}}{\sigma_3} \\ \frac{\phi_{31}}{\sigma_1} & \frac{\phi_{32}}{\sigma_2} & \frac{\phi_{33}}{\sigma_3} \end{pmatrix} \begin{pmatrix} \sigma_1 & 0 & 0 \\ 0 & \sigma_2 & 0 \\ 0 & 0 & \sigma_3 \end{pmatrix} := \hat{\underline{\underline{\phi}}}\ \underline{\underline{\sigma}}$$

  For the computation of the sensitivity coefficients σ_i the transformation of the basevectors has to be considered. Equation (1) transform the components of the fields, whereas

$$\underline{e}^{\mathrm{c}} = \left(\underline{\underline{\phi}}^{\mathrm{T}}\right)^{-1}\ \underline{e}^{\mathrm{m}} := \underline{\underline{\Psi}}\ \underline{e}^{\mathrm{m}}$$

  has to be used for the contragredient base-vector transformation of the skew sensorsystem Σ^{m} into the orthonormal coilsystem Σ^{c}. The length of the column vectors of $\underline{\underline{\psi}}$ define the sensitivity coefficients σ_i:

$$\sigma_1 = \frac{1}{\sqrt{\psi_{11}^2 + \psi_{21}^2 + \psi_{31}^2}}$$

[2] Also the rotation matrix is regarded as temperature dependent being able to consider any thermal setup inadequacies causing fractional rotations.

$$\sigma_2 = \frac{1}{\sqrt{\psi_{12}^2 + \psi_{22}^2 + \psi_{32}^2}}$$
$$\sigma_3 = \frac{1}{\sqrt{\psi_{13}^2 + \psi_{23}^2 + \psi_{33}^2}}$$

- Calculation of the Misalignment matrix $\underline{\underline{\omega}}$

  After the separation of $\underline{\underline{\sigma}}$ the reduced transfer function $\overset{\wedge}{\underline{\underline{\phi}}}$ contains only the misalignment and the real sensor rotation. The misalignment angles $\xi_{xy}, \xi_{xz}, \xi_{yz}$, hence the angles between the base vectors of the affine sensorsystem Σ^{m}, can be evaluated from the scalar products of all these base vectors. The base unit vectors are defined by the inverse transposed matrix of the reduced transfer function:

$$\underline{e}_{\mathrm{x}}^{\mathrm{m}} := \left(\overset{\wedge}{\underline{\underline{\phi}}}^{\mathrm{T}}\right)^{-1} \begin{pmatrix} 1 \\ 0 \\ 0 \end{pmatrix}$$
$$\underline{e}_{\mathrm{y}}^{\mathrm{m}} := \left(\overset{\wedge}{\underline{\underline{\phi}}}^{\mathrm{T}}\right)^{-1} \begin{pmatrix} 0 \\ 1 \\ 0 \end{pmatrix}$$
$$\underline{e}_{\mathrm{z}}^{\mathrm{m}} := \left(\overset{\wedge}{\underline{\underline{\phi}}}^{\mathrm{T}}\right)^{-1} \begin{pmatrix} 0 \\ 0 \\ 1 \end{pmatrix}$$

  The misalignment angles can be derived from the scalar products:

$$\xi_{xy} = \arccos\left(\underline{e}_x^m \cdot \underline{e}_y^m\right)$$
$$\xi_{xz} = \arccos\left(\underline{e}_x^m \cdot \underline{e}_z^m\right)$$
$$\xi_{yz} = \arccos\left(\underline{e}_y^m \cdot \underline{e}_z^m\right)$$

  Let's assume that the x-axis of the reference system $\underline{e}_{\mathrm{x}}^{\mathrm{c}}$ is identical to the $\underline{e}_{\mathrm{x}}^{\mathrm{m}}$-axis of the sensor system. The angle between $\underline{e}_{\mathrm{y}}^{\mathrm{c}}$ and $\underline{e}_{\mathrm{y}}^{\mathrm{m}}$ is β (rotation angle around the $\underline{e}_{\mathrm{z}}^{\mathrm{c}}$ axis). And the sensor $\underline{e}_{\mathrm{z}}^{\mathrm{m}}$ axis can be constructed by a rotation of η in the $\underline{e}_{\mathrm{x}}^{\mathrm{c}}, \underline{e}_{\mathrm{y}}^{\mathrm{c}}$-plane and a second rotation of γ out of this plane. Then this misalignment of the base vectors is given by

$$\underline{\underline{O}} = \begin{pmatrix} 1 & \sin\beta & \sin\gamma \\ 0 & \cos\beta & \cos\gamma\sin\eta \\ 0 & 0 & \cos\gamma\cos\eta \end{pmatrix} \tag{2}$$

  By comparison of the angles β, η, γ with misalignment angles $\xi_{xy}, \xi_{xz}, \xi_{yz}$, the misalignment matrix (2) can be written in the following shape:

$$\underline{\underline{O}} = \begin{pmatrix} 1 & \cos\xi_{xy} & \cos\xi_{xz} \\ 0 & \sin\xi_{xy} & \dfrac{\cos\xi_{yz} - \cos\xi_{xy}\cos\xi_{xz}}{\sin\xi_{xy}} \\ 0 & 0 & \sqrt{\sin^2\xi_{xz} - \dfrac{(\cos\xi_{yz} - \cos\xi_{xy}\cos\xi_{xz})^2}{\sin^2\xi_{xy}}} \end{pmatrix}$$

$\underline{\underline{O}}$ transforms the base vectors. To achieve the transformation between the field components the transposed, inverse matrix of $\underline{\underline{O}}$ has to be calculated as the final misalignment matrix:

$$\underline{\underline{\omega}} = \left(\underline{\underline{O}}^{\mathrm{T}}\right)^{-1}$$

- Calculation of the Rotation matrix $\underline{\underline{\rho}}$
  With the knowledge of $\underline{\underline{\omega}}$ and the nominal Setup matrix $\underline{\underline{R}}_{\mathrm{nom}}$ the rotation matrix $\underline{\underline{\rho}}$ can be evaluated:

  $$\underline{\underline{\rho}} = (\underline{\underline{R}}_{\mathrm{nom}})^{-1} \; \overset{\wedge}{\underline{\underline{\phi}}} \; (\underline{\underline{\omega}})^{-1}$$

  From this rotation matrix the actual rotation angles of the sensor wrt. the coil system can be calculated using again the scalar product:

  $$\begin{aligned} \lambda &:= \arccos\left(\left[\underline{\underline{\rho}}\begin{bmatrix}1\\0\\0\end{bmatrix}\right]\cdot\begin{bmatrix}1\\0\\0\end{bmatrix}\right) \\ \mu &:= \arccos\left(\left[\underline{\underline{\rho}}\begin{bmatrix}0\\1\\0\end{bmatrix}\right]\cdot\begin{bmatrix}0\\1\\0\end{bmatrix}\right) \\ \nu &:= \arccos\left(\left[\underline{\underline{\rho}}\begin{bmatrix}0\\0\\1\end{bmatrix}\right]\cdot\begin{bmatrix}0\\0\\1\end{bmatrix}\right) \end{aligned}$$

  The rotation matrix $\underline{\underline{\rho}}$ and the rotation angles λ, μ, ν are of interest just for the calibration to determine the right magnetometer parameters.

The transfer function for the normal use of the magnetometer is just given by

$$\overset{\sim}{\underline{\underline{\phi}}} = \underline{\underline{\omega}}\;\underline{\underline{\sigma}}$$

16 Nomenclature

Abbreviations in theoretical sections:

Item	Meaning
$\underline{B}^c$	Magnetic calibration field generated by coil system
$\underline{B}^{off}$	Offset of the magnetometer [nT]
$\underline{B}_k^{off}$	Polynomial Fit coefficients for the sensor offset vs. temperature
$\underline{B}^m$	Measured magnetic field raw data, offset & residual field corrected [nT]
$\underline{B}^{or}$	$= \underline{B}^{off} + \underline{B}^{res}$, Offset + Residual field at CoC [enT]
$\underline{B}^r$	Magnetic field raw data
$B^r_{0°}$	Magnetic raw data, measured in normal position (0°)[enT]
$B^r_{180°}$	Magnetic raw data, measured in turned position (180°)[enT]
$\underline{B}^{res}$	Residual field of the coil system
e°C	Engineering degrees centigrade units
enT	Engineering NanoTesla units
c_0, c_1, c_2, c_3	Fit coefficients of the sensor thermistor
i	component x | y | z
CoC	Center of Coil system
DUT	Device under Test
$\underline{\underline{\phi}}$	$= \underline{\underline{R}}_{\text{nom}}\, \underline{\underline{\rho}}\, \underline{\underline{\omega}}\, \underline{\underline{\sigma}}$, Calibration Transfer Matrix
$\tilde{\underline{\underline{\phi}}}$	$= \underline{\underline{\omega}}\, \underline{\underline{\sigma}}$, Transfer Matrix
$\hat{\underline{\underline{\phi}}}$	$= \underline{\underline{\phi}}\, \underline{\underline{\sigma}}^{-1}$, Reduced Transfer Matrix
$\underline{\underline{\psi}}$	$= (\underline{\underline{\phi}}^T)^{-1}$, Auxilliary transfer matrix
$\underline{\underline{O}}$	Base vector Orthogonalisation matrix
$\underline{\underline{\omega}}$	$= (\underline{\underline{O}}^T)^{-1}$, Field components orthogonalisation matrix
$\underline{\underline{R}}_{\text{nom}}$	Nominal Rotation matrix of sensor vs. coil system
$\underline{\underline{\rho}}$	= Actual rotation matrix
$\underline{\underline{\sigma}}$	= Sensitivity matrix
$\sigma_{k,i}$	Polynomial Fit coefficient for sensitivity vs. temperature. Coefficient of order k for the sensor component i
TeMeSys	MRode Temperature Measurement System
T^c_s	Temperature of sensor s, calibrated data [°C]
T^r_s	Temperature of sensor s, raw data [e°C]
s	Sensor IB | OB
$U_{\text{T, IB}}$	IB–Temperature data [V], measured
$U_{\text{T,OB}}$	OB–Temperature data [V], measured
ξ_{ij}	Temperature dependent alignment angle (ij component)
$\xi^0_{k,ij}$	Polynomial Fit coefficient for misalignment angle vs. temperature. Coefficient of order k for the angle ij
λ, μ, ν	Rotation angles wrt. coil system reference coordinates.